

**FUEL OPTIMAL
TRAJECTORY AND GUIDANCE DESIGN
FOR LUNAR SOFT LANDING AT A TARGET SITE**

*A thesis submitted
in partial fulfillment for the award of the degree of*

Doctor of Philosophy

by

REMESH N



**Department of Aerospace Engineering
INDIAN INSTITUTE OF SPACE SCIENCE AND TECHNOLOGY
Thiruvananthapuram, India**

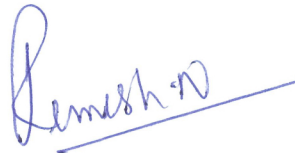
July 2021

DECLARATION

I declare that this thesis titled **Fuel Optimal Trajectory and Guidance Design for Lunar Soft Landing at a Target Site** submitted in partial fulfillment for the award of the degree of **Doctor of Philosophy** is a record of original work carried out by me under the supervision of **Dr. R.V Ramanan** and **Dr. V.R Lalithambika**, and has not formed the basis for the award of any degree, diploma, associateship, fellowship, or other titles in this or any other Institution or University of higher learning. In keeping with the ethical practice in reporting scientific information, due acknowledgments have been made wherever the findings of others have been cited.

Place: Thiruvananthapuram

Date: 2 July 2021



Remesh N

Roll No.:SC11D026



www.iist.ac.in

भारतीय अंतरिक्ष विज्ञान एवं प्रौद्योगिकी संस्थान

(वि.अ.आयोग अधिनियम 1956 की धारा-3 के अधीन भावी मानित विश्वविद्यालय घोषित)

भारत सरकार, अंतरिक्ष विभाग, वलियमला पोस्ट, तिरुवनंतपुरम 695 547 भारत

Indian Institute of Space Science and Technology

(A Deemed to be University u/s 3 of the UGC Act, 1956)

Government of India, Department of Space

Valiamala P.O., Thiruvananthapuram 695 547 India

CERTIFICATE

This is to certify that the thesis titled **Fuel Optimal Trajectory and Guidance Design for Lunar Soft Landing at a Target Site** submitted by **Remesh N (SC11D026)**, to the Indian Institute of Space Science and Technology, Thiruvananthapuram, in partial fulfillment for the award of the degree of **Doctor of Philosophy**, is a bona fide record of the research work carried out by him under our supervision. The contents of this thesis, in full or in parts, have not been submitted to any other Institute or University for the award of any degree or diploma.

Dr. V.R Lalithambika

Research Supervisor,

Director,

Directorate of Human Space Program,

ISRO Head Quarters, Bangalore

Dr. R.V Ramanan

Research Supervisor,

Outstanding Scientist/Adjunct professor (Retd.),

Department of Aerospace Engineering, IIST

डॉ. अरविंद वी./Dr. ARAVIND V.
आचार्य एवं अध्यक्ष/Professor & Head
वांतरिक्ष इंजीनियरी विभाग
Department of Aerospace Engineering
भारतीय अंतरिक्ष विज्ञान एवं प्रौद्योगिकी संस्थान
Indian Institute of Space Science and Technology
अंतरिक्ष विभाग, भारत सरकार
Department of Space, Government of India
तिरुवनंतपुरम/Thiruvananthapuram - 695 547

Counter Signature

The Head-of-Department,

Department of Aerospace Engineering,

IIST.



Seal

Place : Thiruvananthapuram

Date : 2 July 2021

This thesis is dedicated to my beloved parents

ACKNOWLEDGEMENTS

First and foremost, I thank God for enabling me to persevere the research work, whenever I experienced lack of self-confidence, and complete this thesis.

I would like to express my sincere gratitude to my thesis supervisor Dr. R.V Ramanan for his valuable guidance, constant motivation and help throughout the research. It has been a great learning experience in both technical research and personal levels. I thank my internal guide Dr. V.R Lalithambika for her timely advice and suggestions, which helped me to complete my thesis. My sincere heartfelt thanks to Dr. S Swaminathan for the inspiration to do research and questions during the periodic review sessions.

I would also like to thank all the members of my doctoral committee for their insightful comments and questions during the periodic review sessions, which helped me to bridge the gap and provide completeness in my work.

I also thank all my friends and colleagues who supported me during the course of my research activities.

I express my sincere gratitude to Deputy Director-Aeronautics Entity VSSC, Group Director-Aerospace Flight Dynamics and Group Head-Flight Mechanics Group for their encouragement and support for the research.

I also wish to express my gratitude to Director, VSSC for giving me permission to register for the Ph.D. course and supported me during the entire period of this course.

Remesh N

ABSTRACT

The problem of generating optimal landing trajectory design and optimal guidance laws for Moon landing is solved in this research. First, the lunar soft landing trajectory design problem is formulated and the resulting two-point boundary value problem (TPBVP) is solved using different approaches. Two independent approaches i) direct ii) indirect are used to solve the problem. Two of the gradient free (Particle Swarm Optimization-PSO and Differential Evolution-DE) optimization techniques and a gradient based optimization technique (Sequential Quadratic Programming-SQP: fmincon-MATLAB) have been used to solve the problem formulated using both direct and indirect approaches. A scheme based on the indirect approach and DE is evaluated to be superior for the soft landing trajectory design. The challenge in the indirect approach lies in finding suitable initial co-states with no prior knowledge available about them. In the second part of the research, the challenge related to initial co-states is dealt with and overcome. The co-states are determined using the Differential Transformation (DT) technique, for a given flight duration (unknown) and a target site. The only unknown flight time is determined using the DE technique. This novel computational scheme, called DT-DE scheme, uses Differential Transformation in multi steps to ensure the precise landing at the target site. This scheme is uniformly valid for the performance measures like fuel-optimal, energy-optimal or time-optimal. In DT-DE scheme, the major advantage is that the co-state equations need not be numerically integrated to find the control variables at each computational step. Furthermore, the number of unknowns reduces to one, the flight time, resulting in a reduction of computational time. Another important step of a lander mission is to guide the vehicle

to the pre-selected target site. Towards achieving this, a DT based novel guidance algorithm with real time computational strategy for the determination of flight time is developed. Two guidance schemes (i) fuel-optimal (ii) energy-optimal to realize soft landing at a desired location on the Moon are developed using the optimal control laws. The optimal control laws are obtained as functions of co-states. The DT technique is employed to determine the unknown co-states at each time instant of landing trajectory using the information on the current vehicle state, target landing site (loaded on-board a priori), and the time-to-go. The time-to-go, a critical parameter for any guidance scheme, is computed and updated in real time using a simple strategy that uses the current and end states. Further, the new guidance schemes are compared with other popular guidance schemes. Other features of the proposed schemes are that they do not assume a constant gravity field and independent of the reference trajectory. The proposed methods for landing trajectory design and guidance design have been implemented and the numerical results have been analyzed. Some of the important findings are: (i) The computational time (CPU time) to generate optimal trajectory using the DT-DE scheme is significantly less (35 to 40 s) compared to the CPU time required to generate the solution using the DE technique alone (170 s). (ii) The landing mass achieved by fuel-optimal DT guidance is remarkably close (the difference is less than one kg) to the landing mass of open-loop fuel-optimal trajectory. (iii) The Fuel-optimal DT guidance lands more mass than the energy-optimal DT guidance. (iv) The DT based energy-optimal guidance scheme performs better than other energy-optimal guidance schemes (v) The simple strategy proposed for the real-time computation of time-to-go performs very well and helps in achieving the target site precisely.

List of Publications Based on the Current Research

Publications in refereed International Journals

1. Remesh, N., Ramanan R.V., Lalithambika V.R., October 2016. Fuel optimum lunar soft-landing trajectory design using different solution schemes. International Review of Aerospace Engineering (IREASE), 9(5), 131-143.
2. Remesh, N., Ramanan R.V., Lalithambika V.R., March 2021. Fuel-optimal and energy optimal guidance schemes for lunar soft landing at a desired location. Advances in Space Research, 67(6), 1787-1804.
3. Remesh, N., Ramanan R.V., Lalithambika V.R. A novel indirect scheme for optimal lunar soft landing at a target site. Journal of the Institution of Engineers (India) : Series C Aerospace (Under revision)

Publications in International Conferences

4. Remesh, N., Ramanan, R.V., Lalithambika, V. R., 2017. Optimal 3D Lunar soft landing trajectory design and performance evaluation of explicit guidance laws. IEEE Xplore, International Conference on Recent Advances in Aerospace Engineering (ICRAAE 2017), DOI:10.1109/ICRAAE:2017.8297217.

Table of Contents

DESCRIPTION	PAGE NUMBER
DECLARATION	ii
CERTIFICATE	iii
ACKNOWLEDGEMENTS	v
ABSTRACT	vii
PUBLICATIONS BASED ON THIS THESIS	ix
TABLE OF CONTENTS	x
LIST OF FIGURES.....	xiv
LIST OF TABLES	xviii
ABBREVIATIONS.....	xxii
NOMENCLATURE	xxiii
Chapter 1	1
Introduction and Literature Survey	1
1.1 Introduction.....	1
1.2 Historical Perspective.....	2
1.3 Literature Survey	3
1.4 Motivation of the Research.....	15
1.5 Objectives of the Research	17
1.6 Research Summary.....	18
1.7 Thesis Architecture	20
Chapter 2	23
Optimal Lunar Landing Trajectories and Solution Schemes.....	23
2.1 Dynamics of Landing Trajectory	23
2.2 Formulation of Optimal Control Problem – Indirect Approach.....	25
2.3 Solution of the Optimal Control Problem.....	27
2.3.1 Indirect Approach.....	27
2.3.2 Direct Approach	29

2.3.3 Solution Schemes	30
2.4 Optimization Techniques	30
2.4.1 Particle Swarm Optimization (PSO).....	31
2.4.2 Differential Evolution (DE)	32
2.4.3 Gradient Based Optimizer (SQP)	34
2.5 Results and Analysis	34
2.5.1 Performance of Indirect Schemes.....	35
2.5.1.1 Implication of Initial guess on Convergence of Gradient Based Scheme (Solution Scheme 3)	39
2.5.2 Comparison of Indirect Schemes.....	40
2.6 Optimal Landing Trajectories with Different Initial Thrust to Mass Ratio	42
2.7 Results using Direct Approach Based Schemes (4, 5 and 6)	44
2.7.1 Comparison of direct and indirect approaches	52
2.8 Trajectory Design by 3-DOF Dynamics	52
2.9 Conclusion	54
Chapter 3	55
An Indirect Scheme for Optimal Lunar Pinpoint Soft landing Trajectories	55
3.1 Introduction.....	56
3.2 System Dynamics.....	57
3.3 Formulation for Landing Problem (Indirect Approach)	60
3.3.1 Formulation for Energy-optimal.....	61
3.3.1.1 Unlimited Thrust.....	61
3.3.1.2 Limited Thrust.....	62
3.3.2 Formulation for Fuel-optimal.....	63
3.3.3 Formulation for Time-optimal.....	64
3.4 Solution Scheme	66
3.4.1 DT-DE Solution Scheme	66
3.4.2 Initial Co-states using Differential Transformation.....	67
3.4.3 Guidelines for Bounds for Flight time	72
3.5 DT-DE Scheme –Algorithm	72
3.6 Soft Landing Trajectory Design and Analysis with Various Performance Measures	75

3.6.1 Time-optimal Trajectory using Differential Evolution for Target Site Generation	75
3.6.2 Sensitivity of the DT Scheme Parameters.....	77
3.6.3 Time-optimal Trajectory using Multi-step DT Scheme (DT-DE Scheme).....	78
3.6.4 Energy-optimal Trajectory Using DE and DT-DE Schemes (Unlimited Thrust).....	81
3.6.5 Energy-optimal Trajectory using DE and DT-DE Schemes (With Limited Thrust) ..	83
3.6.6 Fuel-optimal Trajectory Using DE and DT-DE Schemes.....	84
3.6.7 Comparison of Optimal Solution with Different Performance Measures	86
3.6.8 Performance of Gradient Based Method with DT	89
3.6.9 Summary of Merits and Demerits of Different Solution Schemes	90
3.7 Strategy for Vertical Landing at Touch down.....	90
3.8 Conclusion	94
Chapter 4	95
Performance and Design analysis using the DT-DE scheme	95
4.1 Optimal Trajectory Design from Different Perilune Altitudes	95
4.2 Realization of a Target Site with Different Descent Flight Durations with a Fixed Periapsis Location.....	98
4.2.1 Performance of Fuel-optimal DT-DE scheme.....	99
4.2.2 Performance of Energy-optimal DT-DE scheme	100
4.3 Realization of a Target site with Different Descent Flight Durations by the Choice of Periapsis Location.....	102
4.3.1 Performance of the Fuel-optimal DT-DE	102
4.3.2 Performance of the Energy-optimal Limited Thrust DT-DE	104
4.4 Conclusions.....	106
Chapter 5	107
DT Guidance Algorithms for Lunar Pinpoint Soft Landing	107
5.1 Introduction.....	107
5.2 Some Guidance Schemes for Landing at a Specified Location – With Variable Thrust.....	108
5.2.1 E-Guidance.....	108
5.2.2 CTVG (Constrained Terminal Velocity) Guidance Scheme.....	111
5.2.3 Polynomial Guidance Scheme.....	114
5.3 Differential Transformation Based Guidance Scheme	115

5.3.1 Energy-optimal Guidance Laws	116
5.3.2 Fuel-optimal Guidance Laws	116
5.3.3 Strategy for Time-to-go	117
5.3.4 Differential Transformation (DT) Based Guidance Algorithms	118
5.4 Results and Discussion	123
5.4.1 Evaluation of Guidance Schemes	124
5.4.2 Fuel-optimal DT Guidance for Throttling Engine (40 % - 100 %)	130
5.4.3 Evaluation of time-to-go Computation Strategy and Guidance Schemes	131
5.4.3.1 Performance comparison of time-to-go computation methods- proposed vs standard method	134
5.4.4 Nominal Landing Site with Higher Thrust.....	135
5.5 Retargeting Capability	136
5.5.1 Retargeting Before Start of Powered Braking.....	136
5.5.2 Retargeting During Powered Braking Phase.....	138
5.6 Monte Carlo Simulations	140
5.7 Constraint on Lander Terminal Thrust Attitude.....	147
5.8 Conclusions.....	149
Chapter 6	151
Conclusions and Future Scope of Work.....	151
Future Scope	155
References	156

LIST OF FIGURES

Fig. 2.1. Parameters for planar trajectory design	24
Fig. 2.2. Indirect approach schematic	28
Fig. 2.3. Direct approach schematic	29
Fig. 2.4. Altitude profile with solution scheme 1,2 and 3	36
Fig. 2.5. Horizontal velocity vs time with solution scheme 1,2 and 3	36
Fig. 2.6. Vertical velocity vs time with solution scheme 1,2 and 3	37
Fig. 2.7. Optimum thrust direction angle with solution scheme 1,2 and 3.....	37
Fig. 2.8. Hamiltonian variation with solution scheme 1,2 and 3	38
Fig. 2.9. Co-state variation for optimal trajectory –Scheme 2.....	38
Fig. 2.10. Optimum thrust direction angle – comparison of solution Scheme 3 sensitivity with initial guess	40
Fig. 2.11. Comparison of solution schemes 1 and 2	41
Fig. 2.12. Altitude variation with different thrust levels	44
Fig. 2.13. Optimum thrust direction angle for different thrust levels	44
Fig. 2.14. Direct approach solution sensitivity with interpolation methods.....	46
Fig. 2.15. Altitude profile comparison for solution scheme 4, 5 and 6.....	47
Fig. 2.16. Optimum thrust direction angle for solution scheme 4,5 and 6	47
Fig. 2.17. Horizontal velocity variation for solution scheme 4, 5 and 6	48
Fig. 2.18. Vertical velocity variation for solution scheme 4, 5 and 6	48
Fig. 2.19. No of function evaluations for solution scheme 4, 5 and 6	49
Fig. 2.20. Schematic RTN frame	52

Fig. 3.1. Soft landing coordinate System and thrust vector schematic	59
Fig. 3.2. Altitude profile comparison – time-optimal solution	80
Fig. 3.3. Velocity profile comparison – time-optimal solution	80
Fig. 3.4. Thrust acceleration components- time-optimal case	80
Fig. 3.5. Required thrust profile comparison: energy-optimal -unlimited thrust.....	82
Fig. 3.6. Required thrust acceleration comparison: energy-optimal -unlimited thrust ...	83
Fig. 3.7. Thrust acceleration profile comparison – energy-optimal with limited thrust .	84
Fig. 3.8. Thrust acceleration components – fuel-optimal.....	85
Fig. 3.9. Fuel-optimal thrust profile	88
Fig. 3.10. Energy-optimal thrust profile- with limited thrust	88
Fig. 3.11. Thrust direction variation for fuel-optimal and energy-optimal DT-DE schemes.....	93
Fig. 4.1. Thrust profile for fuel-optimal formulation for initial perilune altitude of 20 km	97
Fig. 4.2. Thrust profile for energy-optimal (limited thrust) formulation for initial perilune altitude of 20 km.....	97
Fig. 4.3. Fuel-optimal trajectory profile for different fixed flight times	100
Fig. 4.4. Fuel-optimal thrust profiles for different fixed flight times	100
Fig. 4.5. Energy-optimal trajectory profiles for different fixed flight times	101
Fig. 4.6. Energy-optimal thrust profiles for different fixed flight times	102
Fig. 4.7. Fuel-optimal trajectory profiles for different fixed flight times	103
Fig. 4.8. Fuel-optimal thrust profiles for different fixed flight times	104

Fig. 4.9. Energy-optimal trajectory profiles for different fixed flight times with optimum initial argument of perilune	105
Fig. 4.10. Energy-optimal thrust profiles for different fixed flight times	105
Fig. 5.1. Altitude profile for DT guidance schemes (Case 1).....	127
Fig. 5.2. Down-range vs cross-range - Case 1.	127
Fig. 5.3. Thrust profile- for fuel-optimal DT guidance (0 %- Case 1).....	128
Fig. 5.4. Thrust profile for energy-optimal DT guidance (Case 1).....	128
Fig. 5.5. Time vs real time computed time-to-go.	129
Fig. 5.6a. and Fig.5.6b. The time-to-go difference with propagation steps.	129
Fig. 5.7. Profile of demanded thrust by fuel-optimal DT guidance (minimum thrust = 40%).	131
Fig. 5.8. Fuel-optimal trajectories for different thrust levels (case 1).....	133
Fig. 5.9. Profiles of time-to-go differences under various thrust levels.....	134
Fig. 5.10. Guided trajectories (latitude vs longitude) for nominal and with retargeting-energy-optimal	139
Fig. 5.11. Guided trajectories (altitude vs longitude) for nominal and with retargeting - energy optimal	140
Fig. 5.12. Position deviation from target at touch down (fuel-optimal).....	142
Fig. 5.13. Velocity deviation from target at touch down (fuel-optimal)	142
Fig. 5.14. Position deviation from target at touch down (energy-optimal)	143
Fig. 5.15. Velocity deviation from target at touch down (energy-optimal)	143
Fig. 5.16. Touch down (flight) time vs number of fuel-optimal simulations	144
Fig. 5.17. Landing mass vs number of fuel-optimal simulations	144

Fig. 5.18. Touch down time vs number of energy-optimal simulations	145
Fig. 5.19. Landing mass vs number of energy-optimal simulations	145
Fig. 5.20. Altitude, downrange and cross range profiles of energy-optimal simulations	146
Fig. 5.21. Velocity components – energy-optimal simulations	146
Fig. 5.22. Thrust direction variation for fuel-optimal and energy-optimal guidance scheme.....	148

LIST OF TABLES

Table 2.1 Summary of different solution schemes	30
Table 2.2 DE mutation schemes and sensitivity comparison	33
Table 2.3 Initial state parameters	34
Table 2.4 Initial co-states – comparison of converged values for solution scheme 1, 2 and 3	39
Table 2.5 Initial guesses and the sensitivity of solution – Scheme 3	40
Table 2.6 Comparison summary for solution schemes 1, 2 and 3	42
Table 2.7 Optimum landing mass with solution scheme 1 and 2 for different thrust level	43
Table 2.8 Evaluation of interpolation schemes	46
Table 2.9 Performance summary of solution scheme 4, 5 and 6	50
Table 2.10 Converged design using direct approach	50
Table 2.11 Performance of gradient based method with arbitrary initial guess (scheme 6)	51
Table 2.12 Performance of DE and PSO with wide guess of thrust direction angle rate	51
Table 3.1 Input parameters	75
Table 3.2 Unknown initial co-states for time-optimal trajectory using DE	76
Table 3.3 Time-optimal trajectory parameters	76
Table 3.4 Landing site of the time-optimal trajectory.....	76
Table 3.5 Determined initial co-states with single step using DT	77
Table 3.6 Influence of DT step size on DT scheme	78

Table 3.7 Influence of number of terms of series expansion (n) and step size on the DT scheme	78
Table 3.8 Time-optimal trajectory using multi-step DT-DE scheme	79
Table 3.9 Determined initial co-states using multi-step DT-DE scheme	81
Table 3.10 Comparison of computational time	81
Table 3.11 Unknown initial co-states – energy-optimal (unlimited thrust)	81
Table 3.12 Optimal trajectory – energy-optimal (unlimited thrust)	82
Table 3.13 Optimal trajectory parameters – energy-optimal with limited thrust	83
Table 3.14 Unknown initial co-states comparison – energy-optimal with limited thrust	84
Table 3.15 Optimal trajectory – fuel-optimal	85
Table 3.16 Unknown initial co-states – fuel-optimal	85
Table 3.17 Comparison of optimal solutions - DT-DE scheme	86
Table 3.18 Alternate landing site	87
Table 3.19 Comparison of optimal solutions	87
Table 3.20 Performance summary of energy-optimal: alternate landing sites	89
Table 3.21 Performance summary of fuel-optimal: alternate landing sites	89
Table 3.22 Comparison of computational time	90
Table 3.23 Comparison of solution schemes	90
Table 3.24 Target conditions	93
Table 3.25 Performance of the DT-DE scheme (fuel-optimal) for vertical landing	93
Table 3.26 Performance of the DT-DE scheme (energy-optimal) with terminal vertical thrust direction	94

Table 4.1 Sensitivity to Perilune altitudes for fuel-optimal trajectory	96
Table 4.2 Sensitivity to Perilune altitudes for energy-optimal (limited thrust) trajectory	96
Table 4.3 Input parameters	98
Table 4.4 Fuel-optimal DT-DE: touch down parameters with optimum initial true anomaly	99
Table 4.5 Energy-optimal formulation - touch down parameters with optimum initial true anomaly	101
Table 4.6 Fuel-optimal DT-DE : Touch down parameters with optimum initial argument of perilune (AOP).....	103
Table 4.7 Energy-optimal DT-DE : Touch down parameters with optimum initial argument of perilune (AOP).....	104
Table 5.1 Input parameters	123
Table 5.2 Optimal trajectory parameters and the resulting landing target	124
Table 5.3 Performance of DT Guidance scheme and Comparison with other schemes (Case 1).....	125
Table 5.4 Performance of DT Guidance scheme and Comparison with other schemes (Case 2).....	125
Table 5.5 Performance of polynomial guidance with fixed time-to-go (Case 1)	126
Table 5.6 Performance of fuel-optimal DT guidance with minimum thrust 40 %	130
Table 5.7 Optimal trajectory parameters – Fuel-optimal	132
Table 5.8 Performance of the fuel-optimal DT guidance scheme	132
Table 5.9 Performance of the energy-optimal DT guidance scheme.....	133

Table 5.10 Performance of the CTVG scheme	133
Table 5.11 Effect of higher thrust (2500 N) on guidance scheme and time-to-go strategy	135
Table 5.12 Assessment of retargeting capability (Retarget 1).....	137
Table 5.13 Assessment of retargeting capability (Retarget 2).....	137
Table 5.14 Assessment of fuel-optimal DT guidance for cross-range deviation	137
Table 5.15 Assessment of energy-optimal DT guidance for cross-range deviation	138
Table 5.16 Assessment of fuel-optimal DT guidance for retargeting at 7km	139
Table 5.17 Assessment of energy-optimal DT guidance for retargeting at 7km.....	139
Table 5.18 Dispersions for Monte Carlo simulation	141
Table 5.19 Summary of MC simulations for fuel-optimal DT guidance	141
Table 5.20 Summary of MC simulations for energy-optimal DT guidance.....	141
Table 5.21 Target conditions	148
Table 5.22 Performance of DT guidance schemes with terminal vertical thrust direction	148

ABBREVIATIONS

CFSQP	C and Fortran version of Sequential Quadratic Programing
CRS	Controlled Random Search
CTVG	Constrained Terminal Velocity Guidance
DE	Differential Evolution
DIDO	Direct and Indirect Optimization
DT	Differential Transformation
G-FOLD	Guidance for Fuel-Optimal Large Divert
GPOPS	General Purpose OPtimal Control Software
LVLH	Local Vertical Local Horizontal
MCI	Moon Centered Inertial
MISER	Software for Solving Optimal Control Problems
MPSP	Model Predictive Static Programing
NLP	Nonlinear Programming
POST	Program to Optimize Simulated Trajectories
PSO	Particle Swarm Optimization
RTN	Radial-Transversal-Normal
SOCp	Second Order Cone Programming
SQP	Sequential Quadratic Programming
TPBVP	Two Point Boundary Value Problem
ZEM	Zero Effort Miss
ZEV	Zero Effort Velocity

NOMENCLATURE

\mathbf{a}_T	Current thrust acceleration vector of module
\mathbf{a}_t	Target acceleration vector of module
\mathbf{r}_T	Target position vector of module
\mathbf{v}_T	Target velocity vector of module
Ω_p	Inertia parameter of PSO algorithm
A_z	Velocity azimuth, deg.
$C_1, C_2, C_3, C_4, C_5, C_6$	Guidance parameters (Coefficients) of thrust acceleration vector
a_{Tx}, a_{Ty}, a_{Tz}	acceleration components of thrust (T), m/s^2
\dot{m}	Mass flow rate, kg/s
m_0 and m_f	Initial and final mass, kg
p_{vx}, p_{vy}, p_{vz}	Co-state of velocity vector components
p_m	Co-state of mass
p_r	Co-state of radius
p_{vr}	Co-state of radial velocity
$p_{v\theta}$	Co-state of horizontal velocity
p_x, p_y, p_z	Co-state of position vector components
p_θ	Co-state of range angle
\mathbf{r}	Radius vector
r_{ave}	Average radius, m
r_c	Current radius of vehicle, m
r_f	Target radius of vehicle, m
r_p and r_G	Uniform random numbers between 0 and 1
t_0	Initial time, s
t_f	Final (flight) time, s
t_{go}	Time to go, s
\bar{u}	Control variables

\mathbf{v}	Velocity vector
v_c	Current velocity magnitude, m/s
v_f	Target velocity magnitude, m/s
v_x, v_y, v_z	Velocity components of lander module, m/s
v_\emptyset	Lateral velocity of lander module, m/s
v_r	Radial velocity, m/s
v_θ	Horizontal(transversal velocity), m/s
\mathbf{p}	Co-state variables
$\dot{\mathbf{p}}$	Co-state rates variables
\mathbf{p}_r	Co-state vector for position
\mathbf{p}_v	Co-state vector for velocity
\mathbf{v}	Lagrangian multiplier variables
ρ_c	Cross-range angle, rad
ρ_d	Down-range angle, rad
σ_{ub}, σ_{lb}	Upper bound and lower bound of unknown variables
ϕ_p and ϕ_G	Constants used in PSO algorithm
ϕ_t, λ_t	Target site latitude and longitude, deg.
ΔV	Ideal velocity, m/s
CR	Cross over probability
F	Objective function for optimization
F_m	Mutation factor
G_{best}	Global best solution
H	Hamiltonian
h	Current altitude, m
J	Performance measure
k	Thrust throttling parameter
k	Engine throttling parameter
L	Lagrange polynomial

m	Mass of the module, kg
n	Number of DT terms
NP	Number of DE population
P_{best}	Current best position vector among the swarm in PSO algorithm
$P_{current}$	Current Position vector of swarm in PSO algorithm
t	Current time, s
t_{burn}	Total burn time of engine, s
V_{upper}, V_{lower}	Upper bound and lower bound of velocity of particles of swarm in PSO algorithm
x_i, z_i, u_i	Solution vector (i^{th}) in DE algorithm
Ω	Right ascension of ascending node, deg.
I_{sp}	Specific impulse, s
P	Position vector of swarm particles in PSO algorithm
S	Switching function
T	Thrust, N
V	Velocity vector of swarm particles in PSO algorithm
e	Eccentricity of orbit
g	acceleration due to gravity of Earth (at sea level), m/s^2
i	Inclination of orbit, deg.
p	Magnitude of velocity co-states
r	Radius at the module location, m
x, y, z	Position components of module, m
α	In plane thrust angle, deg.
β	Out of plane thrust angle, deg.
μ	Gravitational parameter of moon, m^3s^{-2}
v	True anomaly, deg.
ψ	Terminal boundary condition vector
ω	Argument of periselenium, deg.

Chapter 1

Introduction and Literature Survey

1.1 Introduction

Space exploration is now moving towards planetary landing, asteroid landing and sample return collection etc. For planets like Mars that have an atmosphere, it is possible to decelerate the module using atmospheric braking. Landing on planetary bodies with a weak atmosphere is achieved by reducing the velocity to an acceptable limit at touch down using rocket engines with appropriate thrust level and suitable steering. Asteroid landing is similar to lunar landing mission. The difference lies in the gravity field due to a smaller asteroid size and it causes the possibility of vehicle rebound after touch down. The renewed interest shown by different nations on lunar missions, concentrates on search for water at the South Pole and helium and other minerals on the surface of the Moon. Establishing human habitats and lunar bases are other motives of lander missions. These lander missions rekindled the development of new methods of trajectory, guidance and control designs, robotics, propulsion system, navigation systems etc. The criticality of soft landing mission on a planetary surface is to identify appropriate mechanisms to slow down the lander module to acceptable limits at touchdown. For a successful mission it is important to land at a specified location using minimum fuel, which helps to carry more scientific payloads for planetary exploration closer to the area of interest. Therefore, it is essential to find the fuel-optimum thrust steering and the sequence of landing operations before the actual mission to ensure that all mission and vehicle related constraints are not violated and landing is executed successfully.

A lunar soft landing mission starts from a parking orbit (assumed to be 100 km circular) around Moon and with a de-orbit burn, the module is transferred to an elliptical transfer orbit with periapsis altitude varying between 30 km to 15 km. At a

pre-specified time (based on landing location), descent begins from the periapsis of the elliptical transfer orbit and ends at touchdown by reducing velocity to acceptable velocity level. This powered descent phase of trajectory is the focus of the current research. Generating fuel- optimal descent trajectory is the first requirement of any lander mission during mission planning phase. These open-loop schemes are not used in real-time because the navigation and propulsion dispersions result in deviations in the vehicle state. However, these open loop trajectories serve as reference trajectories for the development of closed loop guidance schemes. They provide the interim target states required for closed loop guidance algorithms. For the successful pinpoint landing at a selected target site, closed loop guidance algorithms play an important role. Towards realizing a successful mission, efficient methods to generate the optimal landing trajectory design and guidance design have been developed and discussed in this research.

1.2 Historical Perspective

The former Soviet Union executed many successful lunar missions starting from Luna 1 (1959) to Luna 24 (1976). A total of eight spacecraft landed on Moon and two of the landers deployed rovers. The Surveyor program of USA focused on unmanned lunar landings. The first lunar lander mass was about 300 kg. At about 96 km in altitude Surveyor was re-oriented (Cheng et al., 1966) and the propulsion system (non-throttleable) was fired continuously to reduce the velocity magnitude by 95%. At about 7 to 8 km altitude, the retro motor jettisoned and the vernier engines (throttleable between thrust of 130 N to 460 N) used for attitude control and to bring the remaining 5% (100 m/s) of velocity to near zero level. The Surveyor project was conceived as a preparation for human missions of the Apollo project.

The Apollo project includes six successful lunar landings on the Moon and one aborted mission (Apollo 13). Apollo 11 became the first human landing on the Moon. The Apollo mission had several phases during descent (Klumpp, 1974). The first phase of landing was to change the orbit size from 110 km circular to 110 km X 15 km

elliptical orbit. At 15 km, a powered descent initiation (PDI) was executed, resulting in continuous firing of the descent propulsion system (DPS). The second and third phases were approach and landing phases respectively designed for crew visibility and manual controllability. The nominal DPS burn time was 676 s and the vertical descent was from 30 m. The total mass of lunar module was about 15 t. The DPS had a maximum thrust of about 44.5 kN and it was capable of maximum 6 deg. gimbal motion for control and it was throttlable to about 10% of maximum thrust. Also it had 16 RCS thrusters of 445 N thrust level each for attitude control along with DPS. The Apollo and Surveyor landing sites are closer to flat visible equator region. However, the trends for future missions are to land at Polar Regions or in the far invisible regions and craters.

The Japanese Hiten satellite (Uesugi, 1996) orbited around Moon in 1990. NASA's Clementine mission (Nozette, 1995) in 1994 and the Lunar prospector in 1998 (Hubbard et al., 1998) provided a clear understanding of Lunar terrain and atmosphere. In November 2004, the first European spacecraft, SMART-1 (Foing et al., 2005), orbited around Moon. Later India's Chandrayaan and Moon Impact Probe (MIP) (AshokKumar et al., 2009) missions provided the valuable information of the lunar terrain and traces of water. LCROSS mission provided additional information of the south poles and traces of water (Ennico et al., 2012). China successfully landed on Moon twice (Donna Lu, 2020). These attempts help to speed up lunar exploration planning by several countries.

1.3 Literature Survey

The soft-landing mission can be direct descent from Lunar transfer trajectory or descent from Lunar parking orbit (Klumpp, 1968). The criticality in direct descent is the timing of Earth departure (lunar transfer injection) maneuver. In addition, the landing mission success is highly dependent on navigation instruments because of availability of very small time for correction maneuver (Klumpp, 1971). These limitations are overcome by the insertion of a module into a lunar parking orbit. In such missions, the landing site can be decided based on the observations of navigation and optical

instruments. Historically, all lunar landing missions followed the powered soft landing from a lunar parking orbit (Klumpp, 1974). In general, the optimal trajectories are generated with one of the following objectives (i) fuel-optimal (ii) energy-optimal (iii) time-optimal. However, most of the early lunar missions did not stress optimality.

Mason and Brainin (1962) generated the descent trajectory with the help of approximations. The main assumption involved is landing trajectory is constrained in a vertical plane with constant gravity. Cheng and Pfeffer (1962) provided a scheme for the generation of real time commands of soft landing trajectory and its sequence of execution during terminal descent phase. Cheng and Conrad (1964) provided the design aspects of terminal descent phase of trajectory of Surveyor mission addressing fuel requirement and sensor characteristics. Surveyor (Lunar) and Viking (Mars) mission used gravity turn concept for soft landing (Cheng et al., 1966). Gravity-turn concept requires the thrust vector of the module to be aligned opposite to the instantaneous velocity vector during the descent phase. The gravity turn law ensures that the module to be vertical on the lunar surface when velocity converges to zero. The main limitation of the algorithm is that the mission must start at higher altitude to ensure enough time for velocity braking. The advantage of gravity turn algorithm is that the velocity losses are minimum. The downside of the algorithm is that it is incapable of landing at a specified location and handling the retargeting capability. Another disadvantage (Sostaric and Rea, 2005) is that touchdown conditions are dependent on the initial conditions selected during gravity turn descent. Pinpoint landing using gravity turn concept requires the complete knowledge of perturbations during the trajectory and in turn, it requires the spacecraft to be at a specific initial state at the start of descent. The modified version of gravity turn algorithm was developed for descent from circular orbit with the approximation of constant gravity by McInnes (2003).

Cavoti (1966) solved the problem of minimum fuel soft lunar landing trajectory by approximating the powered braking phases into two. He derived closed form expressions for the soft-landing trajectory. Bennett and Price (1964) presented an

analytical study for lunar landing maneuver for a constant thrust level. The factors that influence the fuel-optimal performance are the altitude at the initiation of this phase and the thrust level used. The Apollo mission trajectory (Bennett, 1970) was not a truly optimal trajectory with respect to time or fuel. The focus was to achieve high probability of mission success and safety. In addition, the computational power was limited for both offline and real-time computations of trajectory and guidance design. Another limitation was the lack of information about the lunar terrain and the uncertainties in measurements. Hence, to enhance the safety aspects, during the terminal touchdown phase, the pilot assisted landings were followed to assist the landing site evaluation (Bennet, 1972).

Many numerical solution schemes have been explored in literature to generate an optimal powered braking trajectory since the first Apollo mission. Meditch (1964) presented an optimal thrust programming and trajectory design for terminal vertical landing phase and it was shown to be equivalent to minimum time problem. The thrust profile is a bang-bang thrust profile, which switches the thrust between minimum and maximum instantaneously. Bennet (1970) discussed the Apollo lunar landing mission design and he approximated the optimal trajectory as a polynomial for real-time usage.

Wilhite and Wagner (2008) analysed soft-landing mission strategies using POST software (Brauer et al., 1975). Many of the other landing trajectory design schemes are based on optimal control theory (Kirk, 1970; Bryson and Ho, 1975; Subchan and Zikowski, 2009). The optimal control problems are fundamentally different from the nonlinear static optimization problems since they involve unknown functions in time (control and state) and the dynamics of the process must be considered as constraints (Ben Asher, 2010). It is well known that an optimal control problem can be solved mainly by two approaches, (i) direct approach (ii) indirect approach. Different researchers (Betts, 1998; Rao, 2009; Conway, 2012) present comprehensive survey of different solution approaches. Topcu et al. (2007) formulated the problem of a fuel-optimal powered descent for terminal phase of Mars landing. The results showed that

the optimal thrust profile is a bang-bang profile and it stated that the proposed lander propulsion system must be capable of throttling between its minimum and maximum in 30 to 40 milliseconds.

In the direct approach, the optimal control problem is converted into a parameter optimization problem by discretizing the state and control variables (sometimes, state variables are obtained by numerical integration) and it is solved by Non-Linear Programming (NLP) approach. This method of discretization of state and control variables is called collocation scheme (Hargraves and Paris 1987; Stryk, 1993) and it is used for different space vehicle trajectory optimization. Two commercially, available software for collocation scheme of optimal control with gradient based solvers are DIDO (Gong et al., 2008) and GPOPS (Rao et al., 2010). They mainly use pseudo spectral methods to discretize the states and control variables at the selected nodal points along the trajectory. It is well known that the solution accuracy of direct approach depends on the number of nodes and their distribution. When the number of nodes increases, the number of unknowns also increases, making the problem computationally expensive. Further, a good initial guess of state and control variables at each node is essential for rapid convergence.

Vasik and Floberghagen (1998) formulated the soft landing problem in planar form using direct scheme and solved by using Newton's method. The SELENE orbiter and lander trajectory formulation using direct approach for different phases are provided by Kawakatsu et al. (1998). Park et al. (2011) presented a two-dimensional trajectory optimization for soft lunar landing considering a landing site. Also, the same problem was extended to three-dimensional motion and solved by Park and Tahk (2011) using sequential quadratic programming (CFSQP). In this paper, the equations of motion for the system dynamics is formulated in spherical (latitude, longitude and altitude) coordinates and it has singularity when latitude=90 deg. Tu et al. (2007) formulated the planar case of soft landing problem using direct collocation method and solved using nonlinear programming solver. Many authors (Hawkins, 2005; Mathavaraj

et al., 2017) have solved the lunar landing problem by using the software DIDO. Zhou et al. (2010) solved the soft landing problem as an optimal parameter selection problem using the optimal control software package MISER (Jennings et al., 1991). Huiping et al. (2017) used a direct scheme to find the optimal landing trajectory with constraints for a planar case. Henzeh Leeghim et al. (2016) computed the optimal terminal phase landing trajectory with a modified version of gravity turn. In MISER software, the control parameters are expressed as a linear combination of simple basis functions to reduce the computational complexity.

In the indirect scheme, the problem is transformed into a two-point boundary value problem involving the state and co-state variables and the related equations representing their variations. The control law is obtained as a function of time-varying co-state variables. Ramanan and Madan Lal (2005) solved the lunar soft-landing optimal trajectory in planar form using indirect approach. For trajectory optimization in the solution process, these authors used Controlled Random Search (CRS) a gradient free optimization technique.

Vasile et al. (2008) tested different global optimization algorithms for space trajectory design and compared their performances. The evolutionary optimization methods are found to be very powerful methods by Vasile and Minisci (2010) for solving complex aerospace engineering problems. Some of the methods are Genetic algorithms, Particle Swarm Optimization (PSO), Differential Evolution (DE), Simulated Annealing, Ant colony optimization etc. PSO (Venter and Sobieski, 2003) is an evolutionary computational algorithm based on the movement and intelligence of swarms. It is a gradient free stochastic search algorithm and it is suitable for dynamic optimization of continuous systems. Hassan et al. (2005) compare the performance of PSO with Genetic algorithm and concluded that PSO is better in terms of function evaluations. PSO was effectively used (Pontani and Conway, 2010; Pontani et al., 2012) for solving different aerospace trajectory design problems. PSO combined with pattern search algorithm was explored for propulsion system optimization related problem by

Jenkins and Hartfield (2012). DE is now becoming popular due to its convergence capability with lesser number of function evaluations. PSO and DE (Storn and Price, 1997) have fewer procedural steps and are easier to implement compared to Genetic algorithm. Olds et al. (2007) generated interplanetary mission opportunity using DE. It involves complex dynamics like multiple gravity assists and parking orbit considerations. These optimization techniques do not require initial guess of decision variables.

In the indirect approach, determining suitable values of initial co-state variables is a challenging problem. Many researchers attempted to find the initial co-states by introducing assumptions. Fahroo and Ross (2001, 2004) presented a Legendre pseudospectral method and Benson et al. (2006) presented a Gauss pseudo spectral method to find the co-state history. These studies attempted to solve the optimal control problem using direct approach by representing the problem as a nonlinear programming problem through pseudo spectral methods. As pointed out earlier, the number of unknowns depends on the number of nodes. Further, in these formulations, if the final time is unknown, the number and distribution of nodes also change depending on the change in the final time. Taheri et al. (2006) obtained the co-states using shape-based method for trajectory construction. The trajectory construction is carried out using constant thrust. These formulations are specific to some objective function and many of them are valid for minimum time problems only in which the final time is free.

In the current research, the Differential Transformation (DT) technique is employed to determine the initial co-states using the information about the required target site. The DT technique was proposed by Pukhov (1981) in which the solution of a differential equation is expressed as a series expansion of step size on the independent variable. The DT technique converts ordinary differential equations into algebraic equations, which are then computationally easier to solve. This technique has been used for solving a two-point boundary value problem by several authors (Hwang et al., 2008; Huang et al., 2009) when the final state and the time are known. However, for landing

at a target site problem, in general, the final state that represents the target landing site is known but the final time (flight time) is unknown.

The literature on the guidance design which is another important step in achieving a successful mission is abundant. Three different classes of guidance algorithms are mostly in use and they are open loop, explicit guidance schemes with analytical expressions and numerical algorithms. The open loop algorithm depends on the pre-loaded time/altitude/velocity dependent optimal thrust acceleration vector. The drawback of this scheme is that it does not account for the real-time state given by navigation for steering command generation and the dispersions of the propulsion system during the flight.

The explicit scheme uses the current state of the space vehicle and an analytical expression that generates the thrust acceleration vector to guide the space vehicle to the target vector. The advantage of this scheme is that it considers the current state obtained from navigation system. However, the derivation of analytical expression is based on some assumptions. Hence, these algorithms need to be checked extensively prior to flight.

Numerical algorithms are theoretically more robust but need more computational time when compared to explicit schemes. These algorithms must be used with extreme care because of the real-time computational risk related to convergence.

The requirement of guidance algorithm is computing the steering commands in real time to reach the target consuming minimum fuel. The computations should be simple so they can be implemented on-board for real-time use. The guidance computations need to be close to the optimal trajectory if fuel mass required is a major concern during the mission. Mainly guidance algorithms can be divided into open loop and closed loop algorithms. In an open loop mode of guidance, the trajectory steering command is generated offline and used in real-time with appropriate interpolations. Here, the target locations are planned prior to the mission and the freedom of target modification is absent. These modes are sensitive to real-time perturbations and not

suitable for landing that may require changes in target conditions. Closed loop guidance uses the current state information from navigation to compute the steering command to reach the desired location and this computation will repeat in every computational cycle.

The first real-time computation of thrust vector was based on a gravity turn concept (Cheng, 1964) and was used for the Surveyer landing. The main feature of this scheme, as discussed earlier, is that the thrust vector is oriented opposite to the instantaneous velocity vector. In this scheme, to nullify the velocity at touchdown, the guidance law needs to be initiated at an appropriate altitude of parking orbit, which depends on the maximum thrust level available. A guidance law based on gravity turn concept was investigated by McInnis (1995, 1996, and 1999). Viking landers (Ingoldby, 1978) and the terminal descent phase of Phoenix lander (Guo et al., 2012) used gravity turn guidance. A feedback guidance scheme was proposed by Citron et al. (1964) combining gravity turn concept and another algorithm to minimize the horizontal component of velocity. A planar case of fuel-optimal guidance law was proposed by Hall et al. (1963) and used for vertical landing for computing the pitch angle program for thrust orientation. This pitch steering angle was found to be sensitive to the initial altitude, maximum thrust level, and specific impulse and thrust to weight ratio.

Most of the research for guidance was during the Apollo era in the 1960s. Bennett and Price (1964) divided the powered descent phase of the Apollo landing trajectory into three phases for trajectory design and analysis and they are the braking phase, approach phase, and terminal descent phase. Klumpp (1971) provided different methods used for guidance, navigation, and control during the Apollo missions. The Apollo soft landing guidance design approximated the trajectory with polynomials and used variable thrust through throttling. This algorithm requires the information about current and target position, velocity and acceleration vectors and it guides the lander to a specified target state in specified flight time, popularly known as time-to-go (t_{go}). The

altitude at which powered descent starts and the parameter t_{go} are selected through extensive ground simulations.

The merits and demerits of polynomial guidance algorithm for the lunar pinpoint soft landing problem was presented by Guo and Han (2009) and it concluded that the polynomial guidance law could achieve precise pinpoint landing with appropriate t_{go} computation. Lu (2019) presented an augmented version of Apollo guidance algorithm. He introduced autonomous determination of suitable altitude for powered descent initiation and the parameter t_{go} in the near fuel-optimal algorithm. Another enhanced version of Apollo guidance algorithm was presented by Bishop and Azimov (2008).

Explicit guidance law generates the steering commands using the current vehicle state and the current target conditions. The time to reach the target conditions is computed in every computational cycle and the computations are performed until the time to go approaches zero. It generates the steering commands using polynomial or analytical expressions. One of the earliest explicit guidance algorithm, named E-guidance, was formulated by Cherry (1963, 1964) for the Apollo landing missions. It generates the required acceleration vector in every computational cycle for 3-DOF soft landing trajectory. Different versions of this algorithm exist and they are capable to land the vehicle at re-designated target locations. D'Souza (1997) presented a near optimal guidance scheme which is derived based on Pontryagin's maximum principle. This scheme optimizes the energy (control effort) instead of fuel to avoid computational complexities.

Ebrahimi et al. (2008) proposed a feedback guidance algorithm based on the concepts of Zero Effort Miss (ZEM) and Zero Effort Velocity (ZEV) for Mars soft landing. ZEM is the miss distance from the target if no guidance command acceleration is applied from current instant. ZEV is similar to ZEM concept applied to velocity. ZEM/ZEV based guidance algorithms with feedback control are presented by Wang et al. (2008). Based on these concepts, Guo et al. (2011) and Hawkins et al. (2011)

developed Constrained Terminal Velocity Guidance (CTVG). CTVG generates the required thrust acceleration profile using the terminal target boundary conditions of position and velocity vector with the assumption of constant gravity acceleration during the landing phase. ZEM/ZEV guidance algorithm was used for asteroid landing and proximity operations by Hawkins et al. (2012). Further modifications to ZEM/ZEV algorithm were proposed by Guo et al. (2013) to handle waypoint-optimized targeting. A modified version of the ZEM/ZEV guidance scheme (Je Liuyu, et al., 2014) was proposed for Mars landing by including a feature to handle constraints to avoid the impact on surface. This constraint is handled by including in the performance index for minimum control effort.

Lunghi and Lavagna (2015) proposed a semi analytical guidance scheme for lunar soft landing to compute the required acceleration command. This scheme represents the trajectory in polynomial form for the specified flight time. Lunghi et al. (2016) extended this semi-analytical guidance to make it adaptive guidance by using differential algebra. Shuang Li et al. (2016) presented a near fuel-optimal guidance algorithm and this scheme was used in Change E-3 mission. Steinfeld et al. (2010) presented the summary of guidance, navigation, and control technologies that could be used for pinpoint landing on Mars. An analytic optimal lunar trajectory was proposed by Li et al. (2010) by expanding the thrust acceleration, gravitational acceleration and the cosine of the vertical attitude angle to a high-order polynomial. The specified boundary conditions used to get the polynomial coefficients. A three-dimensional guidance algorithm was proposed by Ueno and Yamaguchi (1999) for SELENE mission with certain assumptions and approximations. The terminal landing velocity and altitude are specified as boundary conditions in this algorithm and the terminal landing point is not specified. A guidance algorithm for the terminal phase of lunar soft landing guidance was presented by Najson and Mease (2006) in which the solution of optimal control problem is expressed in analytical closed form. Mehedi and Kubota (2011) presented a guidance algorithm for a powered braking from orbital conditions by

approximating the centrifugal acceleration term and with constant acceleration due to gravity.

Uchiyama et al. (2002, 2005) proposed a jerk based lunar soft landing guidance algorithm and its implementation for real time usage. This algorithm is based on a simplified spacecraft dynamics, which incorporates various assumptions such as a flat lunar surface, a small variation of downrange angle and constant gravity model. An analytical expression for acceleration command during the terminal phase of a lunar landing was derived by Banerjee and Padhi (2017) with minimum jerk-based guidance.

Furfaro et al. (2011) proposed a non-linear sliding guidance algorithm for precision lunar landing and it had a base on non-linear sliding mode control theory (Won and Hedrick 1996). This algorithm generates the thrust acceleration command, which drives the deviation of vehicle position and velocity from the target (i.e sliding surface vectors) to zero in finite time. This non-linear sliding mode guidance algorithm was used by Furfaro et al. (2013) for landing on asteroid. Kozynchenko (2010) had formulated a planar guidance algorithm for a constant thrust magnitude based on a direct approach, which involves finding the solution of non-linear equations for selected boundary conditions. Banerjee et al. (2015) formulated the planar lunar soft landing guidance problem using a model predictive static programming (MPSP). MPSP converts the dynamic programming problem into a static optimization problem with flight time as unknown. The flight time is selected using a gradient based optimizer offline. MPSP based guidance algorithm formulated by Banerjee and Padhi (2020) was used to achieve the terminal position, velocity and terminal orientation requirement. The requirement of spacecraft terminal orientation is embedded in the guidance formulation as soft constraints.

Most of the numerical algorithms reported are in the context of Mars missions. Ploen et al. (2006) presented a survey of various Mars landing guidance schemes. D'Souza et al. (2014) presented a literature survey of past and present planetary entry

guidance algorithms and they categorized them based on the planetary atmosphere that the vehicle is entering. Gerth and Mooij (2014) consolidated a comprehensive review of various types of guidance algorithms. Wong et al. (2006) provided a guidance algorithm for Mars landing similar to the one used for the Apollo Lunar Module to guide the vehicle from its current state to the desired target state. The acceleration profile used to command thrust in that profile is linear in the vertical channel, and quadratic in the horizontal channel. Açıkmeşe and Ploen (2007) proposed a numerical algorithm that solves the terminal powered descent landing problem using direct approach of optimal control and convex optimization theory. In their study, the powered landing problem is converted to a convex optimization problem under certain assumptions. This convex optimization problem is then parameterized and converted into a second-order cone programming problem (SOCP) and numerically solved (proposed for on-board use). Numerical interior point optimization methods are used to solve the SOCP to find a global optimum along with another parameter to find with iterative scheme is optimal time-of-flight. The disadvantage of this scheme is that it needs a numerical solver and unreliable real time convergence capability. To overcome these issues, a scheme was proposed with an augmentation (Açıkmeşe et al., 2008) for generating a set of near optimal, preflight trajectories with different initial conditions. These trajectories were proposed to be used in a table look up form for on-board use. With this background, G-FOLD (Guidance for Fuel Optimal Large Divert) guidance (Blackmore et al., 2010) based on convex programming (Acikmese and Blackmore 2011) was presented for terminal phase of Mars landing. It has advantage of including many constraints, and the disadvantage is the requirement of a numerical solver. The retargeting capabilities of the algorithm and the convergence are yet to be demonstrated for real-time planetary landing applications. Lu et al. (2017, 2018) developed a fully numerical predictor-corrector numerical algorithm for entry guidance of mars missions. Lu et al. (2017) presented a fuel-optimal guidance algorithm, which solves the optimal control problem using indirect approach in the context of Mars landing. Rea et al. (2010) developed an analytical fuel-optimal guidance law assuming constant thrust for Moon landing problem.

Lee et al. (2010) presented the Altair Lunar lander guidance, navigation and control System schematic and preliminary details. Altair Lunar guidance algorithm (Lee, 2011) uses a polynomial to minimize the fuel usage and to maximize the landing point accuracy. The optimal trajectory profile of a lander with a cost function that penalizes both the touchdown velocity and the fuel cost of the descent engine is generated. In this formulation, achievement of a zero-touchdown velocity is not a requirement and only a touchdown velocity that is required to meet the landing gear design.

In many of the studies, the value for t_{go} is either computed based on extensive ground simulations and preloaded or computed in real-time on-board. Some approaches make an estimate of t_{go} assuming gravity turn trajectory and some solve a cubic or quartic equation to get an estimate.

1.4 Motivation of the Research

For safe and precise lunar landing in a pre-specified target location within specified accuracy limits, it is required to steer the lander module to the target site. For the survival of the module after landing it is required to bring the velocity to a near zero level from 1.7 km/s. With the Moon having very weak atmosphere, the reduction of velocity to zero must be achieved using chemical propulsion, which calls for minimizing fuel consumption. To achieve the fuel-optimal design of mission and trajectory, thrust vector need to be steered and throttled in an optimum way. The landing trajectory design problem is to find the optimum thrust-direction profile (in plane and out of plane directions), for maximizing the landing mass while transferring the module from a given parking orbit. Among the two basic approaches, the inherent well known complexities of the direct approach are: (i) number of discrete nodes decides the accuracy of the solution (ii) the dimension of the problem increases when number of nodes increased (iii) good initial guess for the unknowns etc. So, an indirect

approach is adapted for this research because it avoids the complexities of direct approach.

For the indirect scheme of solution approach, determining the unknown co-states is a challenging problem since they do not represent any physical phenomena. This is the major reason for the non-convergence encountered while using gradient-based methods through indirect approach. Many researchers have attempted to find the initial co-states by introducing assumptions. However, these methods are specific to certain objectives either to fuel-optimal or energy-optimal.

So, development of a method to determine the initial co-states, which is uniformly valid for all objectives viz. time-optimal, fuel-optimal and energy-optimal etc., is attempted. With the unknown co-states determined using Differential Transformation technique, the number of unknowns reduces to one viz. the flight time. This indirect approach based method leads to reduction in computational time.

The current research focusses on developing a new computational scheme, in which the computation of initial co-states is carried out using Differential Transformation technique. The DT technique needs a flight duration to determine the initial co-states. This flight duration is selected using the Differential Evolution technique. The scheme uses the pre-specified target state vector and the flight time selected using Differential Evolution for the computation of co-states. With the co-states determined using the DT technique, the soft-landing trajectory problem becomes easily and quickly solvable with reduced number of unknowns and the numerical integration of co-states is avoided.

Furthermore, two main observations based on the guidance algorithms reported in the literature can be made (i) fuel-optimal guidance is not addressed by many studies, especially under variable thrust, because of the theoretical complexity involved in deriving analytical design. Most of the studies are based on energy optimal approach (ii) all the guidance algorithms depend heavily on the parameter time-to-go ' t_{go} '. In many

of the studies, the value for t_{go} is either computed based on large ground simulations and preloaded or computed in real-time on-board. The current research is motivated to develop a fuel-optimal guidance scheme and analyze various mission scenarios. It is well known that the use of optimal control theory makes any guidance scheme robust. This motivated the use of optimal control theory to derive the fuel-optimal guidance laws and energy- optimal guidance laws as a function of co-states. In the proposed guidance scheme, the Differential Transformation (DT) technique is employed to determine the unknown co-states using the information on the current vehicle state (obtained from navigation), target landing site (loaded on-board apriori) and time to go. A simple strategy to compute t_{go} based on current and end states is introduced. The retargeting capability is another main feature of guidance.

1.5 Objectives of the Research

The main aim of the research work is to develop an optimal lunar soft landing trajectory design technique along with a real time implementable guidance scheme that meets the following objectives,

- i. Use indirect approach to avoid the complexities of direct approach. The determination of unknowns of this approach, although in small number, is challenging.
- ii. Reduce the number of unknowns for the trajectory design process for faster convergence.
- iii. Avoid any initial guess for the unknown variables involved for trajectory design process.
- iv. Develop a computational scheme, which is uniformly valid for all performance measures.
- v. Develop real time implementable computational fuel-optimal and energy-optimal guidance scheme. In addition, the scheme should be independent of any reference optimal trajectory and optimal flight time.

- vi. Develop a simple computational strategy to compute t_{go} based on current and end states.

1.6 Research Summary

At first, the soft landing trajectory design problem is formulated using different approaches and the resulting two-point boundary value problem (TPBVP) is solved using different optimization techniques. Two independent approaches i) direct ii) indirect are used to formulate the problem. Two of the gradient free (Particle Swarm optimization-PSO and Differential Evolution-DE) optimization techniques and a gradient based optimization technique (SQP) are explored to solve the problem for both direct and indirect approaches. In all, six solution schemes, each consisting of one of the approaches and one of the optimization techniques have been explored and evaluated. As is well known, the gradient based methods work well with good initial guesses on unknowns and the accuracy of the solution increases (control profile) with more number of discrete points. Among the gradient free methods (i) PSO (ii) DE, the performance of DE is found to be better in terms of number of function evaluations and computational time for both direct and indirect approaches.

The challenge in the indirect approach lies in finding suitable initial co-states with no prior knowledge available about them. In the above study, the number of unknowns are seven initial co-states and the flight time. In the second part of the research, an attempt to reduce the number of unknowns has been made. A new computational scheme that combines DT and DE techniques has been developed to realize the objective of reducing the number of unknowns. The co-states are computed using Differential Transformation (DT) technique, for a given flight duration. The unknown flight time is determined using the DE technique. DT is a recently proposed method in which the solution of a differential equation is expressed as a series expansion of step size on the independent variable. The DT technique converts ordinary differential equations into algebraic equations, which are then computationally easier to

solve. This novel computational scheme uses Differential Transformation in multi steps, to ensure the precise landing at the target site. In the DT-DE scheme, the major advantage is that the co-state equations need not be numerically integrated to find the control variables at each computational step. Furthermore, the number of unknowns reduces to one, the flight time. In a conventional indirect approach without DT, the numbers of unknowns are eight and numbers of equations are fourteen including the co-state equations. The robustness and validity of the proposed scheme is demonstrated for three popular objectives (i) energy-optimal (minimum control effort): a) with variable thrust; b) with limited thrust and throttling (ii) fuel-optimal: with limited thrust and throttling (iii) time-optimal: with limited thrust and throttling.

In the final part of the research, optimal analytical guidance schemes with objectives as (i) fuel-optimal (ii) energy-optimal are developed. These analytical schemes compute the time varying optimal thrust acceleration vector during the powered descent phase. First, the soft landing problem is transformed into a two point boundary value problem using Pontryagin's principle and the control laws for the three objectives are obtained. These control laws, which produce the optimal thrust acceleration components, are used in the proposed guidance scheme. In the control laws, the components of thrust acceleration at a time instant are dependent on instantaneous co-states. **The challenge of finding analytically suitable co-states, with no prior knowledge available about them, is handled.** In the proposed guidance scheme, the Differential Transformation (DT) technique is employed to determine the unknown co-states using the information on the current vehicle state (obtained from navigation), target landing site (loaded on-board a priori) and the flight time required to land from the current state.

The DT based approach provides a unified approach to handle all the performance measures in the context of guidance. For guidance scheme, the parameter time-to-go (t_{go}) is to be updated in real-time for the computation of thrust acceleration commands. In the proposed scheme, the parameter t_{go} is determined in real time. A

simple strategy is used to compute t_{go} based on current and end states. The real time computation of t_{go} helps the algorithm to guide the lander to the landing site even when the trajectory is nonlinear. The fuel-optimal and energy-optimal guidance schemes are compared for test cases and the fuel consumptions are quantified. **The advantage of this novel scheme is the fast computation of optimal real-time trajectory without any prior guess of initial co-states and it requires only the information on the current vehicle state with terminal state along with flight time.** The DT guidance scheme is an optimal fuel-optimal guidance scheme in closed form on which there are not many studies. Guidance schemes are evaluated for both limited and unlimited thrust cases. For thrust limit case thrust is assumed to be limited to some value and throttleable between a maximum and minimum level. The ideal navigation is assumed which is substituted by numerical integration.

1.7 Thesis Architecture

The current thesis has six chapters, which are outlined below.

- **Chapter 1:** This chapter introduces the topic of the research. A survey of the available literature for trajectory and guidance design schemes is consolidated. The limitations of the existing schemes, which motivated the current research, are discussed. The objectives of the research and a brief research summary are presented along with thesis architecture.
- **Chapter 2:** The problem of lunar soft landing is formulated and solved using different solution schemes. A formulation using planar dynamics is presented. Two evolutionary optimization methods i.e Particle Swarm Optimization (PSO) and Differential Evolution (DE) along with MATLAB based gradient optimization scheme are tested independently for solving the optimal control problem of lunar soft landing trajectory design. The details of six direct and indirect approach solution schemes and their merits and demerits are

highlighted. The evaluation of all schemes, results in the selection of an indirect solution scheme that uses Differential Evolution.

- **Chapter 3:** This chapter outlines the formulation of soft landing problem using three degree of freedom (3-DOF) system dynamics. The formulations of the optimal control problem using indirect approach (Pontryagin's principle) for different performance measures such as, energy-optimal (or minimum control effort), fuel-optimal, time-optimal are provided. This chapter also includes the details of a new scheme introduced to find the unknown co-states to compute the control history for the above mentioned performance measures. This new scheme that is based on Differential Transformation (DT) is described and the number of unknowns needs to be obtained using optimizer is reduced to one, i.e flight time. The single unknown (flight time) is selected using Differential Evolution(DE). The new technique named as DT-DE scheme that uses DT and DE to find the unknown co-states at different time instants during the descent phase of trajectory is presented. A comparison of DT-DE scheme with the other conventional techniques are briefly presented.
- **Chapter 4:** This chapter discusses the performance of DT-DE scheme to generate the optimal open loop trajectory for different mission scenarios.
- **Chapter 5:** This chapter includes the details of fuel-optimal and energy-optimal guidance methods using DT for real-time computation of instantaneous thrust acceleration vector. The unknown instantaneous time-to-go parameter is computed using a new technique which involves the downrange and cross range to be covered and current altitude at every computational step. The fuel-optimal and energy-optimal guidance schemes are compared and evaluated and the details are presented in this chapter. The proposed guidance schemes are compared with the other popular guidance schemes and the details are highlighted in this chapter. The performance of the scheme for retargeting is

discussed. The robustness of DT based guidance schemes is demonstrated using Monte Carlo analysis.

- **Chapter 6:** This chapter consolidates the major inferences for the proposed DT-DE trajectory optimization scheme and DT guidance schemes. The future scope of the research is also presented.

Chapter 2

Optimal Lunar Landing Trajectories and Solution Schemes

Chapter Summary

The problem of soft landing on Moon is formulated and solved using different solution schemes. Each solution scheme consists of one of the two approaches i) direct ii) indirect and one of different optimization techniques. Gradient free (Particle Swarm Optimization and Differential Evolution) and gradient based optimization techniques have been used to solve the problem through both direct and indirect approaches. In the indirect approach, the optimal control problem is transformed into a two-point boundary value problem (TPBVP) using Pontryagin's minimum principle and the appropriate initial co-states are selected using different optimization techniques. In the direct approach, it is transformed into a nonlinear programming (NLP) problem and is solved by using an optimizer. The performance of the direct schemes is compared with indirect schemes. A scheme based on the indirect approach and Differential Evolution technique is evaluated to be better than other schemes for the soft landing trajectory problem.

2.1 Dynamics of Landing Trajectory

As the main aim of this chapter is to evaluate different solution schemes and to select one for use in further research, planar motion for landing trajectory design is considered. The number of unknown design variables are less and so, it helps for quick evaluation of the solution schemes. Also, it provides deep insight for 3-DOF formulation and solver. The lander module is assumed to be a point mass (cf. Fig. 2.1). The vehicle state equations in radial transversal coordinates used for the trajectory simulation are as follows.

$$\dot{r} = v_r \quad (2.1a)$$

$$\dot{\theta} = \frac{v_\theta}{r} \quad (2.1b)$$

$$\dot{v}_\theta = \frac{-v_r v_\theta}{r} + \frac{T}{m} \cos(\alpha) \quad (2.1c)$$

$$\dot{v}_r = \frac{v_\theta^2}{r} - \frac{\mu}{r^2} + \frac{T}{m} \sin(\alpha) \quad (2.1d)$$

$$\dot{m} = -\frac{T}{g I_{sp}} \quad (2.1e)$$

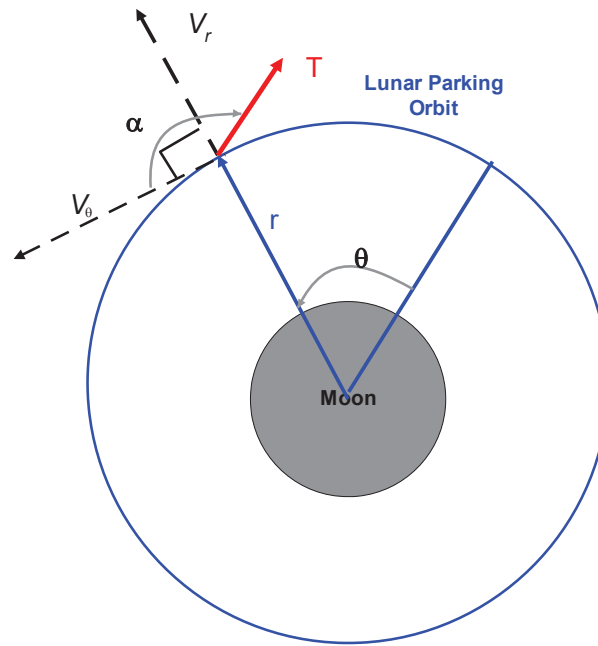


Fig. 2.1. Parameters for planar trajectory design

where r is radius at the module location; v_θ is the horizontal velocity; v_r is the vertical velocity; T is thrust level; m is mass; θ is the angle between the initial position and the current position (range angle) of space module and α is the angle from the local horizontal to the thrust direction. In the planar motion, the state vector is $[r \ \theta \ v_\theta \ v_r \ m]$. The following assumptions have been used.

- i. The tenuous atmosphere of Moon is ignored
- ii. Moon is assumed to be spherical and non-rotating.

- iii. Gravity perturbations due to the Earth and Sun are neglected.
- iv. Constant thrust and constant specific impulse assumed for planar case of trajectory
- v. Mass consumption is dependent only on constant propellant mass flow rate.

The constants used are:

- i. Lunar equatorial radius 1738000 m
- ii. Lunar gravitational parameter $4.902800476 \times 10^{12} \text{ m}^3/\text{s}^2$

The trajectory design problem is to find the thrust-direction profile, $\alpha(t)$, to maximize the landing mass while transferring the module from a given initial orbital conditions to the specified target conditions with the given constant thrust level and I_{sp} . This optimal control problem to find the optimal thrust steering formulated with direct and indirect approach. In indirect approach, the problem is transformed into a two-point boundary value problem using Pontryagin's principle and solved. The challenge in the indirect approach lies in finding suitable initial co-states with no prior knowledge available about them. To solve this problem an NLP solver and the Evolutionary optimization technique of Particle Swarm (PSO) and Differential Evolution (DE) are used and their performances highlighted.

2.2 Formulation of Optimal Control Problem – Indirect Approach

Because the mass consumption is dependent only on the constant propellant flow rate, the problem of maximizing the landing mass is equivalent to minimizing the time. The present problem is treated as a minimum time problem that results in a Lagrange problem. Accordingly, the performance measure is set as,

$$\min J = \int_0^{t_f} dt = t_f \quad (2.2)$$

The Hamiltonian is given by

$$H = 1 + \mathbf{p} [\dot{r} \ \dot{\theta} \ v_\theta \ v_r \ m]^T \quad (2.3)$$

The co-state variables are:

$$\mathbf{p} = [p_r \ p_\theta \ p_{v_\theta} \ p_{v_r} \ p_m] \quad (2.4)$$

The co-state rates variables are given by

$$\dot{\mathbf{p}} = - \left[\frac{\partial H}{\partial r} \quad \frac{\partial H}{\partial \theta} \quad \frac{\partial H}{\partial v_\theta} \quad \frac{\partial H}{\partial v_r} \quad \frac{\partial H}{\partial m} \right] \quad (2.5)$$

The co-state equations are :

$$\dot{p}_r = p_{vr} \frac{v_\theta^2}{r^2} + p_\theta \frac{v_\theta}{r^2} - p_{v\theta} \frac{v_\theta v_r}{r^2} - 2\mu \frac{p_{vr}}{r^3} \quad (2.6a)$$

$$\dot{p}_\theta = 0 \quad (2.6b)$$

$$\dot{p}_{v\theta} = -p_{vr} \frac{2v_\theta}{r} + p_{v\theta} \frac{v_r}{r} - \frac{p_\theta}{r} \quad (2.6c)$$

$$\dot{p}_{vr} = -p_r + p_{v\theta} \frac{v_\theta}{r} \quad (2.6d)$$

$$\dot{p}_m = \frac{T}{m^2} (p_{vr} \sin(\alpha) + p_{v\theta} \cos(\alpha)) \quad (2.6e)$$

The optimum thrust steering angle (α) is found by minimizing the Hamiltonian with respect to the control variable ' α ' at every instant of time.

$$\frac{\partial H}{\partial \alpha} = 0 \quad (2.7)$$

The optimal thrust angle is given by

$$\alpha = \tan^{-1} \left(\frac{p_{vr}}{p_{v\theta}} \right) \quad (2.8)$$

At the end of powered braking phase (at touch down), the velocity must be brought to near zero. So the terminal boundary conditions are given by Eq.(2.9).

$$\psi(t_f) = \begin{bmatrix} r(t_f) \\ \theta(t_f) \\ v_r(t_f) \\ v_\theta(t_f) \\ m(t_f) - (m_0 + \dot{m} t_f) \end{bmatrix} = \begin{Bmatrix} r_m \\ free \\ 0 \\ 0 \\ 0 \end{Bmatrix} \quad (2.9)$$

Where r_m is radius of the spherical Moon. Because the range angle at time t_f is free, we have $p_\theta(t_f) = 0$. Also, we have that its co-state rate is zero, i.e $\dot{p}_\theta = 0$. So, it leads to $p_\theta(t) = 0$, $\forall t \in [0, t_f]$. Furthermore, the Hamiltonian is not an explicit function of time and so it will be constant for all $t \in [t_0, t_f]$. The value of the Hamiltonian depends on the boundary conditions at the end of horizontal braking phase. The transversality (boundary) conditions are:

$$\left[\frac{\partial \psi^T}{\partial \mathbf{x}} \mathbf{v} - \mathbf{p} \right]_{t=t_f} d\vec{\mathbf{x}}(t_f) + \left[\frac{\partial \psi^T}{\partial t} \mathbf{v} + H \right]_{t=t_f} dt_f = 0 \quad (2.10a)$$

where $\mathbf{x} = [r \ \theta \ v_r \ v_\theta \ m]$; $\mathbf{v} = [v_1 \ v_2 \ v_3 \ v_4 \ v_5]$ is Lagrange multiplier variables associated with the terminal state constraints. An additional relation for the Hamiltonian is derived from the transversality conditions. Consider the second term in Eq. (2.10a). It is the boundary condition for the terminal time and because the final time is free,

$$dt_f \neq 0 \quad \text{and} \quad \left[\frac{\partial \psi^T}{\partial t} \mathbf{v} + H \right]_{t=t_f} = 0 \quad (2.10b)$$

$$H = - \left[\frac{\partial \psi^T}{\partial t} \mathbf{v} \right]_{t=t_f} \quad (2.10c)$$

$$\frac{\partial \psi^T}{\partial t} = (0 \ 0 \ 0 \ 0 - \dot{m}) \quad (2.10d)$$

$$H = v_5 \dot{m} \quad (2.10e)$$

The constant Hamiltonian depends on mass flow rate and the Lagrange multiplier for boundary conditions of mass (cf. Eq. (2.9)). To get the multiplier value use the first term from Eq.(2.10a). Because the final mass is free (final time free), we have,

$$\left[\frac{\partial \psi^T}{\partial m} v_5 - p_m \right]_{t=t_f} = 0 \quad (2.10f)$$

$$[p_m]_{t=t_f} = \frac{\partial \psi^T}{\partial m} v_5 = v_5 \quad (2.10g)$$

$$H = v_5 \dot{m} = [p_m]_{t_f} * \dot{m} \quad (2.10h)$$

Eq. (2.10h) provide additional help in verifying the optimal solution.

2.3 Solution of the Optimal Control Problem

Any optimal control problem can be solved using two approaches (i) Indirect approach (ii) Direct approach. In this study, both the approaches have been tried.

2.3.1 Indirect Approach

The time dependent control variable is a function of instantaneous values of the co-state variables (Eq. 2.8). If suitable initial value of co-states (at $t = 0$) are known

then the co-states can be propagated numerically and so, control variable can be determined. But the initial co-states are unknown. Because the Hamiltonian H is homogenous in co-state variables, it is possible to fix the initial value of one of the co-states. Also, we already have that the co-state of the state variable θ , p_θ is zero at $t = 0$. So there are only three unknown co-states and are found using an optimizer. Equation (2.9) presents the boundary conditions for the states and the cost function at the terminal time for optimal trajectory design problem, used in the optimization technique is set as

$$OBJ = (v_\theta - 0)^2 + (v_r - 0)^2 \quad (2.11)$$

The third variable ' $r(t_f)$ ' is used for terminating the numerical integration of the state variables. With the initial state and the co-state variables known (chosen by optimizer), the equations of motion (state and co-state) are integrated and the optimum thrust steering angle computed using the control law (Eq. (2.8)).

Three optimizers i) Particle Swarm Optimization ii) Differential Evolution iii) SQP of MATLAB have been used to solve this problem. So, three solution schemes have been explored through indirect approach. The functional block diagram for indirect approach is shown in Fig. 2.2.

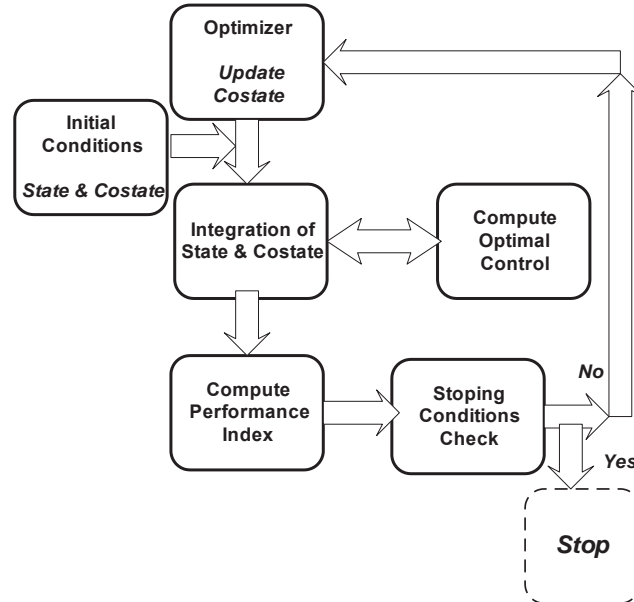


Fig. 2.2. Indirect approach schematic

2.3.2 Direct Approach

In this approach, the control variable is dealt without the help of co-state variables. The control parameter is selected at discrete time intervals and the state equation alone is numerically integrated (schematic is shown in Fig. 2.3). The solid line in Fig. 2.3 represents the state (radius) obtained by numerical integration. Another control variable is the final time since the flight time is unknown. The control parameters are interpolated between the time intervals. The performance of the scheme depends on the number of discrete time intervals at which control parameter is selected.

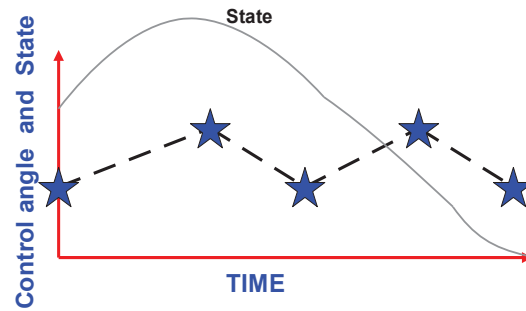


Fig. 2.3. Direct approach schematic

For the soft landing problem, the control variable is set as the rate of change of the control variable (thrust direction angle). With a guess on initial thrust direction angle ($@time = 0$) and guessed angular rates at different times, thrust direction angles are computed at different time intervals. For the interpolation of rates at timings different from the discrete times, linear and Lagrange interpolation methods are explored. A fourth-order Runge–Kutta (RK4) method is used for the propagation of the state equations. The guesses on the thrust angle rates are updated using an optimizer. As discussed in the previous section three optimization techniques have been used to generate the solution using the direct approach.

2.3.3 Solution Schemes

The soft landing problem is solved (to find appropriate initial co-state or control angle history) using different solution schemes listed in Table 2.1. Each solution scheme consists of one of the two approaches and an optimizer.

Table 2.1 Summary of different solution schemes

Soft Landing Trajectory Design Problem		
Solution Scheme	Approach	Optimizer Selected
Scheme 1	Indirect	PSO
Scheme 2	Indirect	DE
Scheme 3	Indirect	MATLAB (SQP)
Scheme 4	Direct	PSO
Scheme 5	Direct	DE
Scheme 6	Direct	MATLAB (SQP)

2.4 Optimization Techniques

Most of the traditional optimization techniques calculate the first derivatives to locate the optima on a given constrained surface and the second derivatives are used to establish the optimality. To overcome the difficulties in evaluation of the first and the second derivatives for discontinuous optimization spaces, several derivatives-free optimization methods have been developed in recent time. In the present study, Particle Swarm Optimization (PSO) and Differential Evolution (DE) techniques are used to solve the soft landing trajectory optimization problem and the results are compared. Also MATLAB based gradient constrained optimization (SQP) is tried to solve the problem with initial guess from PSO/DE. The different optimization techniques are briefly discussed below.

2.4.1 Particle Swarm Optimization (PSO)

In PSO algorithm, a number of swarms (possible solution vector) are considered in the design space and these swarms are moving with their own individual experience and the experiences of other particles. Every particle will keep track of its position (P) and velocity (V) and it will move according to the best solution (fitness) achieved (Venter and Sobieski, 2003). Another value that is tracked by the PSO is the best value (G_{best}) achieved so far by any particle. The concept lies in changing the velocity of each particle toward its P_{best} and the G_{best} position at each step. Each particle tries to modify its current position and velocity according to the distance between its current position and P_{best} , and the distance between its current position and G_{best} .

$$P_{n+1} = P_n + V_{n+1} \Delta t \quad (2.12)$$

where P_n, P_{n+1} : position of particle at n^{th} and $n+1^{th}$ iteration, V_{n+1} : particle velocity at $n+1^{th}$ iteration. $\Delta t = 1$ (unit time step); The velocity update is given by

$$V_{n+1} = \Omega_p V_n + \frac{\phi_p r_p (P_{best} - P_{current})}{\Delta t} + \frac{\phi_G r_G (G_{best} - P_{current})}{\Delta t} \quad (2.13)$$

where Ω_p is the inertia weight $=(r_u+1)/2$; r_u is a uniform random number between 0 and 1 and controls the momentum of particles by weighting the contribution of the previous velocity; r_p and r_G are the uniform random numbers between 0 and 1; ϕ_p and ϕ_G are constants that fix how much the particles directed towards good positions. In the current problem after few trials, the values have been fixed at 1.5 for both ϕ_p and ϕ_G which results in faster convergence. Similarly, the swarm population size is fixed at 40. The termination criteria for PSO is fixed based on number of iterations or by keeping track of global best solution or the particle positions. If all particles converge to a same feasible point, then the global optimum is ensured. The unknown values of position of particles (initial co-states in this problem) are chosen from predefined bounds.

$$X = r_u (\sigma_{ub} - \sigma_{Lb}) + \sigma_{Lb} \quad (2.14)$$

where σ_{ub} and σ_{lb} are the upper and the lower bound and r_u is the uniform random number between 0 and 1. PSO velocity vector is defined as

$$V_{upper} = (\sigma_{ub} - \sigma_{lb}) \quad (2.15)$$

$$V_{lower} = -V_{upper}$$

Initialization of the velocity of the particles is as follows,

$$V = r_u(V_{upper} - V_{lower}) + V_{lower} \quad (2.16)$$

Equation (2.16) provides the initial velocity of the particles and Eq.(2.13) provides the velocity updates in subsequent iterations. The advantages of the PSO scheme are the initial guess is not necessary and there are only few algorithm parameters for tuning.

2.4.2 Differential Evolution (DE)

This algorithm has three steps namely mutation, crossover and selection. Mutation will expand the search space by adding the difference between two individual population members to a base element (Storn and Price, 1997). DE randomly selects two population vectors x_2 and x_3 and makes use of the difference between them with a scaling factor (F_m) to mutate x_1 . Some of the popular mutation schemes are presented in Table 2.2 along with the performance for the soft landing trajectory design problem. Performance of mutation scheme 3 in terms of function evaluations and the CPU time required is better than other schemes. The results are generated according to third mutation scheme. The mutation factor F_m is fixed at 0.8 and the population size is fixed at 30 after a few trial runs with the present problem.

Table 2.2 DE mutation schemes and sensitivity comparison

S.no	Mutation Scheme	Mutation	No. of function evaluation required	CPU time (s)
1	DE/rand/1	$z_i = x_1 + F_m (x_2 - x_3)$	4085	1290
2	DE/best/1	$z_i = x_{best} + F_m (x_2 - x_3)$	2734	987
3	DE/rand to best/1	$z_i = x_1 + F_m (x_2 - x_3) + F_m (x_{best} - x_3)$	2397	764
4	DE/rand/2	$z_i = x_1 + F_m (x_2 - x_3 + x_4 - x_5)$	4426	1412
5	DE/best/2	$z_i = x_{best} + F_m (x_2 - x_3 + x_4 - x_5)$	3594	1076

After the mutation, a binominal crossover operates on the selected vector z_i to expand the diversity of the population. The purpose of this phase is to mix the successful solutions from the previous generation with the current vector. This is done as follows:

$$u_i = \begin{cases} z_i & \text{if } r_i \leq CR \\ x_i & \text{otherwise} \end{cases} \quad (2.17)$$

CR is the cross over probability which is usually set a fixed value between (0, 1) and in the present case it is set as 0.9 and r_i is a uniform random number between 0 and 1.

In the third step i.e selection, u_i is compared with x_i based on function evaluation and the one with better function value will be selected to be a member of DE population for the next generation. The selection scheme is as follows

$$x_i^{k+1} = u_i^k \quad ; \quad \text{if } f(u_i^k) < f(x_i^k) \quad (2.18a)$$

$$x_i^{k+1} = x_i^k \quad ; \quad \text{if } f(u_i^k) \geq f(x_i^k) \quad (2.18b)$$

In the first step of Differential Evolution technique, an initial population of a fixed size (NP) is built. If there are 'N' unknown variables, the population matrix is of the size NP x (N+1). Of the N+1 elements of each row, first 'N' of them are unknown variables selected randomly from their respective bounds according to uniform distribution and the (N+1)th element is the objective function value. The set of randomly selected unknowns are used to evaluate the objective function at touchdown after numerical propagation. In the second step, each row (say z_i) of the population undergoes three operations: mutation, crossover and selection and a new set of elements

is constructed. These two steps are repeated until the value of objective function is less than a prefixed small tolerance value.

2.4.3 Gradient Based Optimizer (SQP)

The Sequential Quadratic Programming (SQP) is used in the current research and the function ‘fmincon’, a built in MATLAB function for constrained optimization, is utilized in this study. Apart from SQP, the function ‘fmincon’ has provision to use other methods such as (i) active-set (ii) interior point (iii) trust-region-reflective. It finds the constrained minimum of a function of several variables (Venkataraman, 2009). The function requires initial guesses of the unknown variables along with their bounds (lower and upper). The search starts from initial guess and moves towards the optimum. The initial guess must be provided within the parameter bounds. It uses finite differences to compute the gradients and Hessian using the selected unknown parameters within the bounds. It uses one of the four methods (user selected) to update the initial guess. The user needs to supply the maximum number of function evaluations and tolerance level of objective functions.

2.5 Results and Analysis

The initial mass is set as 880 kg in a 100x 100 km orbit with engine thrust level of 2200 N and I_{sp} of 315 s. Typical initial conditions for a planar case are provided in Table 2.3

Table 2.3 Initial state parameters

Parameter	Value
Radius - m	1753000
Horizontal velocity (v_θ) – m/s	1692
Vertical Velocity (v_r) – m/s	0.0
Range angle (θ)– deg.	0.0
Mass at 100 x 100km orbit (kg)	880
Mass at 100 x 15km orbit (kg)	874.4

The terminal boundary conditions to be achieved are:

$$\begin{bmatrix} r(t_f) \\ v_r(t_f) \\ v_\theta(t_f) \end{bmatrix} = \begin{cases} 1738.003 \text{ km} \\ 0 \text{ m/s} \\ 0 \end{cases} \quad (2.19)$$

2.5.1 Performance of Indirect Schemes

The initial co-states are selected by using PSO, DE and SQP independently and their results have been compared. To ensure consistency, the codes for PSO and DE have also been implemented in the MATLAB environment. Three results match very closely (Fig. 2.4) and the maximum difference in altitude between the schemes is about 0.08m. It is to be noted that for scheme 3 (gradient based scheme) requires a good initial guess and bounds for unknown variables for convergence. The sensitivity to the initial guess for scheme 3 is discussed in a separate subsection. Fig. 2.5 and 2.6 shows the comparison of horizontal and vertical velocity. Fig. 2.7 depicts the optimum thrust direction angle for safe landing. During the descent phase, the optimum control angle varies from 180 to 145 deg. The initial co-state for mass is fixed at one and the other appropriate co-states are selected using the optimizer. Fig. 2.8 and 2.9 show the Hamiltonian and co-state variation for the optimal trajectory design. Clearly, the Hamiltonian is constant on the optimal trajectory, since it is not an explicit function of time. The optimum converged values of the initial co-states are listed in Table 2.4 for solution scheme 1, 2 and 3.

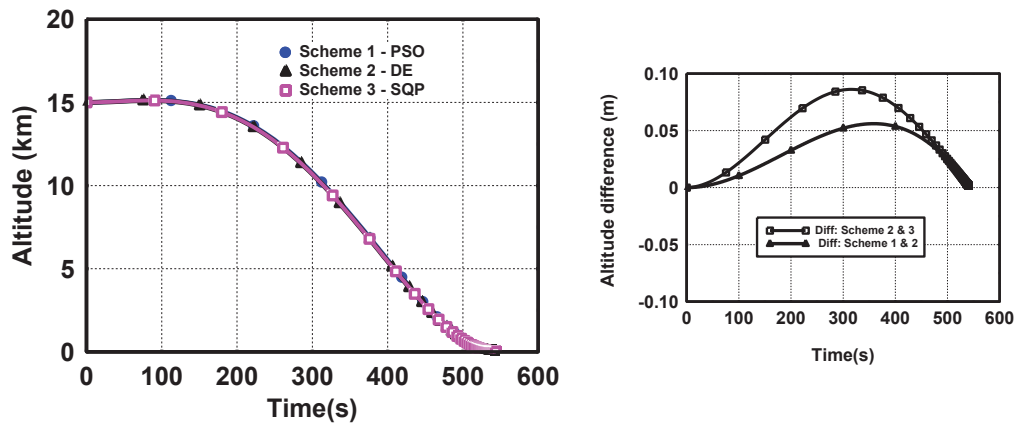


Fig. 2.4. Altitude profile with solution scheme 1,2 and 3

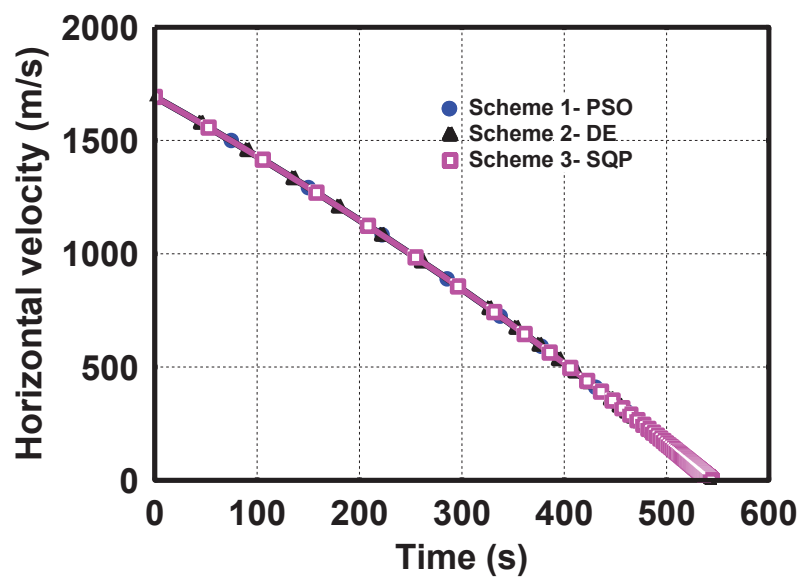


Fig. 2.5. Horizontal velocity vs time with solution scheme 1,2 and 3

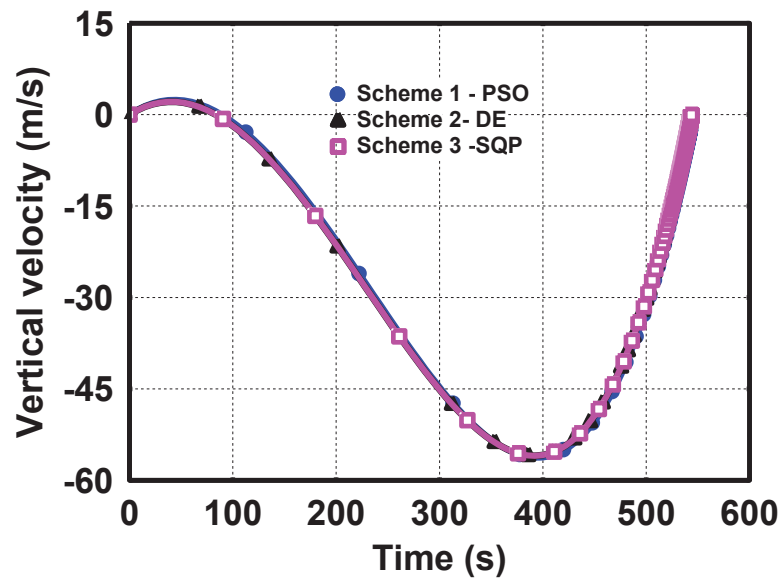


Fig. 2.6. Vertical velocity vs time with solution scheme 1,2 and 3

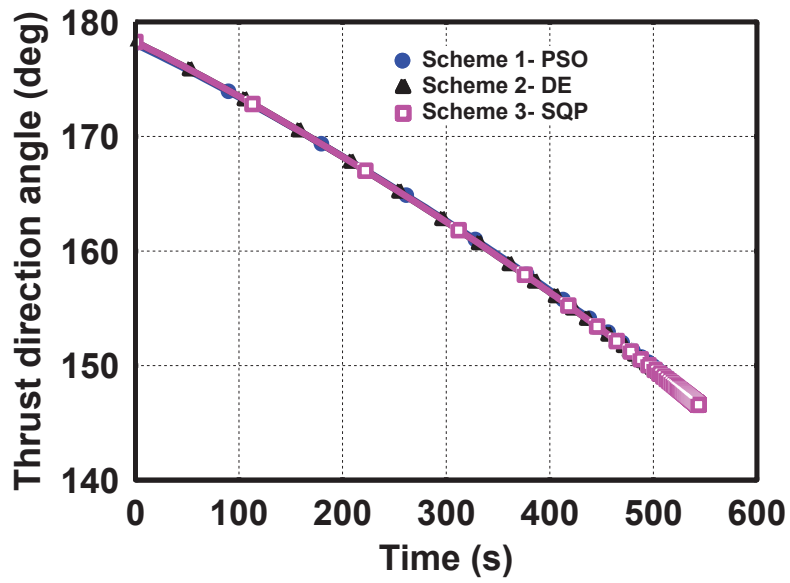


Fig. 2.7. Optimum thrust direction angle with solution scheme 1,2 and 3

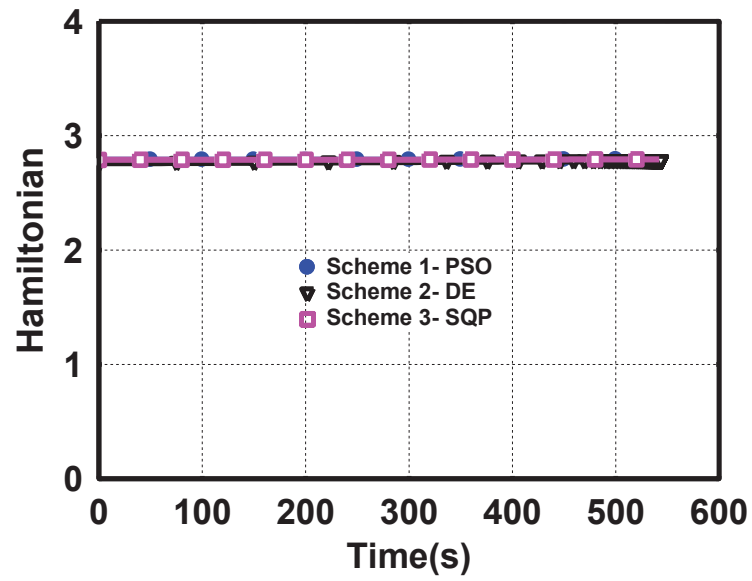


Fig. 2.8. Hamiltonian variation with solution scheme 1,2 and 3

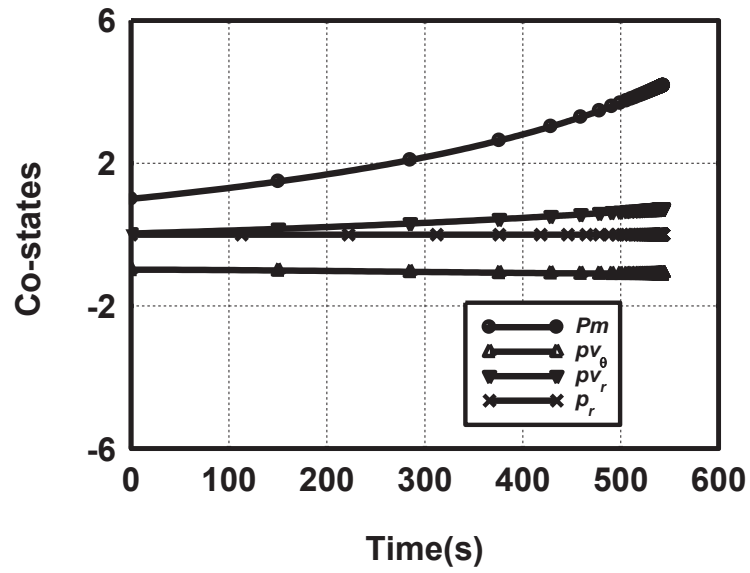


Fig. 2.9. Co-state variation for optimal trajectory –Scheme 2

Table 2.4 Initial co-states – comparison of converged values for solution scheme 1, 2 and 3

Co-state	Optimizer		
	PSO Scheme - 1	DE Scheme -2	SQP (with close initial guess) Scheme -3
p_m	1	1	1
p_r	-0.001589	-0.001588	-0.001577
p_{v_r}	0.027866	0.027865	0.027855
p_{v_θ}	-0.907962	-0.907960	-0.907957

2.5.1.1 Implication of Initial guess on Convergence of Gradient Based Scheme (Solution Scheme 3)

Figure 2.10 shows the optimal thrust direction variation with time for SQP with different initial guesses to assess the sensitivity of the solution. If the initial guess is widely off from the solution, SQP does not converge. Also, when the initial co-state guess far-away from the actual value the thrust direction angle profile shows the sudden variation of about ± 180 deg. This discontinuity leads to the non-convergence of gradient based scheme. Table 2.5 provides the sensitivity of the solution to the initial guess and the converged co-states for Scheme 3. Four different initial guesses considered for SQP are provided in Table 2.5. The bounds for all these initial guesses is set as ± 1 . With the initial guess sets ig_1 and ig_2 , convergence did not happen because of high sensitivity of the solution to the low magnitude co-states. With the close initial guess (ig_4), SQP converges (cf. Fig.2.10) and the results match well with scheme 1 and 2. It is well known that arriving at good initial guess for a completely new problem will require numerous iterations and sometimes even after iterations solution may elude.

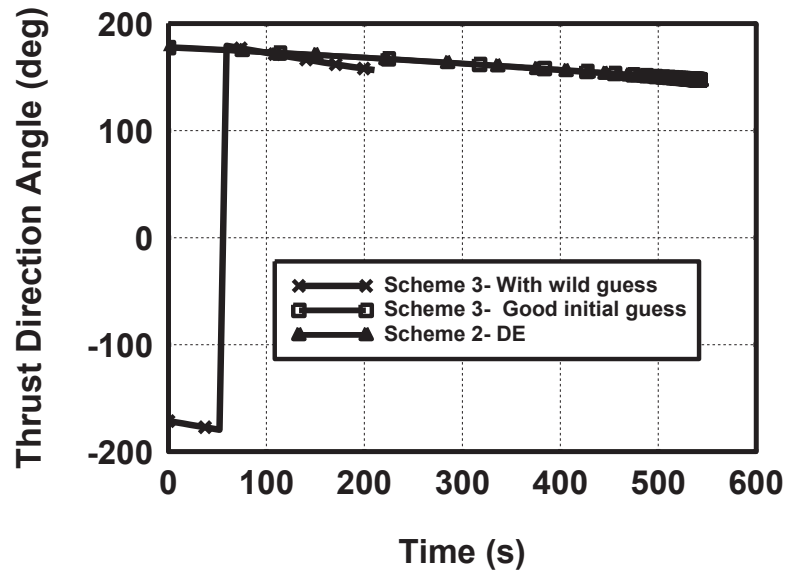


Fig. 2.10. Optimum thrust direction angle – comparison of solution Scheme 3 sensitivity with initial guess

Table 2.5 Initial guesses and the sensitivity of solution – Scheme 3

Initial guess No	Initial guess and Converged co-states			Landing mass (kg)
	p_r	p_{vr}	$p_{v\theta}$	
ig ₁	1.0	1.0	1.0	Not converged
ig ₂	0.01	0.1	-1.0	Not converged
	-0.003657	-0.150808	-0.996084	
ig ₃	-0.002	0.03	-1.0	485.6
	-0.00175	0.0287	-0.973	
ig ₄	-0.0016	0.026	-0.91	486.924
	-0.001577	0.027855	-0.907957	

2.5.2 Comparison of Indirect Schemes

Table 2.6 summarizes the performance of the schemes 1 and 2 for two sets of bounds on initial co-states (i) ± 1000 (ii) ± 1 and the performance of the scheme 3 for the initial guess ig₄. The PSO technique requires more computational time than DE, while the optimum landing mass and flight time are very close (the problem has a unique solution). As is well known, SQP requires good initial guess as well as close bounds to

achieve convergence. Figure 2.11 shows the cost function variation for the two-optimization schemes, Scheme 1 and 2 for initial co-state bounds of ± 1000 .

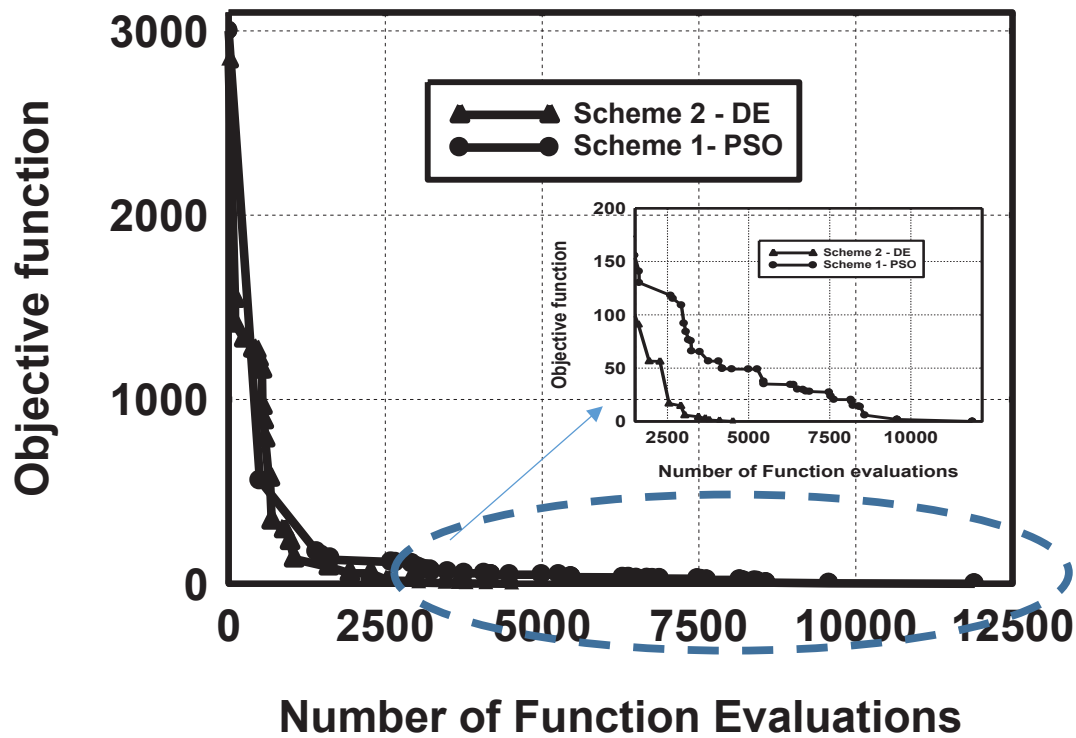


Fig. 2.11. Comparison of solution schemes 1 and 2

Note that both PSO and DE converge even for a very wide bound on the initial co-states. If the bounds on the co-states are restricted to ± 1 , there is a 30 to 50% reduction in number of function evaluations and the computational time. The DE technique clearly performs better than PSO in terms of number of function evaluations for convergence and computation time for both the sets of bounds on the co-states.

Table 2.6 Comparison summary for solution schemes 1, 2 and 3

Optimizer	Optimum landing mass (kg)	Optimum flight time (s)	CPU time required (s)		Number of function evaluations	
			Co-state bounds ± 1000	Co-state bounds ± 1	Co-state bounds ± 1000	Co-state bounds ± 1
PSO-Scheme 1	486.924	544.086	3312	1586	11898	7689
DE-Scheme 2	486.925	544.085	1120	764	4512	2397
SQP (with closer initial guess (ig_4)) - Scheme 3	486.924	544.086	No convergence	712	No convergence	2007

If the initial guess for SQP is closer to a global minimum, the convergence will be faster than PSO and DE. In indirect approach a good guess of co-states is not possible and so, the performance of the gradient based scheme cannot be compared with PSO and DE. With the results of the above cases, it can be concluded that PSO and DE are capable of locating the global minimum while DE requires less number of function evaluations and hence less time for convergence. So, scheme 2 is selected out of the three indirect schemes for further analysis.

2.6 Optimal Landing Trajectories with Different Initial Thrust to Mass Ratio

The soft landing optimal trajectory design is generated with various constant thrust levels for powered braking maneuver represented by initial thrust to mass ratio. The initial mass is set as 880 kg and I_{sp} is 315 s.

The number of function evaluations and the computational time are provided in Table 2.7 for Scheme 1 and Scheme 2 by varying initial thrust to mass ratios between 1 and 3. The number of function evaluations required to generate the optimal solution is insensitive with different thrust to mass ratio. Figure 2.12 shows the altitude variation with different constant thrust levels. The plot shown corresponds to the design with the DE technique (scheme 2). The PSO results (solution scheme 1) are very close hence it is

not shown. The altitude rise and the time required for soft landing depends on the thrust level. If thrust level increases the flight time required for soft landing reduces and also the peak altitude. It can be concluded that with sufficient energy available for braking, the rise in altitude is minimum. Figure 2.13 shows the thrust direction profiles for different thrust levels. With the reduction in the thrust levels the nonlinearity of the solution (thrust direction angle profile) decreases except for the thrust to mass ratio of one.

Table 2.7 Optimum landing mass with solution scheme 1 and 2 for different thrust level

Initial thrust to Mass ratio	Optimum landing mass (kg) and flight time (s).		Number of function evaluations and CPU time required (s)	
	Scheme 1- PSO	Scheme 2- DE	Scheme 1- PSO	Scheme 2- DE
1.0	385.71 (1715.5)	385.72 (1715.46)	7896 (2169)	2534 (1265)
1.5	457.296 (976.253)	457.3 (976.2)	7738 (1984)	2498 (1078)
2.0	479.2 (693.6)	479.2 (693.6)	7630 (1821)	2420 (877)
2.5	486.924 (544.086)	486.925 (544.085)	7689 (1586)	2397 (764)
3.0	491.7 (447.7)	491.7 (447.7)	7525 (1367)	2278 (723)

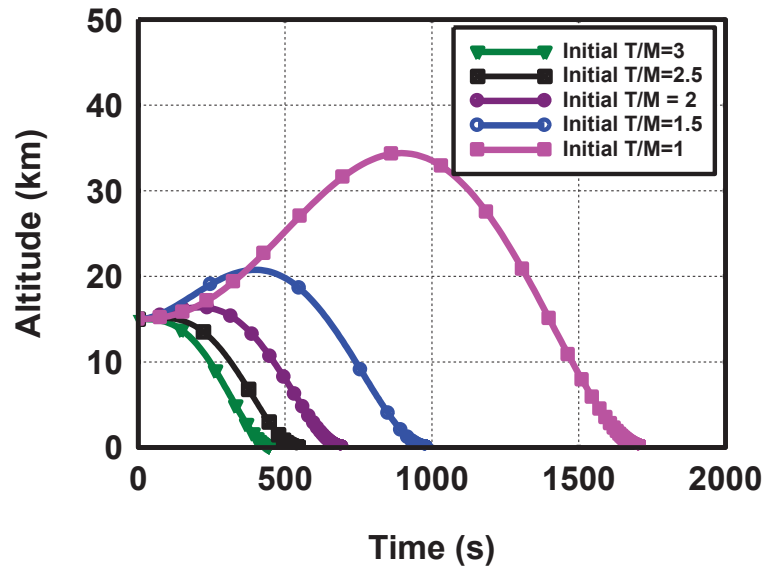


Fig. 2.12. Altitude variation with different thrust levels

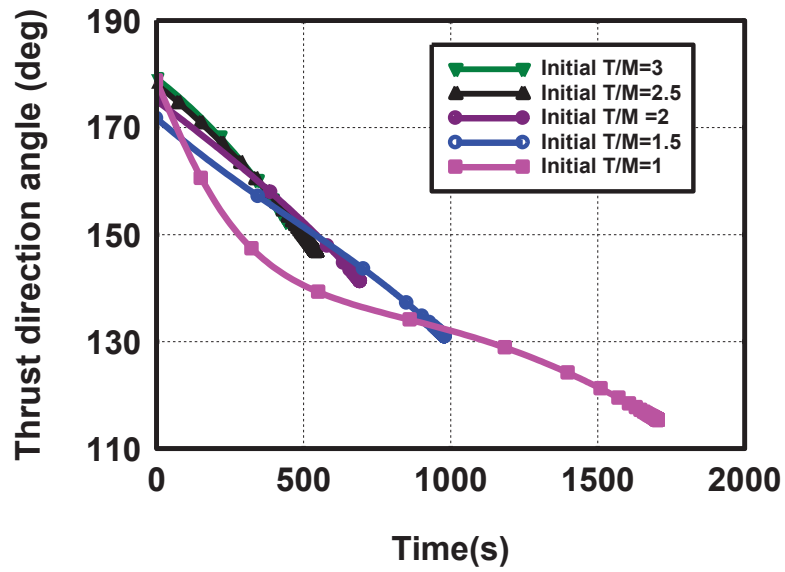


Fig. 2.13. Optimum thrust direction angle for different thrust levels

2.7 Results using Direct Approach Based Schemes (4, 5 and 6)

In the present case, initial control angle (@time=0) and thrust direction angle rates at different time instants are the unknown design variables and selected using the optimizer. The angular rates are interpolated at different time steps to find the

instantaneous control angle. The performance of the direct approach is dependent on the interpolation method used to compute the control angles at different nodes. An optimal landing trajectory is generated using direct scheme 5 and the solutions are generated using linear and Lagrange interpolation techniques. The solutions are compared with the solution of scheme 2. It is found that when Lagrange interpolation scheme is used the results are very close to the solution of indirect scheme compared to linear interpolation scheme. The optimum thrust angle is plotted in Fig.2.14. Five thrust angle rates (at different time intervals) are selected for linear interpolation whereas for Lagrange interpolation three thrust angle rates are found to be sufficient to get close match with the indirect approach (cf. Table 2.8). So, for further analysis, Lagrangian interpolation method is adapted. A brief account of Lagrange interpolation is provided below.

Lagrange polynomial interpolation involves finding a polynomial of order 'N' that passes through the 'N+1' data points. Let x_i and y_i - vectors of (N+1) data values. N is the degree of interpolation polynomial which represents the function $y=f(x)$. The data points are $(x_0, y_0), (x_1, y_1), (x_2, y_2) \dots (x_N, y_N)$. The Lagrange interpolating polynomial is given by

$$f_N(x) = \sum_{i=0}^N L_i(x) f(x_i) \quad (2.20a)$$

$$L_i(x) = \prod_{\substack{j=0 \\ j \neq i}}^N \frac{x - x_j}{x_i - x_j} \quad (2.20b)$$

where $L_i(x)$ is a weighting function that includes a product of $N-1$ terms except $j=i$.

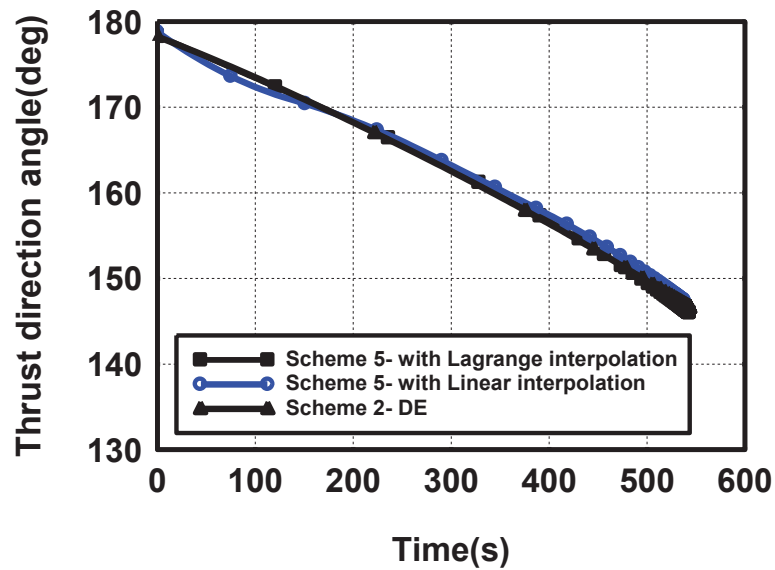


Fig. 2.14. Direct approach solution sensitivity with interpolation methods

Table 2.8 Evaluation of interpolation schemes

Solution Scheme	Interpolation scheme of thrust angular rates	Converged values of thrust angular rates at discrete time interval (deg/s)	Flight Time (s)	Landing Mass (kg)
Scheme 5	Linear with 5 angular rates	-0.026149 -0.026953 -0.027853 -0.039853 -0.044462	544.088	486.918
Scheme 5	Lagrangian	-0.027149 -0.027253 -0.047462	544.086	486.924

The performance of Schemes 4, 5 and 6 is assessed in terms of altitude profile (Fig. 2.15) and thrust direction profile (Fig. 2.16). The altitude profiles for the schemes 4, 5 and 6 are very close. It is experienced that for SQP, the initial guess must be very close to the solution along with close bounds for the unknowns for quick convergence. Figure 2.17 and 2.18 show the horizontal velocity and the vertical velocity variations on the optimal trajectory.

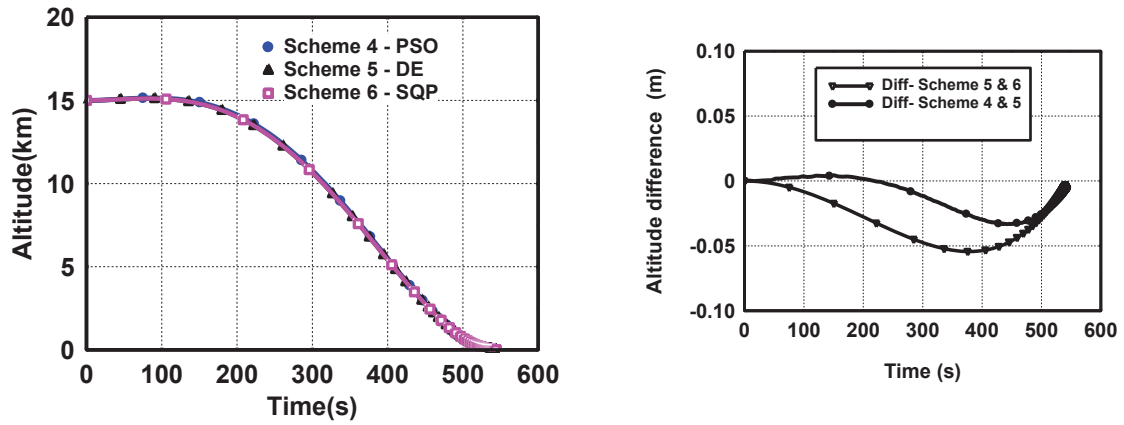


Fig. 2.15. Altitude profile comparison for solution scheme 4, 5 and 6

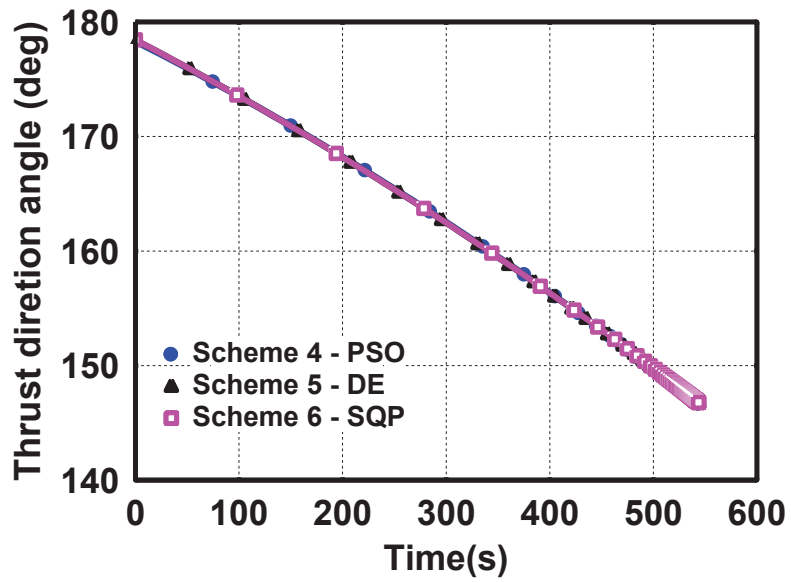


Fig. 2.16. Optimum thrust direction angle for solution scheme 4,5 and 6

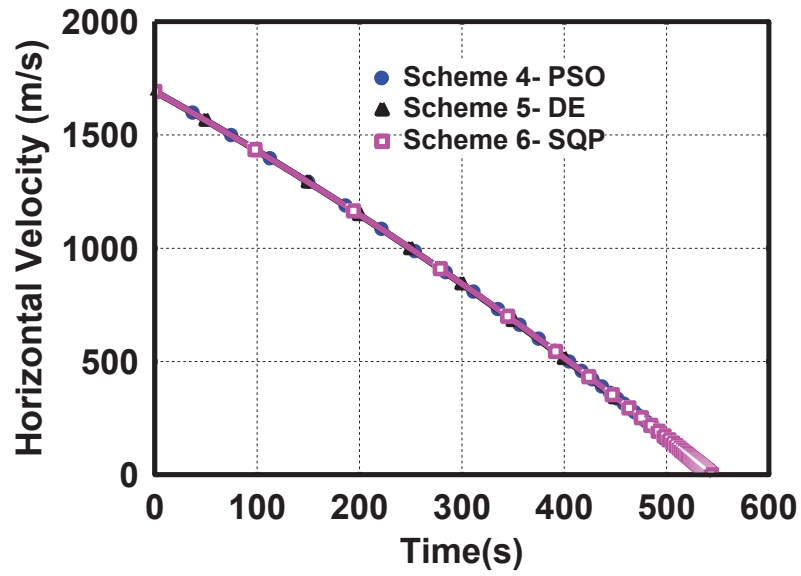


Fig. 2.17. Horizontal velocity variation for solution scheme 4, 5 and 6

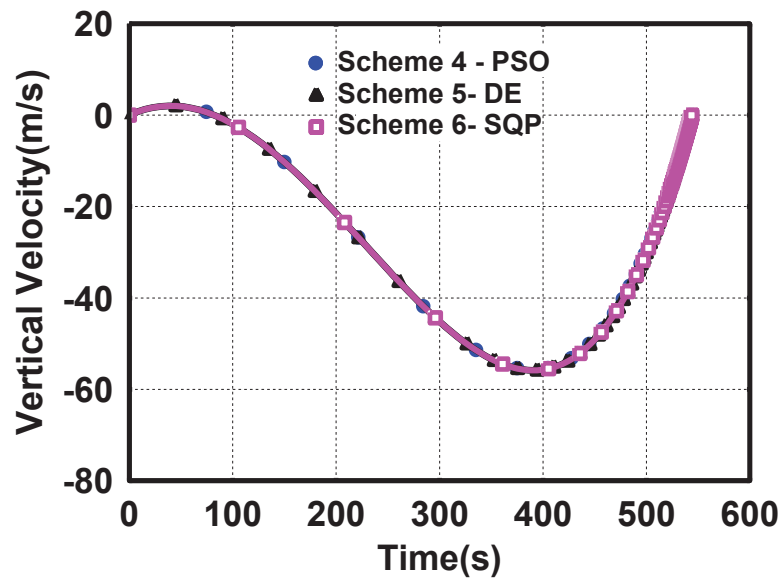


Fig. 2.18. Vertical velocity variation for solution scheme 4, 5 and 6

Figure 2.19 shows the variation of objective function with the number of function evaluations. Table 2.9 provides the summary of the performance of optimizers and the various parameters of interest. The optimum landing masses and the flight time for different schemes are very close. With the close initial guess, SQP convergence is faster. The techniques PSO and DE require no initial guess and it is capable of generating the optimum solution within about 5000 function evaluations without the a prior knowledge of the solution. Also, the DE performance is better than PSO in terms of function evaluations. The converged design is given in Table 2.10. Scheme 6 requires closer bounds of ± 0.05 deg/s (cf. Table 2.10) and closer initial guess (cf. Table 2.11) for convergence. The implication of initial guess and the wider bounds for SQP is given in Tables 2.10 and 2.11. The computational time increases for non-closer initial guess and there is no convergence for some guesses for SQP.

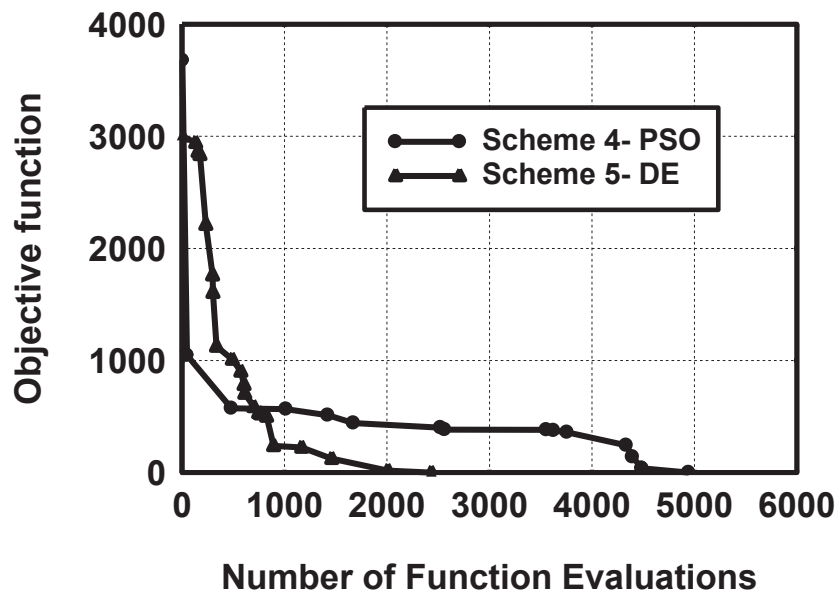


Fig. 2.19. No of function evaluations for solution scheme 4, 5 and 6

Table 2.9 Performance summary of solution scheme 4, 5 and 6

Optimizer	Optimum landing mass(kg)	Optimum flight time (s)	CPU time required (s)	No of function evaluations
PSO (Scheme 4)	486.921	544.087	606	4945
DE (Scheme 5)	486.924	544.086	267	2434
SQP - with close initial guess (Scheme 6)	486.92	544.088	79	412

Table 2.10 Converged design using direct approach

Optimizer	Converged Design				Landing mass (kg)
	Initial Thrust direction angle (α @ time=0)	Thrust direction angle rate bounds	Thrust direction angle rates (deg/s)	Flight time (s)	
PSO (Scheme 4)	178.255	± 1 deg/s	-0.027152 -0.027301 -0.047457	544.087	486.921
DE (Scheme 5)	178.26	± 1 deg/s	-0.027149 -0.027253 -0.047462	544.086	486.924
SQP (Scheme 6)	178.3	-0.05 deg/s	-0.027152 -0.027605 -0.046907	544.088	486.92

Table 2.11 Performance of gradient based method with arbitrary initial guess (scheme 6)

Initial guess No	Initial guess and Converged co-states				Landing mass
	Initial Thrust direction angle (α @ time=0) and Converged angle	Guess of thrust direction angle rate	Converged thrust direction angle rate (deg/s)	Initial guess on flight time and converged flight time	
1	177	-0.5 -0.5 -0.5	Not converged		
2	177 175.3	-0.1 -0.1 -0.1	-0.034535 -0.029033 -0.05565	550 544.6	485.2*
3	170 178.8	-0.05 -0.05 -0.05	-0.037016 -0.026311 -0.041005	550 544.3	486.1*
4	177 178.3	-0.05 -0.05 -0.05	-0.027152 -0.027605 -0.046907	550 544.088	486.92

*Results after 5000 function evaluations

The number of function evaluations and CPU time required for convergence are provided in Table 2.12 for DE and PSO with wider bounds on thrust direction angle rates. Scheme 6 requires close bounds for convergence hence it is not added in Table 2.12 for comparison.

Table 2.12 Performance of DE and PSO with wide guess of thrust direction angle rate

Bounds on Thrust direction angle rate (deg/s)	No of Function evaluations		CPU time (s)	
	DE	PSO	DE	PSO
± 1	2434	4945	267	606
± 1.5	6544	12986	595	1280
± 2	>20000	>20000	>5000	>5000

2.7.1 Comparison of direct and indirect approaches

By comparison of Table 2.6 and Table 2.12, it is clear that in direct approach, if the bounds are wide, then even the evolutionary techniques take more function evaluations and computing time compared to indirect approach. Also, the performance of DE is better than that of PSO. So, the scheme 2 that uses indirect approach and DE for optimization is used for further studies of this research.

2.8 Trajectory Design by 3-DOF Dynamics

For further studies of this research, 3-DOF equations of motion are used to deal with out-of-plane motion also. The natural extension of the equations of motion for planar motion is use of equations of motion represented in radial-transversal-normal (RTN) frame (Fig.2.20). Here the vehicle motion evaluation is done in 3D space (x, y, z) without considering the attitude dynamics of the vehicle.

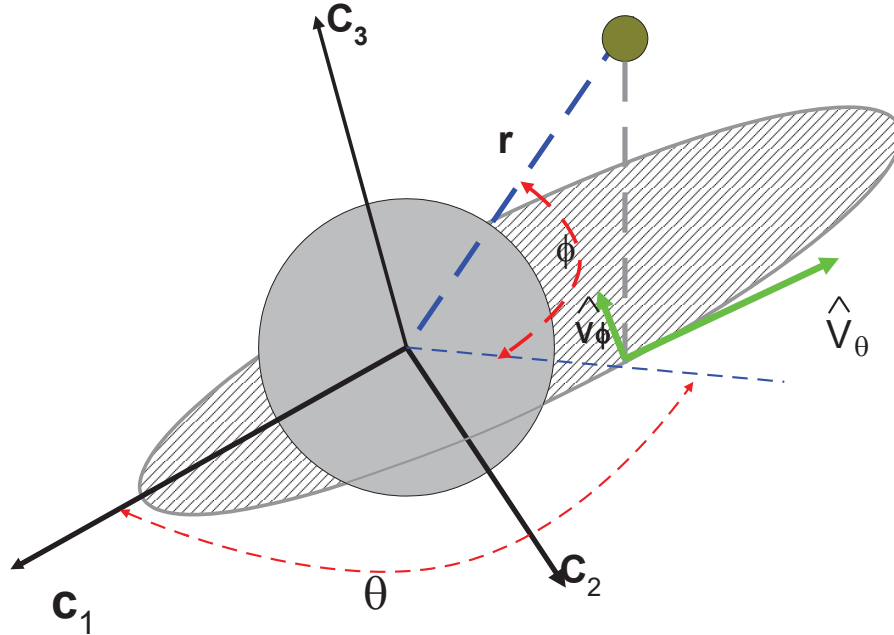


Fig. 2.20. Schematic RTN frame

In the RTN frame, the axes C_1 is towards periapsis of the orbit at the start of descent, C_2 is towards transversal direction, and C_3 forms the right handed system (orbit normal). The fundamental plane is the orbital plane at the start of descent with origin at the center of the Moon. The motion of the lander module is represented by three variables, r - radius, θ and ϕ , the in-plane and out-of-plane angles respectively. The velocity vector is represented by the components of the frame denoted by v_r is the vertical (radial) velocity; v_θ is the horizontal (parallel) velocity v_ϕ is lateral (normal) velocity. The equations of motion (Pontani, 2015) are:

$$\dot{r} = v_r \quad (2.20a)$$

$$\dot{\theta} = \frac{v_\theta}{r \cos(\phi)} \quad (2.20b)$$

$$\dot{\phi} = \frac{v_\phi}{r} \quad (2.20c)$$

$$\dot{v}_\theta = \frac{-v_r v_\theta}{r} + \frac{-v_\phi v_\theta}{r} \tan(\phi) + \frac{T}{m} \cos(\alpha) \cos(\beta) \quad (2.20d)$$

$$\dot{v}_r = \frac{(v_\theta^2 + v_\phi^2)}{r} - \frac{\mu}{r^2} + \frac{T}{m} \sin(\alpha) \cos(\beta) \quad (2.20e)$$

$$\dot{v}_\phi = \frac{-v_\theta v_r}{r} - \frac{v_\theta^2}{r} \tan(\phi) + \frac{T}{m} \sin(\beta) \quad (2.20f)$$

$$\dot{m} = -\frac{T}{g I_{sp}} \quad (2.20g)$$

where T is thrust level; m is mass; α is the angle from the horizontal velocity vector (in local horizontal plane) to the thrust direction; β is the out of plane angle from the horizontal velocity vector (in local horizontal plane) to the thrust direction and g is acceleration due to gravity of Earth(at sea level) .

The above set of equations has singularity for $\phi=90$ deg. Also the co-state equations are complicated and lengthy. Another option is velocity and its spherical angles flight path angle and azimuth. They also have singularity at the time of touch down. So, a set of variables (position and velocity components) in Moon Centered Inertial (MCI) coordinate frame is used. The details are provided in Chapter 3.

2.9 Conclusion

Six direct and indirect schemes have been evaluated using two evolutionary optimization methods i.e PSO and DE along with MATLAB based gradient optimization method (SQP) for soft landing trajectory optimization. Both the evolutionary optimization methods are found to be capable of locating the optimum solution even with very wide bounds. However, PSO requires more function evaluations compared to DE to arrive at the global optimum. Gradient based optimization schemes require reasonably accurate initial guess of the solution. Among the direct approach based schemes, the computational times of even the evolutionary techniques depend on the bounds on the unknown design variables. Apart from good initial guess, the solution accuracy of the direct approach depends on the number of discrete points and the interpolation schemes. For a new problem prior information about nature of the solution is unknown. So, the indirect approach using the Differential Evolution technique is recommended for the design of optimal soft landing trajectory on the Moon.

Chapter 3

An Indirect Scheme for Optimal Lunar Pinpoint Soft landing Trajectories

Chapter Summary

In this chapter, the problem of precise and soft lunar landing in a pre-specified target location, is solved using a numerical scheme based on an indirect approach. In the indirect approach, the problem is transformed into a two point boundary value problem using Pontryagin's principle and solved. The state vector components and their variations are used to study the motion. Three formulations to meet three different objectives are presented. The challenge in the indirect approach lies in finding suitable initial co-states with no prior knowledge available about them. The Differential Transformation (DT) technique is employed to determine the unknown initial co-states using the information on the target site and the flight time. The proposed new scheme reduces the number of unknowns to one from eight. The flight time, the only unknown, is determined by Differential Evolution, an optimization technique. The novel computational scheme that combines Differential Transformation and Differential Evolution techniques uses Differential Transformation in multi steps, to ensure the precise landing at the target site. The guidelines that help fixing the bounds for the flight time are provided. The proposed scheme, named as DT-DE scheme is uniformly valid for various performance measures like fuel-optimal, energy-optimal, and time-optimal. Also, it is capable of introducing coasting during descent while maximizing the landing mass. Numerical results are provided to demonstrate the numerical scheme for all performance measures.

3.1 Introduction

The problem of precise and soft lunar landing in a pre-specified target location, is formulated with a scheme based on indirect approach. In the indirect approach, the problem is transformed into a two-point boundary value problem using Pontryagin's principle and solved. The two-point boundary value problem involves the state and co-state variables and the related equations representing their variations. The control law is obtained as a function of time-variant co-state variables. The variation of co-states is governed by co-state dynamics which is derived using Pontryagin's principle. But the initial co-states (corresponding to the components of the state vector) are unknown and are obtained using, in general, some optimization technique. The challenge in the indirect approach lies in finding suitable initial co-states with no prior knowledge available about them. Many researchers attempted to find the initial co-states by introducing assumptions and these approaches are mainly restricted a certain objective.

In the current research, a computational scheme to determine the initial co-states, which is uniformly valid for all performance measures Viz. fuel-optimal, energy-optimal and time-optimal, etc, is developed. In the proposed computational scheme, the computation of initial co-states is carried out in a multi-step Differential Transformation (DT) technique using the pre-specified target state vector and the randomly selected flight time. The process of selection of flight time and the computation of initial co-states is continued until the touchdown boundary conditions are met. This novel scheme is named as DT-DE scheme. The technique DE needs only bounds for the unknown parameter. The guidelines to arrive at narrow bounds for the only unknown the flight time are also discussed herein. With the co-states determined using multi-step DT technique and the guidelines, for selecting bounds for the unknown flight time available, the soft landing trajectory problem becomes easily solvable. The robustness and validity of the proposed scheme is demonstrated for three popular performance measures (i) energy-optimal (ii) fuel-optimal (iii) time-optimal. For all three problems,

the thrust is assumed to be limited and throttling is available. For the energy-optimal case, it is capable to handle unlimited thrust also.

First, the system dynamics are given, and in subsequent sections, different formulations are described. In another section, the solution scheme based on DT and DE is discussed. Subsequently, the performance of the scheme and its advantages are discussed.

3.2 System Dynamics

As discussed in Chapter 2, the equations of motion in terms of the state variables: the spherical coordinates of the position vector and components of velocity vector in radial-transversal-normal frame has singularity. So, to represent the dynamics of motion, the Moon Centered Inertial (MCI) coordinate frame (XYZ) is used with origin at Moon's centre. The schematic of coordinate system and landing trajectory is shown in Fig. 3.1. In this frame, X –axis is toward the 0 deg. longitude (prime meridian of moon) and XY plane coincides with equatorial plane of Moon and Z axis is toward north pole of moon. This coordinate system is not inertial because of the rotation of Moon about its axis. However, this effect is very small during the landing phase (landing duration is very small compared to rotation period) and so, it is neglected.

The orbital elements at the start of the final maneuver (from periselenium of intermediate orbit) are the inputs for the state equations. The orbital elements converted to MCI frame using the transformation of Eq. (3.1a). The lander module to be transferred from an initial orbit to a target site such that the touchdown velocity is zero. The state vector of target site is computed using Eqs. (3.1b)- (3.1d).

$$\begin{Bmatrix} x \\ y \\ z \\ v_x \\ v_y \\ v_z \end{Bmatrix} = \begin{Bmatrix} r(\cos(\Omega)\cos(\omega+\nu) - \sin(\Omega)\sin(\omega+\nu)\cos(i)) \\ r(\sin(\Omega)\cos(\omega+\nu) + \cos(\Omega)\sin(\omega+\nu)\cos(i)) \\ r(\sin(i)\sin(\omega+\nu)) \\ -\sqrt{\frac{\mu}{p}}[\cos(\Omega)\{\sin(\omega+\nu) + e\sin(\omega)\} + \sin(\Omega)\cos(i)\{\cos(\omega+\nu) + e\cos(\omega)\}] \\ -\sqrt{\frac{\mu}{p}}[\sin(\Omega)\{\sin(\omega+\nu) + e\sin(\omega)\} - \cos(\Omega)\cos(i)\{\cos(\omega+\nu) + e\cos(\omega)\}] \\ \sqrt{\frac{\mu}{p}}[\sin(i)\{\cos(\omega+\nu) + e\cos(\omega)\}] \end{Bmatrix} \quad (3.1a)$$

where, r is the radial distance from Moon's center, μ is the gravitational parameter of Moon. The orbital parameters at the start of final maneuver are the following: ω is argument of periselenium, ν is true anomaly, Ω is right ascension of ascending node, e is eccentricity, i is inclination of the orbit, p is semi latus rectum ($p = a(1 - e^2)$) and a is semi major axis of orbit. The Cartesian components of the target site are

$$x_T = r_T \cos(\phi_t) \cos(\lambda_t) \quad (3.1b)$$

$$y_T = r_T \cos(\phi_t) \sin(\lambda_t) \quad (3.1c)$$

$$z_T = r_T \sin(\phi_t) \quad (3.1d)$$

where r_T, ϕ_T, λ_T are radial distance, selenocentric latitude and selenocentric longitude respectively. To achieve precise and soft landing, the thrust magnitude and direction along the trajectory must be chosen satisfying the appropriate performance measure.

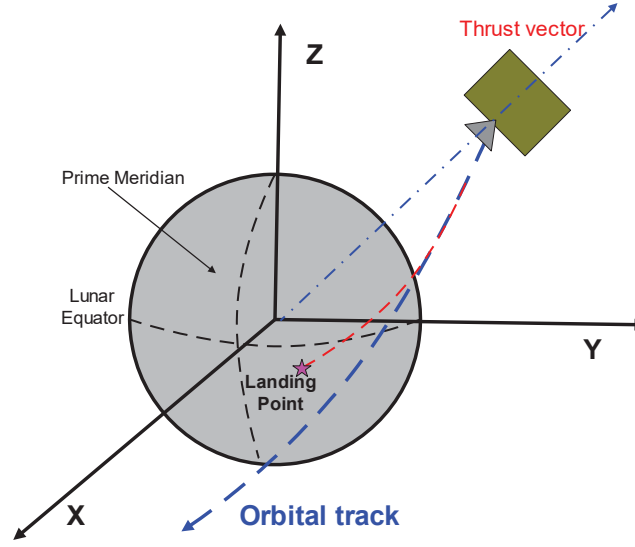


Fig. 3.1. Soft landing coordinate System and thrust vector schematic

The assumptions used in the formulations are : (i) lander is a point mass with 3 degree of freedom (ii) specific impulse of engine is constant (iii) Moon is spherical (iv) rotational effect of the Moon on the landing trajectory is negligible. The equations of motion in vector form are:

$$\dot{\mathbf{r}} = \mathbf{v} \quad (3.2a)$$

$$\dot{\mathbf{v}} = \frac{-\mu}{r^3} \mathbf{r} + k \mathbf{a}_T \quad (3.2b)$$

$$\dot{m} = \frac{-k T_{max}}{g I_{sp}} = \frac{-k m \sqrt{a_{Tx}^2 + a_{Ty}^2 + a_{Tz}^2}}{g I_{sp}} \quad (3.2c)$$

where $\mathbf{r} = [x, y, z]$, $\mathbf{v} = [v_x, v_y, v_z]$, $\mathbf{a}_T = [a_{Tx}, a_{Ty}, a_{Tz}]$, x, y, z are position and v_x, v_y, v_z are velocity components, r is the radial distance from Moon's centre. All these quantities are in SI units i.e position in meter and velocity in meter per second. The quantities a_{Tx}, a_{Ty}, a_{Tz} are acceleration components of thrust (T) and k is the throttling parameter. The parameters $m, T_{max}, I_{sp}, g, \mu$ are the mass of the lander module, maximum thrust, specific impulse, sea level acceleration due to gravity of Earth (9.80665 ms^{-2}) and gravitational parameter of Moon ($4.902800476\text{E}12 \text{ m}^3\text{s}^{-2}$)

respectively. Note that for propulsion system in which the thrust is restricted (referred to as limited thrust), the throttling parameter k varies between 0 and 1. For a propulsion system with unlimited thrust, the actual required thrust will be computed.

3.3 Formulation for Landing Problem (Indirect Approach)

Introduce co-state variables ($\mathbf{p} = [p_x, p_y, p_z, p_{v_x}, p_{v_y}, p_{v_z}, p_m]$) corresponding to the state variables ($\mathbf{X} = [x, y, z, v_x, v_y, v_z, m]$). The control variables of the problem are given by $\bar{u} = (k, a_{Tx}, a_{Ty}, a_{Tz})$.

Let the performance measure be

$$\min J = \int_{t_0}^{t_f} \Gamma(t) dt \quad (3.3a)$$

$\Gamma(t)$ is the generic representation of the minimization parameter and it depends on the formulation cases. The representations for the three cases are as follows,

$$\text{Energy-optimal} \quad \Gamma(t) = \frac{1}{2} k^2 (a_{Tx}^2 + a_{Ty}^2 + a_{Tz}^2) \quad (3.3b)$$

$$\text{Fuel-optimal} \quad \Gamma(t) = -\frac{dm}{dt} \quad (3.3c)$$

$$\text{Time-optimal} \quad \Gamma(t) = 1.0 \quad (3.3d)$$

For energy-optimal case, the term k can be avoided or it can be assumed to unity.

Following Pontryagin's principle, the Hamiltonian H is written as

$$H = \Gamma + \mathbf{p} \dot{\mathbf{X}}^T \quad (3.4)$$

The co-state dynamics is derived using

$$\dot{\mathbf{p}} = - \left[\frac{\partial H}{\partial x} \frac{\partial H}{\partial y} \frac{\partial H}{\partial z} \frac{\partial H}{\partial v_x} \frac{\partial H}{\partial v_y} \frac{\partial H}{\partial v_z} \frac{\partial H}{\partial m} \right] \quad (3.5)$$

The control law by the optimality condition is given by

$$\frac{\partial H}{\partial \bar{u}} = 0 \quad \forall t \in [t_o, t_f] \quad (3.6)$$

3.3.1 Formulation for Energy-optimal

The performance measure of energy-optimal problem with variable thrust is given by

$$\min J = \int_{t_0}^{t_f} \frac{1}{2} k^2 (a_{Tx}^2 + a_{Ty}^2 + a_{Tz}^2) dt \quad (3.7)$$

The Hamiltonian H is written as

$$H = \frac{1}{2} k^2 (a_{Tx}^2 + a_{Ty}^2 + a_{Tz}^2) + \mathbf{p} \dot{\mathbf{X}}^T \quad (3.8)$$

The co-state equations of motion (cf. Eq. (3.5)) are

$$\dot{p}_x = \frac{\mu}{r^5} [p_{v_x} (y^2 + z^2 - 2x^2) - 3x(p_{v_y} y + p_{v_z} z)] \quad (3.9a)$$

$$\dot{p}_y = \frac{\mu}{r^5} [p_{v_y} (x^2 + z^2 - 2y^2) - 3y(p_{v_x} x + p_{v_z} z)] \quad (3.9b)$$

$$\dot{p}_z = \frac{\mu}{r^5} [p_{v_z} (x^2 + y^2 - 2z^2) - 3z(p_{v_x} x + p_{v_y} y)] \quad (3.9c)$$

$$\dot{p}_{v_x} = -p_x \quad (3.9d)$$

$$\dot{p}_{v_y} = -p_y \quad (3.9e)$$

$$\dot{p}_{v_z} = -p_z \quad (3.9f)$$

$$\dot{p}_m = \frac{p_m k \sqrt{a_{Tx}^2 + a_{Ty}^2 + a_{Tz}^2}}{I_{sp} g} \quad (3.9g)$$

3.3.1.1 Unlimited Thrust

For energy-optimal, ideally, the thrust available must be unbounded. So, for unlimited thrust, the control variables are considered as $\bar{u} = (ka_{Tx}, ka_{Ty}, ka_{Tz})$. That means the product of the acceleration component and the throttling parameter is considered as a single parameter. So, there are only three control parameters for this formulation and they are, given by the control laws [cf. Eq.(3.6)] for $\forall t \in [t_0, t_f]$

$$\frac{\partial H}{\partial a_{Tx}} = 0 \quad (3.10a)$$

$$\frac{\partial H}{\partial a_{Ty}} = 0 \quad (3.10b)$$

$$\frac{\partial H}{\partial a_{Tz}} = 0 \quad (3.10c)$$

The control laws obtained using Eq. (3.10a)-(3.10c) are given by

$$k a_{T_x} = -p_{v_x} \quad (3.11a)$$

$$k a_{T_y} = -p_{v_y} \quad (3.11b)$$

$$k a_{T_z} = -p_{v_z} \quad (3.11c)$$

$$k \sqrt{a_{T_x}^2 + a_{T_y}^2 + a_{T_z}^2} = \frac{\text{Thrust required}}{m} \quad (3.11d)$$

For computation purposes, the parameter ‘ k ’ is set to equal to 1. The above control laws (cf. Eqs.(3.11a)-3.11c) are valid for unbounded thrust. But, in actual missions, the thrust available is limited.

3.3.1.2 Limited Thrust

If the required thrust computed using the Eq.(3.11d) is higher than the available maximum thrust, the control laws are modified using Pontryagin’s principle. According to Pontryagin’s principle, the thrust must be chosen satisfying the constraint on the maximum thrust and still minimizing the Hamiltonian. It can easily be verified by selecting the terms that contain control variables that H is minimum when the thrust is set to the maximum permissible value. The unit vector along the co-state of velocity vector, which is optimally, computed using Eqs. (3.11a)-(3.11c), is used for thrust direction. Combining these strategies, to suit the limited thrust conditions, the maximum thrust acceleration is resolved along the unit vector of the co-state velocity vector ($\mathbf{p}_v = [p_{v_x}, p_{v_y}, p_{v_z}]$). The energy-optimal control laws that provide the thrust acceleration components are

$$k a_{T_x} = -\frac{p_{v_x}}{p_v} \frac{T_{max}}{m} \quad (3.12a)$$

$$k a_{T_y} = -\frac{p_{v_y}}{p_v} \frac{T_{max}}{m} \quad (3.12b)$$

$$k a_{T_z} = -\frac{p_{v_z}}{p_v} \frac{T_{max}}{m} \quad (3.12c)$$

where

$$p_v = \sqrt{p_{v_x}^2 + p_{v_y}^2 + p_{v_z}^2}$$

To summarize, the Eqs. (3.12a)-(3.12c) are used as control laws if the required thrust is less than the maximum thrust. Otherwise the Eqs. (3.11a)-(3.12c) are used as control laws. For computation purposes, the parameter ‘ k ’ is set to equal to 1. Note that the control laws are independent of the co-state of the mass (p_m).

3.3.2 Formulation for Fuel-optimal

For the fuel-optimal problem, the thrust is limited to a maximum value and the thrust variation is handled using the throttling parameter (k). The flight time of the fuel-optimal problem can be either free or fixed. Note that the minimizing the fuel consumption leads to maximum landing mass. The performance measure of the fuel-optimal problem with limited thrust is given by

$$\min J = \int_{t_0}^{t_f} -\frac{dm}{dt} dt = \int_{t_0}^{t_f} \frac{k m \sqrt{a_{T_x}^2 + a_{T_y}^2 + a_{T_z}^2}}{I_{sp} g} dt \quad (3.13)$$

The Hamiltonian H is written as

$$H = \frac{k m \sqrt{a_{T_x}^2 + a_{T_y}^2 + a_{T_z}^2}}{I_{sp} g} + \mathbf{p} \dot{\mathbf{X}}^T \quad (3.14)$$

The co-state equations of motion (cf. Eq. (3.5)) except for mass are as given in Eqs. (3.9a)–(3.9f). The co-state equation for mass is

$$\dot{p}_m = \frac{(p_m - 1) k T_{max}}{m I_{sp} g} \quad (3.15)$$

Note that the Eq. (3.15) and Eq. (3.9g) are not same. The optimal thrust acceleration components and magnitude are found using the optimality condition (Eq. (3.6)) and they are as given below.

$$a_{T_x} = -\frac{k g I_{sp} T_{max} p_{v_x}}{m^2 (1 - p_m)} \quad (3.16a)$$

$$a_{T_y} = -\frac{k g I_{sp} T_{max} p_{v_y}}{m^2 (1 - p_m)} \quad (3.16b)$$

$$a_{T_z} = -\frac{k g I_{sp} T_{max} p_{v_z}}{m^2 (1 - p_m)} \quad (3.16c)$$

$$\sqrt{a_{T_x}^2 + a_{T_y}^2 + a_{T_z}^2} = \frac{T_{max}}{m} \quad (3.16d)$$

Equation (3.16d) represents the constraint on maximum thrust. To solve for the throttling parameter k , group the terms containing k in Hamiltonian (cf. Eq. (3.14))

$$H_k = k \frac{T_{max}}{m} \left(\frac{m(1-p_m)}{g I_{sp}} - \frac{g I_{sp}}{m(1-p_m)} (p_{v_x}^2 + p_{v_y}^2 + p_{v_z}^2) \right) \quad (3.17a)$$

$$\text{Let} \quad H_k = k \frac{T_{max}}{m} S \quad (3.17b)$$

where,

$$S = \left(\frac{m(1-p_m)}{g I_{sp}} - \frac{g I_{sp}}{m(1-p_m)} (p_{v_x}^2 + p_{v_y}^2 + p_{v_z}^2) \right) \quad (3.17c)$$

It can also be easily verified that the quantity $[m(1-p_m)]$ is invariant along the trajectory. Clearly, the minimum of H_k is controlled by the function (S), known as switching function. The function H_k is minimum, when

$$k = \begin{cases} 0 & \text{for } S > 0 \\ 1 & \text{for } S < 0 \end{cases} \quad (3.18)$$

When $S = 0$, the value of k is set to zero or one based on the previous value of S . This clearly, is a bang-bang type of control. That means, for fuel-optimal problem, the thrust level is set either to maximum or to zero, along the trajectory. Note that the initial value of co-state of mass (p_m), cannot be equal to one. When set to one, $\dot{p}_m = 0$ and the co-state of m is frozen to one always and the Eq. (3.17) becomes indeterminate. This observation will be used in the formulation for the Differential Transformation technique.

3.3.3 Formulation for Time-optimal

The performance measure of time-optimal problem is given by

$$\min J = \int_{t_0}^{t_f} dt \quad (3.19)$$

The Hamiltonian H is written as

$$H = 1 + \mathbf{p} \dot{\mathbf{X}}^T \quad (3.20)$$

The co-state equations of motion (cf. Eq. (3.5)) except for mass are as given in Eqs. (3.9a)–(3.9f)

The co-state equation for mass is

$$\dot{p}_m = \frac{p_m k T_{max}}{m I_{sp} g} \quad (3.21)$$

The optimal thrust acceleration components obtained using the optimality condition (Eq. (3.6)) is:

$$a_{T_x} = -\frac{k g I_{sp} T_{max} p_{v_x}}{m^2 p_m} \quad (3.22a)$$

$$a_{T_y} = -\frac{k g I_{sp} T_{max} p_{v_y}}{m^2 p_m} \quad (3.22b)$$

$$a_{T_z} = -\frac{k g I_{sp} T_{max} p_{v_z}}{m^2 p_m} \quad (3.22c)$$

$$a_{T_{max}} = \sqrt{a_{T_x}^2 + a_{T_y}^2 + a_{T_z}^2} \quad (3.22d)$$

As in the case of fuel-optimal, to find the throttling parameter k , group the terms containing k in Hamiltonian (cf. Eq. (3.20)) and the resulting switching function is

$$S = \left(-\frac{m p_m}{g I_{sp}} - \frac{g I_{sp}}{m p_m} (p_{v_x}^2 + p_{v_y}^2 + p_{v_z}^2) \right) \quad (3.23)$$

It can also be easily verified that the quantity $(m p_m)$ is constant along the trajectory. The minimum of H_k is controlled by the function S . For H_k to be minimum, the choice of k is as follows:

$$k = \begin{cases} 0 & \text{for } S > 0 \\ 1 & \text{for } S < 0 \end{cases} \quad (3.24)$$

When $S = 0$, the value of k is set to zero or one, based on the previous value of S . The sign of the switching function (S) (refer Eq.(3.23)) depends on the sign of the co-state p_m . If $p_m(t_0) < 0$, then $S(t_0) > 0$ and hence $k(t_0) = 0$ which implies that $\dot{p}_m(t_0) = 0$. So, p_m remains negative in the time interval $[t_0, t_f]$ which, in turn, leads to no thrust throughout which means the probe is not descending. Therefore, the initial co-state p_m cannot have a negative value or zero. It must remain always positive which makes the throttling parameter k as one always.

3.4 Solution Scheme

In all the above formulations, the control variables are expressed as functions of co-state variables (cf. Eqs. (3.11), (3.12), (3.16), (3.22)). As pointed out earlier, in the indirect approach, if the initial co-states are known, the time history of control can be computed. The determination of co-states is attempted, in general, using optimization techniques. The objective function for optimization (different from the one for optimal control) represents the achievement of the target site with zero velocity.

$$F = \sqrt{(x(t_f) - x_T)^2 + (y(t_f) - y_T)^2 + (z(t_f) - z_T)^2 + v_x^2(t_f) + v_y^2(t_f) + v_z^2(t_f)} \quad (3.25)$$

It is well known that the gradient based technique fails in the absence of good initial guess. In this problem, there is no prior knowledge of initial co-states and so gradient techniques are not suitable for solving an optimal control problem using indirect approach. In Chapter 2, the Differential Evolution (DE) technique has been used to determine the unknown co-states. The advantage of the DE technique is that it does not need an initial guess for the unknown and needs only bounds within which the unknown varies. When very wide bounds for the unknowns are used, the process requires large computational time.

3.4.1 DT-DE Solution Scheme

To overcome the complexity in determining the co-states and reduce the computational time, a novel computation scheme is proposed in this chapter. The unknown initial co-states are determined using the Differential Transformation (DT) technique. However, in addition to target state, the time of flight must be known for the use of the DT technique. Although for landing problem the target site is known, the flight time is an unknown quantity. So, in this computation scheme, the unknown flight time is randomly selected using the DE technique and DT determines the initial co-states using the selected flight time. Both DE and DT operate concurrently to minimize the function ‘ F ’. In the following sections, procedure to determine the co-states using DT is explained. Finally, the computation scheme is presented.

3.4.2 Initial Co-states using Differential Transformation

DT is a technique that is used for solving a two point boundary value problem when the final state and the time are known. DT transforms the equations from time domain into a set of nonlinear algebraic equations in a transformed domain. In DT, unlike Fourier and Laplace transforms, the transformed function is expressed in terms of differential operators. That is, if $f(t_e)$ is a function where $t_e \in [t_0, t_f]$, the image of this function ($F(t_e, j)$) for $t_e \in [t_0, t_f]$ in the transformed domain is given by

$$F(t_e, j) = \frac{1}{j!} \left[\frac{d^j f(t)}{dt^j} \right]_{t=t_e}, \quad j = 0, 1, 2, \dots \quad (3.26)$$

and $F(t_e, j)$ is the j^{th} order differential spectra of $f(t)$ at the time instant t_e . Now the solution to the function $f(t)$ in the original domain is obtained using inverse transformation as given below:

$$f(t) = \sum_{j=0}^{\infty} F(t_e, j)(t - t_e)^j \quad (3.27)$$

The solution is obtained as a Taylor series expansion about the step size of the independent variable. For various types of functions, the expressions for images are available in the literature (Pukhov, 1981; Hwang et al., 2008). Some examples are: when the function is a differential function ($f(t) = \dot{x}$), the j^{th} order transformed function is given by $(j + 1) X(t_e, j + 1)$; when the function is an algebraic expression ($f(t) = b x$), the j^{th} order transformed function is given by $b X(t_e, j)$.

The following example is used to demonstrate the DT technique. Consider a system of differential equations,

$$\frac{dx}{dt} = 2x - 3y ; \quad \frac{dy}{dt} = -2x + y ; \quad x(0) = 8 ; \quad y(0) = 3$$

The exact solution is given by

$$x(t) = 5e^{-t} + 3e^{4t} ; \quad y(t) = 5e^{-t} - 2e^{4t}$$

By applying DT scheme,

$$(k+1)X_{(k+1)} = 2X_{(k)} - 3Y_{(k)} ; (k+1)Y_{(k+1)} = -2X_{(k)} + Y_{(k)} ; X_{(0)} = 8 ; Y_{(0)} = 3$$

$$k = 0 \rightarrow X_{(1)} = 7 ; Y_{(1)} = -13$$

$$k = 1 \rightarrow X_{(2)} = \frac{53}{2} ; Y_{(2)} = -\frac{27}{2}$$

$$k = 2 \rightarrow X_{(3)} = \frac{187}{6} ; Y_{(3)} = -\frac{135}{6}$$

and so on. The solution of the system is given by

$$x(t) = \sum_{k=0}^{k=n} X_{(k)} t^k ; y(t) = \sum_{k=0}^{k=n} Y_{(k)} t^k$$

So,

$$x(t) = 8 + 7t + \frac{53}{2}t^2 + \frac{187}{6}t^3 + \dots ; y(t) = 3 - 13t - \frac{27}{2}t^2 - \frac{135}{6}t^3 + \dots$$

It is found that for this problem when the number of terms in the series expansion is 15 or higher, the solution is very close to exact solution. For the soft landing problem an assessment on number of terms is included in later section.

In the current problem, the unknown initial co-states are obtained using the DT technique. The details of the procedure are given below. For use in DT, it is convenient to express the state and co-state equations (Eqs. (3.2) and (3.9)) in state space matrix form. Let \mathbf{x} , \mathbf{p} , \mathbf{u} be the state, co-state and the control vectors of the system, where

$$\mathbf{x} = [x \ y \ z \ v_x \ v_y \ v_z]^T$$

$$\mathbf{p} = [p_x \ p_y \ p_z \ p_{v_x} \ p_{v_y} \ p_{v_z}]^T$$

$$\mathbf{u} = [0 \ 0 \ 0 \ ka_{T_x} \ ka_{T_y} \ ka_{T_z}]^T$$

The mass state (m) is not considered in the DT process because of the following reasons (i) the co-state equation of m does not explicitly depend on either \mathbf{x} or \mathbf{p} (ii) the control law does not depend on the co-state of ' m ' for minimum control effort case (iii) there are invariant quantities ($m p_m$) and $[m(1 - p_m)]$ for time-optimal and fuel-optimal cases. For these reasons, the co-state of m need not be determined through DT technique.

For all performance measures, the co-state equations are same except for co-state equation of mass. So, the state and co-state equations (Eqs. (3.2) and (3.9)) are rewritten as

$$\dot{\mathbf{x}} = A_1 \mathbf{x}(t) + C_1 \mathbf{u}(t) \quad (3.28a)$$

$$\dot{\mathbf{p}} = A_2 \mathbf{p}(t) \quad (3.28b)$$

where

$$A_1 = \begin{bmatrix} 0 & 0 & 0 & 1 & 0 & 0 \\ 0 & 0 & 0 & 0 & 1 & 0 \\ 0 & 0 & 0 & 0 & 0 & 1 \\ \frac{-\mu}{r^3} & 0 & 0 & 0 & 0 & 0 \\ 0 & \frac{-\mu}{r^3} & 0 & 0 & 0 & 0 \\ 0 & 0 & \frac{-\mu}{r^3} & 0 & 0 & 0 \end{bmatrix} \quad (3.28c)$$

$$C_1 = (0 \ 0 \ 0 \ 1 \ 1 \ 1) \quad (3.28d)$$

$$A_2 = \begin{bmatrix} 0 & 0 & 0 & \frac{\mu(y^2+z^2-2x^2)}{r^5} & \frac{-3\mu xy}{r^5} & \frac{-3\mu xz}{r^5} \\ 0 & 0 & 0 & \frac{-3\mu xy}{r^5} & \frac{\mu(x^2+z^2-2y^2)}{r^5} & \frac{-3\mu zy}{r^5} \\ 0 & 0 & 0 & \frac{-3\mu xz}{r^5} & \frac{-3\mu zy}{r^5} & \frac{\mu(y^2+x^2-2z^2)}{r^5} \\ -1 & 0 & 0 & 0 & 0 & 0 \\ 0 & -1 & 0 & 0 & 0 & 0 \\ 0 & 0 & -1 & 0 & 0 & 0 \end{bmatrix} \quad (3.28e)$$

Eqs. (3.28a) and (3.28b) can be written in the matrix form by substituting optimal control law (ref. Eq. (3.11) of energy-optimal).

$$\begin{bmatrix} \dot{\mathbf{x}} \\ \dot{\mathbf{p}} \end{bmatrix} = \begin{bmatrix} A_1 & B_1 \\ 0 & A_2 \end{bmatrix} \begin{bmatrix} \mathbf{x} \\ \mathbf{p} \end{bmatrix} \quad (3.29a)$$

where

$$B_1 = \begin{bmatrix} 0 & 0 & 0 & 0 & 0 & 0 \\ 0 & 0 & 0 & 0 & 0 & 0 \\ 0 & 0 & 0 & 0 & 0 & 0 \\ 0 & 0 & 0 & -1 & 0 & 0 \\ 0 & 0 & 0 & 0 & -1 & 0 \\ 0 & 0 & 0 & 0 & 0 & -1 \end{bmatrix} \quad (3.29b)$$

The matrix B_1 will have to be set according to the performance measure.

Let $B_T = B_1$

Then, for time-optimal case, matrix B_1 becomes

$$B_1 = \left(\frac{g I_{sp} T_{max}}{m^2 p_m} \right) B_T \quad (3.29c)$$

For fuel-optimal case, matrix B_1 becomes

$$B_1 = \left(\frac{g I_{sp} T_{max}}{m^2 (1-p_m)} \right) B_T \quad (3.29d)$$

Let the matrix A be

$$A = \begin{bmatrix} A_1 & B_1 \\ 0 & A_2 \end{bmatrix}_{12 \times 12} \quad (3.29e)$$

The initial and final conditions are given by

$$\mathbf{x}(t_0) = \mathbf{x}_0 \text{ and } \mathbf{x}(t_f) = \mathbf{x}_f \quad (3.30)$$

Now, define a single vector to represent state and co-state variables together as follows.

$$\mathbf{y} = [\mathbf{x} \quad \mathbf{p}]_{12 \times 1}^T \quad (3.31)$$

and the Eq. (3.28) becomes

$$\dot{\mathbf{y}} = A \mathbf{y} \quad (3.32)$$

Let the variables $\mathbf{y}(t), \mathbf{x}(t), \mathbf{p}(t)$ be represented by $\mathbf{Y}, \mathbf{X}, \mathbf{P}$ respectively in the transformed domain. Applying the DT concept for the Eq. (3.32), we get

$$(j+1)\mathbf{Y}(j+1) = A\mathbf{Y}(j) \quad (3.33)$$

for $j = 0, 1, \dots, n$ (the infinite series is restricted to 'n' terms). The value for 'n' depends on the problem sensitivity. Using the above recursive relation (cf. Eq. (3.33)) we get

$$\mathbf{Y}(j) = \frac{1}{j!} A^j \begin{bmatrix} \mathbf{X}(0) \\ \mathbf{P}(0) \end{bmatrix} \quad (3.34a)$$

where $[A^j]_{12 \times 12} = A \times A \times A \dots \times A$, j times. It is represented as

$$[A^j]_{12 \times 12} = \begin{bmatrix} [A_{j1}]_{6 \times 6} & [A_{j2}]_{6 \times 6} \\ [A_{j3}]_{6 \times 6} & [A_{j4}]_{6 \times 6} \end{bmatrix} \quad (3.34b)$$

Applying inverse transformation, we get

$$\mathbf{x}(t) = \sum_{j=0}^n (t - t_0)^j \mathbf{X}(j) \quad (3.35)$$

$$\mathbf{p}(t) = \sum_{j=0}^n (t - t_0)^j \mathbf{P}(j) \quad (3.36)$$

When $t = t_0$, and on expansion of Eqs. (3.35) and (3.36) we have

$$\mathbf{x}(t_0) = \mathbf{X}(0) \text{ and } \mathbf{p}(t_0) = \mathbf{P}(0) \quad (3.37)$$

The state vector at the flight time is given by,

$$\mathbf{x}(t_f) = \sum_{j=0}^n (t_f - t_0)^j \mathbf{X}(j) \quad (3.38)$$

Equation (3.38) can be rewritten using Eq.(3.34), as

$$\mathbf{x}(t_f) = \sum_{j=0}^n \frac{(t_f - t_0)^j}{j!} [A_{j1} \quad A_{j2}] \begin{bmatrix} \mathbf{X}(0) \\ \mathbf{P}(0) \end{bmatrix} \quad (3.39)$$

Expanding Eq.(3.39),

$$\mathbf{x}(t_f) = \sum_{j=0}^n \frac{(t_f - t_0)^j}{j!} A_{j1} \mathbf{X}(0) + \sum_{j=0}^n \frac{(t_f - t_0)^j}{j!} A_{j2} \mathbf{P}(0) \quad (3.40)$$

$$\mathbf{x}(t_f) = \mathbf{Q} + \mathbf{R} * \mathbf{p}(t_0) \quad (\text{using Eq. (3.37)}) \quad (3.41a)$$

where

$$\mathbf{Q} = \sum_{j=0}^n \frac{(t_f - t_0)^j}{j!} A_{j1} \mathbf{x}(t_0) \text{ and } \mathbf{R} = \sum_{j=0}^n \frac{(t_f - t_0)^j}{j!} A_{j2} \quad (3.41b)$$

Rearranging the Eq. (3.41a) we get,

$$\mathbf{p}(t_0) = \mathbf{R}^{-1} [\mathbf{x}(t_f) - \mathbf{Q}] \quad (3.42)$$

Using Eq. (3.42), the initial co-state can be computed if the final state is known. The step size $(t_f - t_0)$ used in the determination of initial co-states is referred to as the DT step size.

In the proposed computational scheme, the computation of initial co-states is carried out in multiple steps for DT technique using the pre-specified target state vector and the randomly selected flight time. The process of selection of flight time and the computation of initial co-states is continued till the touchdown boundary conditions are met. This novel scheme is named as the DT-DE scheme. The technique DE needs only bounds for the unknown parameter. So, guidelines to arrive at narrow bounds for the only unknown the flight time are discussed herein.

3.4.3 Guidelines for Bounds for Flight time

For DT-DE scheme, the flight time is selected using Differential Evolution. The DE technique needs bounds for the unknown flight time. The bounds for the flight time are fixed by using the ideal rocket equation and the burn duration.

$$\Delta v = g I_{sp} \ln \frac{m_0}{m_f} \quad (3.43)$$

$$t_{burn} = m_0 \frac{\left(1 - \frac{1}{e^{\frac{\Delta v}{g I_{sp}}}}\right)}{\dot{m}} \quad (3.44)$$

where m_0 and m_f are initial and final masses. For this computation, it is assumed that the thrust is continuous and constant throughout the descent. The constant mass flow rate is given by,

$$\dot{m} = -\frac{T}{g I_{sp}} \quad (3.45)$$

In general, the thrust level (T), I_{sp} , and initial mass are the known quantities. To derive the guidelines, the orbital velocity is treated as the minimum velocity impulse the propulsion system needs to produce. The burn time required for the reduction of orbital velocity provides the minimum limiting value for the actual flight time. However, these guidelines are not applicable, for the performance measure of energy-optimal with unlimited variable thrust case which is, however, practically improbable scenario.

3.5 DT-DE Scheme –Algorithm

Combining Differential Evolution and Differential Transformation techniques, a novel computational scheme is presented. With the co-states determined using multi-step DT technique and the guidelines, for selecting bounds for the unknown flight time available, the soft landing trajectory problem becomes easily solvable. The robustness and validity of the proposed scheme is demonstrated for three popular performance measures (i) energy-optimal (ii) fuel-optimal (iii) time-optimal. For all three problems, the thrust is assumed to be limited and throttling is available. For the energy-optimal case, it is capable to handle, unlimited thrust also.

In the landing problem on hand, there are eight unknowns in all, namely flight time and the seven initial co-states. As pointed out earlier, the co-state p_m need not be determined in the DT scheme and it can be assigned an arbitrary value. The remaining six co-states are determined using the DT scheme as described in the previous section. For the DT process, the flight time must be a known parameter. But in the landing problem, as pointed out earlier, the flight time is an unknown parameter. In the proposed scheme, the unknown flight time is selected using the DE technique. The DE technique explores over a range of values to obtain the optimal flight time. With each randomly selected value of flight time from DE, the co-states are computed using DT. Using these co-states, the state equations are propagated to find the objective function (cf. Eq. (3.25) of the optimization process.

The performance of the DT process with step size as the whole flight time (chosen using DE) is found to result in large target deviations. So, the chosen flight time is split into several intervals resulting in discrete time instants $(t_0, t_1 \dots t_f)$ and at each time instant DT is applied to determine the co-states at that instant. So, there are two step sizes in this scheme (i) propagation step size (eg. $(t_1 - t_0), (t_2 - t_1)$ etc.), used for the numerical propagation of system dynamics (ii) DT step size (initially $(t_f - t_0)$, then reduces to $(t_f - t_1), (t_f - t_2) \dots$ and so on), used for the determination of co-states at different time instants of numerical propagation. The multi-step DT process along with DE is named as DT-DE scheme.

The steps of the DT-DE algorithm are the following.

- I. By fixing 'NP' as the size of the population, a population matrix (NP x 2) each row of which consists of the unknown flight time and the objective function is constructed. The objective function is evaluated after propagating system dynamics. The steps involved in constructing initial population are given below.
 1. Choose t_f randomly from its bounds.
 2. Compute the co-states at t_0 using the specified terminal states and $(t_f - t_0)$ as the DT step size

3. Compute the thrust accelerations at t_0 as in Eq. (3.11) or (3.12) or (3.16) or (3.22) (depending on the performance measure) using the determined co-states.
4. Propagate the state equations to next time step (t_1) using numerical integration.
5. Update the DT step size as $t_{go} = (t_f - t_1)$. Compute the co-state at t_1 using t_{go} and the states at t_f . During propagation, at different time instants (t_i), $t_{go} = (t_f - t_i)$.
6. Repeat the steps 3 to 5 until t_f is reached and evaluate the final objective function given by Eq. (3.25)

At the end of step (6) one row of the population is generated.

7. Repeat the steps (1) to (6) for different randomly selected flight times until the population is built.
- II. Find the minimum of the objective function values of the population matrix. If Objective function $< \epsilon$ (a small prefixed tolerance value), the solution is obtained.
- III. Otherwise update the population. In the update process, each row is subjected to three operations (mutation, crossover and selection) as mentioned in section 2.4.2. For each trial parameter (flight time, t_f), steps I-(2) to I-(6) are executed to evaluate the objective function.

IV. Steps (II) and (III) are repeated till convergence

In the DT-DE scheme, the major advantage is that the co-state equations need not be numerically integrated to find the control variables at each computational step. Furthermore, the number of unknowns reduces to one. FORTRAN codes developed for the proposed DT-DE scheme and existing DE scheme have been implemented in a desktop computer with specification of Intel Core i5 (3570 CPU @3.4GHz) processor and 4GB RAM.

3.6 Soft Landing Trajectory Design and Analysis with Various Performance Measures

For the case studies presented in this thesis, the parking orbit size and shape correspond to a 100 x 15 km lunar orbit. The braking maneuver starts from the perilune, i.e when true anomaly is zero. The values of physical constants are : Equatorial radius of Moon (r_m) = 1738000 m and gravitational constant of Moon (μ) = 4.902800476E12 m³/s². The initial location is chosen on the equator (0 deg. latitude and 0 deg. longitude). The initial state at which the landing starts corresponds to the orbital elements given in Table 3.1. To demonstrate the performance of the DT-DE scheme a target landing site is required. For this purpose, the time-optimal formulation is solved using Differential Evolution and the resulting landing site is used as the target site. To have confidence in the optimal solution of DT-DE scheme, all problems have been solved using DE scheme also for which all the initial co-states are the unknowns.

Table 3.1 Input parameters

Parameters	Value
Semi-major axis (m)	1795.5E3
Eccentricity	0.023670287
Inclination (deg.)	90
Argument of perilune (deg.)	0
Longitude of ascending node (deg.)	0
True anomaly (deg.)	0
Maximum Thrust (N)	2200
Specific Impulse (s)	315
Mass (kg) @ 100x15km orbit	874.4
Mass (kg) @ 100x100km orbit	880.0

3.6.1 Time-optimal Trajectory using Differential Evolution for Target Site Generation

To generate a target site for use in the DT-DE algorithm, the time-optimal problem is solved using the DE scheme. As pointed out earlier, there are eight

unknowns: seven co-states and the flight time for this scheme. Considering the conditions that the co-state of mass cannot be negative and equal to zero (section 3.3.3), the initial co-state of mass is arbitrarily fixed at +3. For all other initial co-states, $[-3, 3]$ is used as bounds. Because the flight time is unknown, the objective function given in Eq. (3.25) is computed by terminating the numerical integration at touchdown. By this choice of termination, determination of one of the unknowns, flight time is eliminated. The threshold value for convergence is kept as $1.0\text{E-}02$. This value ensures an accuracy of < 1 cm/s in velocity and < 1 mm in position. Table 3.2 presents the initial co-states obtained for the minimum time landing trajectory. The values of the ratio ($\frac{p_{vz}}{p_i}$) are given for comparison with the result of the DT-DE algorithm. The optimal flight time and the related landing mass are given in Table 3.3. The landing site of the optimal trajectory is given in Table 3.4 and is used as the target site in the studies with the DT-DE algorithm.

Table 3.2 Unknown initial co-states for time-optimal trajectory using DE

Co-state	Initial co-states	$\frac{p_{vz}}{p_i}$ ($i = x, y, z, vx, vy, vz$)
p_x	0.00219852	-385.63
p_y	-0.0000000006	1.413E9
p_z	-0.000079799	10624
p_{vx}	-0.0473366245	17.911
p_{vy}	1.7490189757E-07	-4.8474E6
p_{vz}	-0.84782335801	1

Table 3.3 Time-optimal trajectory parameters

Parameter	DE scheme
Flight time (s)	543.955
Landing Mass(kg)	487.043

Table 3.4 Landing site of the time-optimal trajectory

Parameter	Value
Latitude (deg. North)	16.1508
Longitude (deg.)	0.0

3.6.2 Sensitivity of the DT Scheme Parameters

To assess the performance of the DT scheme, the optimal flight time obtained in the previous section is used as the flight time (cf. Table 3.3) with other input parameters remaining same as given in Table 3.1 and Table 3.4. As discussed in section 3.4.2, the number of DT terms is fixed as 15 to assess the sensitivity of time step to be used for trajectory design. The critical parameter in the DT scheme is the size of the time step used, referred to as the DT step size. To demonstrate the criticality of the time step, first the whole flight time is used as the step size, which means that determination of co-states using the DT scheme is attempted in a single step at descent phase initiation. The co-states determined using single step is given in Table 3.5 using whole flight time obtained by the DE scheme (cf. Table 3.3) as single step. To assess the accuracy of these initial co-states, the equations of motion of state (Eqs. (3.2a)– (3.2b)) and co-states (Eqs. (3.9a)–(3.9f) and Eq. (3.21)) are numerically integrated until the final flight time. The deviations in the position and velocity from the target site are found to be large. So, in order to reduce the deviations, a multi-step DT scheme is proposed to get the co-states at a regular interval of time during the descent phase. The computed co-states are used (to find the thrust acceleration components) along with numerical integration of state (Eqs. (3.2a)– (3.2b)) equations to get the soft landing trajectory. The advantage of a multi-step DT scheme is that numerical integration of co-states avoided. The deviations in the target state are given in Table 3.6 for different DT step sizes. It was noted that with the decrease in the DT step size the deviations in the target state decrease. The error stabilizes after the DT step size of 0.5 s and so, for all further studies a step size of 0.5 s is used.

Table 3.5 Determined initial co-states with single step using DT

Co-state	Initial co-states
p_x	0.0021967561
p_y	-0.0000000005
p_z	-0.0000821967
p_{vx}	-0.0499497483
p_{vy}	0.0001835
p_{vz}	-0.8887777192

Table 3.6 Influence of DT step size on DT scheme

Target Parameter deviations	Single step (step size=543.955 s)	Multi-step DT				
		Step size 50 s	Step size 5 s	Step size 1s	Step size 0.5 s	Step size 0.1 s
Position (m)	17890	14726	1270	1.02	0.35	0.35
Velocity (m/s)	520	65	6.48	0.76	0.036	0.036

Another parameter that influences the performances of DT is the number of terms to be considered in the series expansion (as discussed in the example provided in section 3.4.2). Table 3.7 provides the summary of the deviations from the target state for different number of DT terms and DT step size together. When the number of term is ≥ 15 the deviations remain same. So, for further studies, the number of DT terms is fixed at 15 and the step size for multi-step DT scheme is fixed as 0.5s. The term multi-step DT scheme is named as the DT scheme for further cases studies.

Table 3.7 Influence of number of terms of series expansion (n) and step size on the DT scheme

Number of DT terms	DT step size 5.0 s		DT step size 1.0 s		DT step size 0.5 s		DT step size 0.1 s	
	Position deviation from target (m)	Velocity deviation from target (m/s)	Position deviation from target (m)	Velocity deviation from target (m/s)	Position deviation from target (m)	Velocity deviation from target (m/s)	Position deviation from target (m)	Velocity deviation from target (m/s)
3	16570	102	65	98	8	95	8	80
5	1522	93	15	32	3	26.5	3	25.5
10	1310	6.9	8.4	1.6	0.382	0.04	0.382	0.0393
15	1270	6.48	1.02	0.76	0.35	0.036	0.35	0.036
20	1270	6.48	1.02	0.76	0.35	0.036	0.35	0.036
50	1270	6.48	1.02	0.76	0.35	0.036	0.35	0.036

3.6.3 Time-optimal Trajectory using Multi-step DT Scheme (DT-DE Scheme)

As discussed earlier, in the DT-DE scheme, the flight time is an unknown parameter. The unknown flight time is selected using DE and the multi-step DT scheme is employed to find the deviation of state from target state. at the selected flight time. The objective function for the optimization process is the deviation in the position and velocity components of corresponding to the target site (cf. Eq. (3.25)). The target site

given in Table 3.4, as mentioned earlier, is used. The optimal flight time and the landing mass obtained using DT-DE scheme are given in Table 3.8. Note that the optimal trajectory with DE scheme (cf. section 3.6.1) is reproduced and the target site is achieved using the DT-DE scheme.

The profiles of altitude, velocity and thrust acceleration components are given in Figs. 3.2 -3.4 for both DE and multi-step DT-DE schemes. Also the differences between the altitudes and velocities of the two schemes are given in Fig. 3.2 and Fig.3.3. A perfect match of the profiles for the two schemes can be seen.

The initial co-states determined using DT is given in Table 3.9. Note that the initial co-states determined using the DT scheme (cf. Table 3.9) close to the initial co-states obtained using the DE scheme (cf. Table 3.2). The profiles of the control variables of the two schemes are exactly same. Further, the ratios of z-component of velocity to other co-state variables given in Table 3.2 and Table 3.9 are nearly same.

The computational time for the DT-DE scheme is very less compared to DE scheme (cf. Table 3.10). The computational time for the DE scheme will be even larger than 170 s if wider bounds are used for the unknowns.

Table 3.8 Time-optimal trajectory using multi-step DT-DE scheme

Parameter	Value
Flight time (s)	543.96
Landing Mass(kg)	487.04

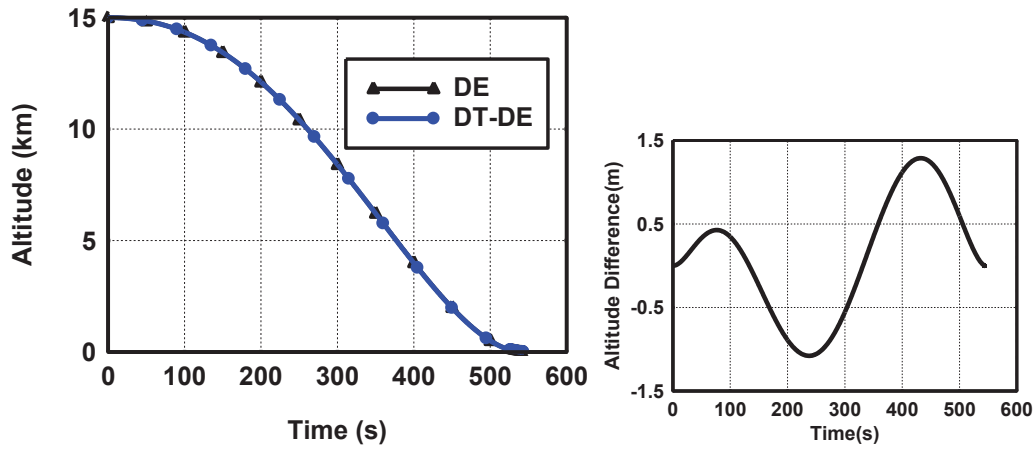


Fig. 3.2. Altitude profile comparison – time-optimal solution

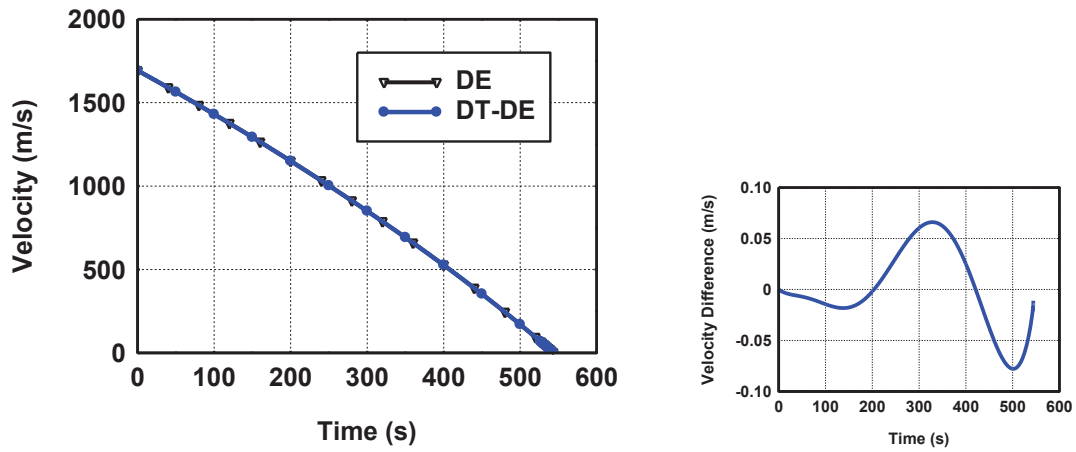


Fig. 3.3. Velocity profile comparison – time-optimal solution

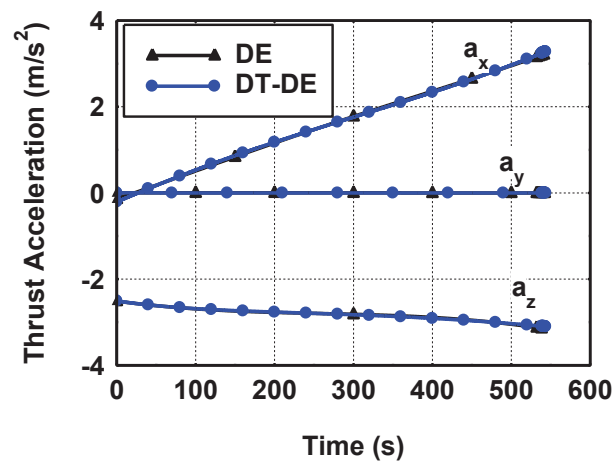


Fig. 3.4. Thrust acceleration components- time-optimal case

Table 3.9 Determined initial co-states using multi-step DT-DE scheme

Co-state	Initial co-states	$\frac{p_{vz}}{p_i}$ ($i = x, y, z, vx, vy, vz$)
p_x	0.0021950378	-386.27
p_y	-0.0000000005	1.6957E9
p_z	-0.0000783060	10828
p_{vx}	-.047307780	17.923
p_{vy}	1.7490112E-007	-4.8477E6
p_{vz}	-0.84787407188	1

Table 3.10 Comparison of computational time

Solution scheme	Computational time (CPU time) s
DE	170
DT-DE	35

3.6.4 Energy-optimal Trajectory Using DE and DT-DE Schemes (Unlimited Thrust)

For energy-optimal case, ideally, the thrust available needs to be unbounded and the optimal thrust acceleration components are computed as given in Eqs. (3.11a)–(3.11c). In this formulation, the control variables do not depend on the co-state of mass of the lander module. Therefore, the computation of co-state of mass is not necessary in the solution process.

Table 3.11 Unknown initial co-states – energy-optimal (unlimited thrust)

co-states	DE scheme		DT-DE Scheme	
	initial co-states	$\frac{p_{vz}}{p_i}$ ($i = x, y, z, vx, vy, vz$)	initial co-states	$\frac{p_{vz}}{p_i}$ ($i = x, y, z, vx, vy, vz$)
p_x	0.01027842	71.595	0.01027986	71.529
p_y	-0.0000002	-3.6794E6	-0.0000002	-3.6765E6
p_z	-0.01224733	-60.085	-0.01225106	-60.02
p_{vx}	0.79802162	0.92213	0.79823871	0.92116
p_{vy}	-0.00000064	-1.1498E6	-0.00000064	-1.1489E6
p_{vz}	0.73588012	1	0.73530857	1

Table 3.12 Optimal trajectory – energy-optimal (unlimited thrust)

Parameter	DE scheme	DT-DE Scheme
Flight time (s)	454.140	454.149
Final Mass(kg)	494.317	494.311
Computational Time (s)	168	40

For the DT-DE scheme as in the case time-optimal problem, the flight time is an unknown parameter. The unknown flight time is selected using DE and the multi-step DT scheme is employed to find the deviation at the selected flight time. The target site given in Table 3.4, as mentioned earlier, is used for demonstration. The initial co-states and trajectory parameters obtained using the two schemes are provided in Table 3.11 and 3.12 for the optimal trajectory. The flight time is less compared to time-optimal problem because of the assumption of unlimited thrust. The profiles of thrust and thrust acceleration components are given in Figs. 3.5-3.6 for both DE and multi-step DT-DE schemes. A perfect match of the profiles from the two schemes can be seen.

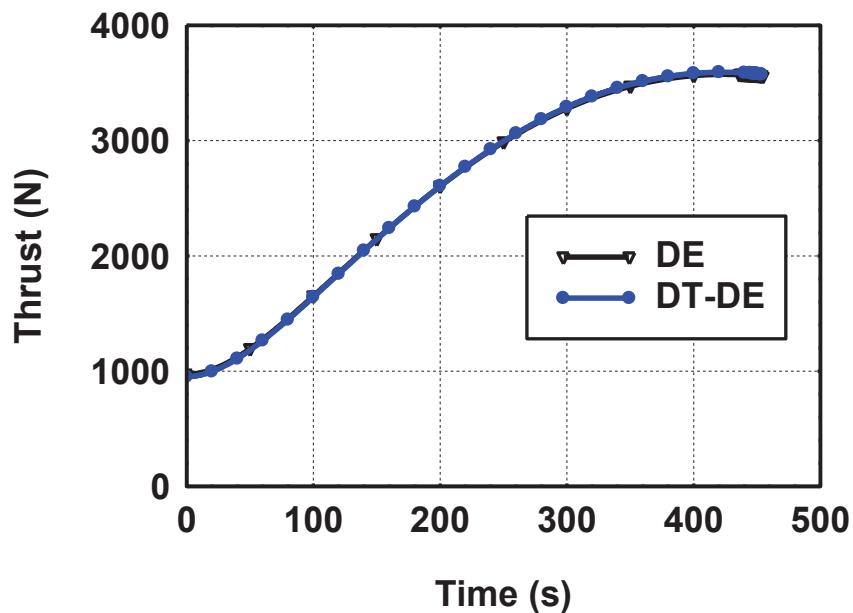


Fig. 3.5. Required thrust profile comparison: energy-optimal -unlimited thrust

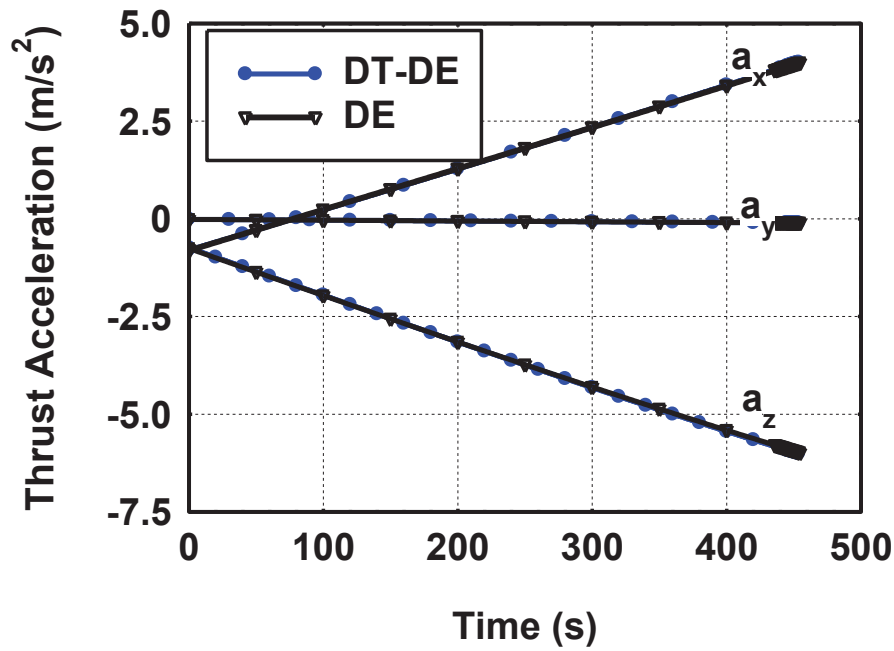


Fig. 3.6. Required thrust acceleration comparison: energy-optimal -unlimited thrust

3.6.5 Energy-optimal Trajectory using DE and DT-DE Schemes (With Limited Thrust)

For demonstration, the thrust limit is kept as 2200 N. Table 3.13 provides the optimal trajectory parameters. The final landing mass is close to the landing mass obtained in minimum time solution (cf. Table 3.3). Figure 3.7 depicts the thrust acceleration profiles. The initial co-states obtained using both schemes are given in Table 3.14 and ratios are also provided in Table 3.14. The optimal trajectory parameters and the control parameters are same.

Table 3.13 Optimal trajectory parameters – energy-optimal with limited thrust

Parameter	DE scheme	DT-DE scheme
Flight time (s)	543.982	543.99
Final Mass(kg)	487.02	487.01
Computational Time (s)	172	38

Table 3.14 Unknown initial co-states comparison – energy-optimal with limited thrust

Co-state	Initial values			
	DE scheme		DT-DE scheme	
	initial co-states	$\frac{p_{vz}}{p_i}$ ($i = x, y, z, vx, vy, vz$)	initial co-states	$\frac{p_{vz}}{p_i}$ ($i = x, y, z, vx, vy, vz$)
p_x	0.00553760	458.2	0.00553760	458.21
p_y	-0.000000101	-2.5123E7	-0.000000103	-2.4635E7
p_z	-0.00143334	-1770.3	-0.00143334	-1770.3
p_{vx}	0.02238520	113.35	0.02238524	113.35
p_{vy}	-0.00000053	-4.7876E6	-0.00000053	-4.7876E6
p_{vz}	2.53740946	1	2.53740936	1

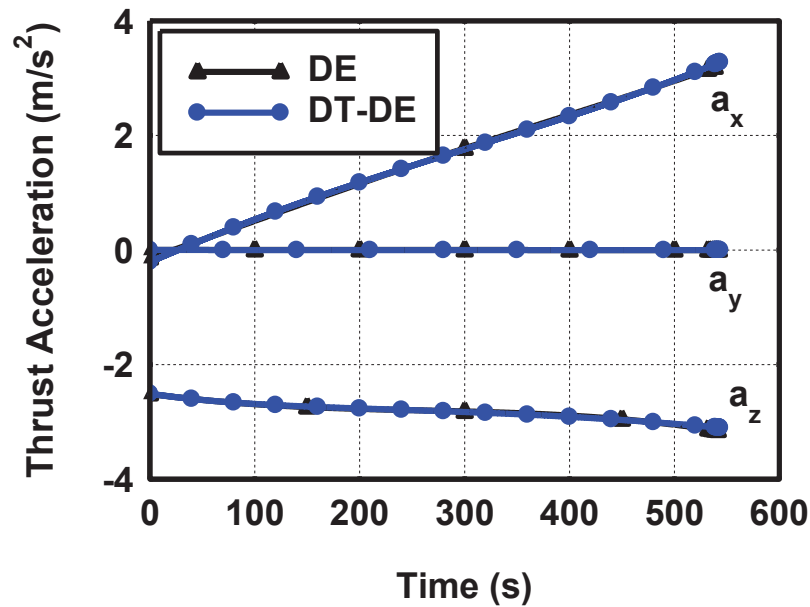


Fig. 3.7. Thrust acceleration profile comparison – energy-optimal with limited thrust

3.6.6 Fuel-optimal Trajectory Using DE and DT-DE Schemes

The fuel-optimal trajectory is generated using the DE scheme and the DT-DE scheme and is provided in Table 3.15. The trajectory corresponds to the input conditions provided in Table 3.1 and target site as given in Table 3.4. As in other cases, the initial co-states obtained using the two schemes are given in Table 3.16. The optimal trajectory is generated by both the schemes are very close.

Table 3.15 Optimal trajectory – fuel-optimal

Parameter	DE scheme	DT-DE scheme
Flight time (s)	543.96	543.97
Landing Mass(kg)	487.04	487.03
Computational time	167	35

Table 3.16 Unknown initial co-states – fuel-optimal

Co-states at time=0	DE scheme		DT-DE scheme	
	Initial co-states	$\frac{p_{vz}}{p_i}$ ($i = x, y, z, vx, vy, vz$)	Initial co-states	$\frac{p_{vz}}{p_i}$ ($i = x, y, z, vx, vy, vz$)
p_x	-0.0012602	448.15	-0.0012636	446.94
p_y	0.00000009	-6.2751E6	0.000000091	-6.2061E6
p_z	0.0003581	-1577.1	0.0003559	-1586.8
p_{vx}	-8.093487E-3	69.78	-8.19694E-3	69.899
p_{vy}	1.20203E-07	-4.6984E6	1.201609E-7	-4.771E6
p_{vz}	-0.56476102	1.0	-0.56475694	1.0

The profiles of thrust acceleration components are given in Fig. 3.8 for both DE and multi-step DT-DE scheme. A perfect match of the profiles from the two schemes can be seen.

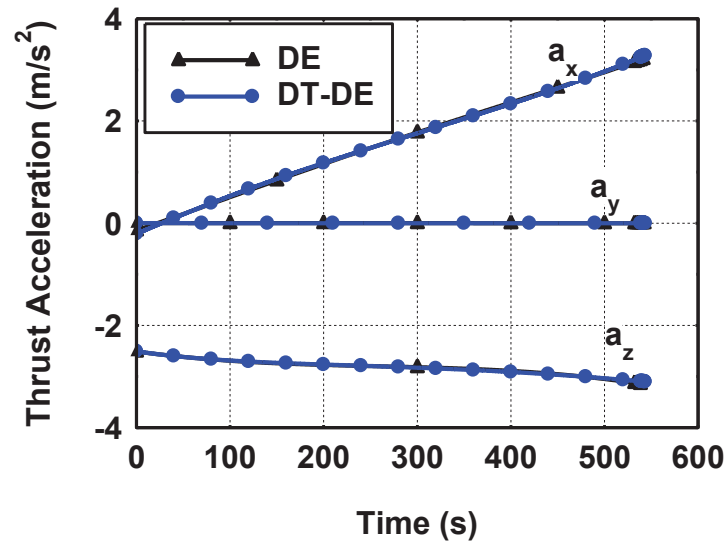


Fig. 3.8. Thrust acceleration components – fuel-optimal

3.6.7 Comparison of Optimal Solution with Different Performance Measures

The optimal solution with the DT-DE scheme as discussed in sections 3.6.3, 3.6.5 and 3.6.6 for time-optimal, energy-optimal (with limited thrust) and fuel-optimal are summarized in Table 3.17. It is to be noted that results for all three formulations are nearly same. These results are nearly the same because of the following reasons (i) the target landing site of minimum time solution is used as the target in all cases (ii) energy-optimal case thrust limited to a maximum value (iii) time-free problem. For the time-optimal trajectory, the thrust settles at maximum throughout the descent phase. For the fuel-optimal trajectory (for final time free problem) to the target landing site of minimum time solution, the thrust settles to the maximum throughout the descent. For the energy-optimal trajectory, (for final time free problem), to the target landing site of minimum time solution, the thrust settles to maximum value in the limited thrust case. So in all cases the optimal solution is nearly same. The theoretical formulations given in sections 3.3.1, 3.3.2 and 3.3.3 also clearly support these phenomena.

Table 3.17 Comparison of optimal solutions - DT-DE scheme

Parameter	Value		
	Time-optimal	Energy-optimal with thrust limit	Fuel-optimal
Flight time (s)	543.96	543.99	543.97
Landing Mass (kg)	487.04	487.01	487.03

For a time-fixed problem for fuel-optimal/energy-optimal (limited thrust) the results could be different. Also, if there is a change in the target site the solutions will be different. To demonstrate this, an alternate landing site very close to the minimum time trajectory is selected along the orbital track which is 2 deg. ahead of minimum time impact latitude (cf. Table 3.4) and it is provided in Table 3.18. The optimal solutions that lead to soft landing on this site under fuel-optimal and energy-optimal performance measures are given Table 3.19. Note that although the landing site is different from the reference target site, the landing masses are only marginally different from the solutions of reference target. The fuel-optimal formulation introduces coasting

(zero thrust) and achieves the optimal landing mass. Furthermore, the solution of energy-optimal, especially flight time, is different from the other two solutions. The thrust is varied within the limit (no zero thrusting periods) throughout the descent and the target site is achieved. Whereas, for fuel-optimal trajectory, zero thrusting duration is introduced by the formulation. The thrust-time profiles are given in Fig.3.9 and Fig.3.10. In Fig.3.9, the vertical line during the thrusting phase indicates zero thrust for certain time instants and introduction of optimal coasting duration realizes the maximum landing mass. The landing target longitude and latitude are varied and the performance of fuel-optimal and energy-optimal are summarized in Table 3.20 and 3.21. The penalties on landing mass are marginal for different along track target site (0 deg. longitude cases). The landing mass penalty observed for 2 deg. and 4 deg. out of plane targets (cf. Table 3.20 and Table 3.21) are 5 kg and 17 kg respectively.

Table 3.18 Alternate landing site

Parameter	Value
Latitude (deg. North)	18.1508
Longitude (deg.)	0.0

Table 3.19 Comparison of optimal solutions

Parameter	Value	
	Energy-optimal with thrust limit	Fuel-optimal
Flight time (s)	588.06	579.98
Landing Mass (kg)	486.6	486.671
Zero thrust duration (s)	-	35.98

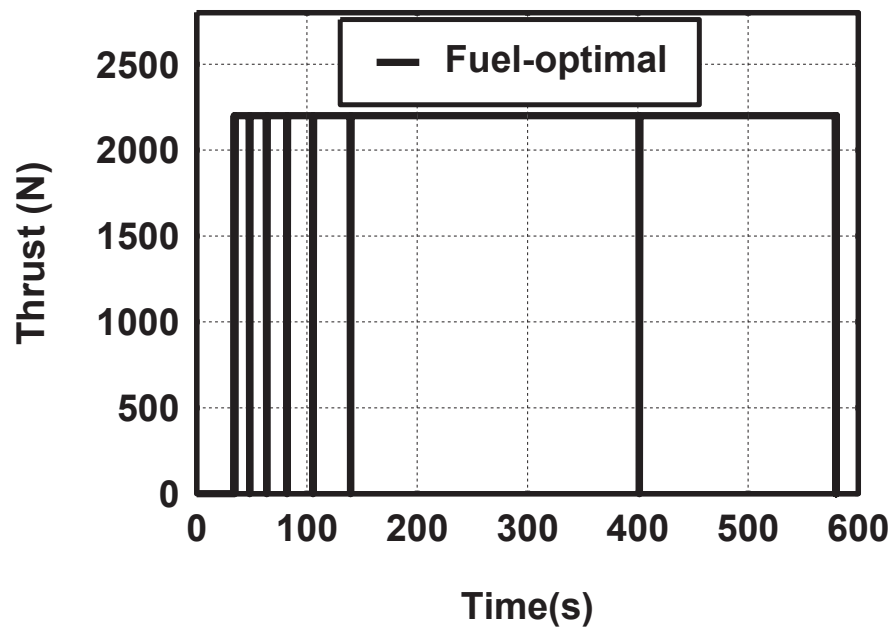


Fig. 3.9. Fuel-optimal thrust profile

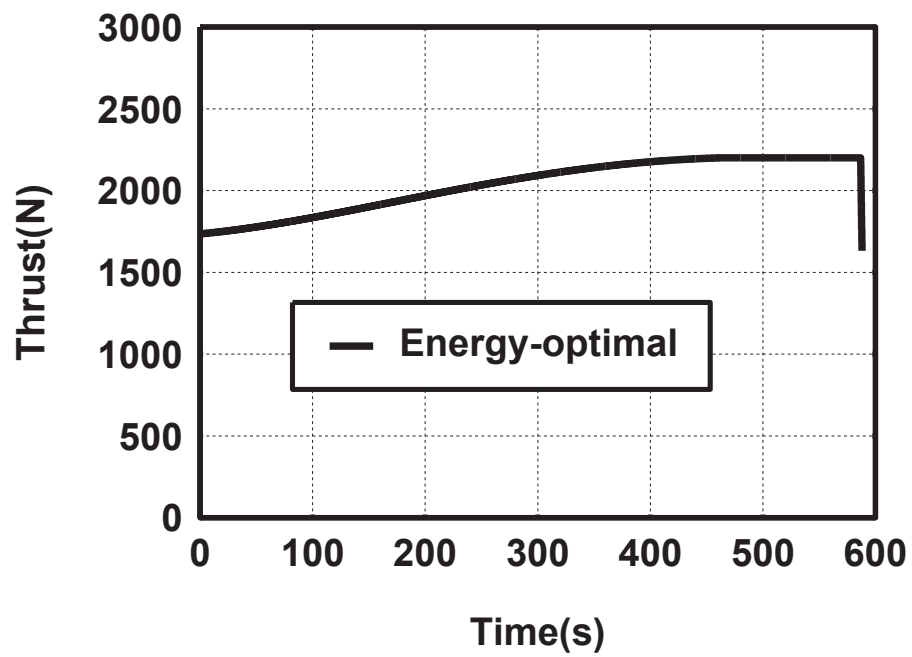


Fig. 3.10. Energy-optimal thrust profile- with limited thrust

Table 3.20 Performance summary of energy-optimal: alternate landing sites

Latitude (deg. North)	Longitude (deg.)	Flight time (s)	Landing mass (kg)
16.1508	0.0	543.99	487.01
18.1508	0.0	588.06	486.6
20.1508	0.0	630.46	485.8
18.1508	2.0	590.17	481.06
20.1508	4.0	636.56	468.27

Table 3.21 Performance summary of fuel-optimal: alternate landing sites

Latitude (deg. North)	Longitude (deg.)	Flight time (s)	Zero thrust duration (s)	Landing mass (kg)
16.1508	0.0	543.97	0.0	487.03
18.1508	0.0	579.98	35.98	486.67
20.1508	0.0	615.5	71.5	486.65
18.1508	2.0	583.2	32.6	482.4
20.1508	4.0	625.9	56.1	469.8

3.6.8 Performance of Gradient Based Method with DT

In this section, the efficiency of gradient based scheme in selecting the single unknown parameter of flight time is explored. In this study, the MATLAB function ‘fmincon’ is used to find the flight time and used in DT scheme. This scheme is named as the DT-SQP scheme and its performance is compared with the DT-DE scheme. The performance measure chosen for this assessment is energy-optimal with unlimited thrust. For this case, the guidelines for getting the bounds for flight time are not applicable. Both DE as well as SQP needs a range of values (bounds) for the unknown and additionally, SQP needs an initial guess for the unknown parameter. For the flight time bounds [400 s 600 s], DT-SQP scheme converges and the solution closer to the DT-DE scheme (cf. Table 3.22). However, when the range is wider, SQP converges to a local minimum with the initial guess as 400 s. Therefore, the DT-DE scheme which avoids non-convergence is preferred over DT-SQP.

Table 3.22 Comparison of computational time

Bounds on Flight time	DT – DE Scheme	DT-SQP (Initial guess = 400 s)
	Landing mass (kg)	Landing mass (kg)
400 s – 600 s	494.311	494.309
300 s – 1000 s	494.311	486.6 (local minimum)

3.6.9 Summary of Merits and Demerits of Different Solution Schemes

The merits and demerits of different solution schemes are compared in Table 3.23. In DT-DE scheme, the major advantage is that the co-state equations need not be numerically integrated to find the control variables at each computational step. Furthermore, the number of unknowns reduces to one. In a conventional indirect approach without DT, the numbers of unknowns are eight and numbers of equations are fourteen including the co-state equations. In direct scheme, the number of unknowns depends on the number of nodes selected.

Table 3.23 Comparison of solution schemes

Solution Scheme	Number of unknowns	Unknown variables	Number of equations numerically integrated
Indirect approach (Conventional)	Eight	Initial co-states and flight time ($p_x, p_y, p_z, p_{v_x}, p_{v_y}, p_{v_z}, p_m, t_f$)	Fourteen
Direct approach using NLP	3*No. of Nodes selected + flight time	Depends on number of Nodes. At each node the thrust acceleration components are the unknowns along with flight time	Seven
DT-DE (proposed)	One	Flight time (t_f)	Seven

3.7 Strategy for Vertical Landing at Touch down

In this section a strategy is included in the DT-DE formulation to achieve vertical landing at the time of touchdown. In this strategy, the horizontal velocity is nullified and an appropriate vertical velocity is achieved at a chosen altitude. This strategy results

in zero acceleration components (except vertical) at the chosen altitude ensuring vertical orientation for landing. Required vertical velocity at chosen altitude can be selected using DE along with unknown flight time. Therefore, the number of unknown becomes two for this strategy. The bounds on the vertical velocity for DE can be computed with acceleration level (assumed to be constant) during the vertical braking phase using one-dimensional kinematic equation $v^2 = u^2 + 2aS$. The procedural steps for the strategy are the following,

1. Input target longitude and latitude and the altitude at horizontal braking end (say 30m) and find the initial position vector

$$x_T = r_T \cos(\phi_T) \cos(\lambda_T) \quad (3.46a)$$

$$y_T = r_T \cos(\phi_T) \sin(\lambda_T) \quad (3.46b)$$

$$z_T = r_T \sin(\phi_T) \quad (3.46c)$$

Where r_T, ϕ_T, λ_T are radial distance (Moon radius +30 m), lunar centric latitude and lunar centric longitude respectively.

2. Select the flight time and vertical velocity (v_v) at the end of horizontal braking using DE
3. Use the vertical velocity (v_v) at the end of braking to compute the target velocity vector at the end of horizontal braking

$$vx_T = v_v \cos(-\phi_T) \cos(\lambda_T + 180) \quad (3.47a)$$

$$vy_T = v_v \cos(-\phi_T) \sin(\lambda_T + 180) \quad (3.47b)$$

$$vz_T = v_v \sin(-\phi_T) \quad (3.47c)$$

4. Simulate the trajectory up to chosen altitude (using DT for co-state computation in multi steps). Further simulate from chosen altitude till touchdown. In this phase, the co-state computation with DT not required since thrust direction is vertical.
5. Compute the deviation in target velocity at chosen altitude and position at touchdown. If the deviation is within threshold stop the computation
6. If the deviation is more, go to step 2.

The next step is to find the thrust attitude angle which needs to be vertical at the end of horizontal braking phase. The formulation uses a Local-Vertical Local-Horizontal (LVLH) coordinate frame. LVLH frame is aligned such that the x-direction is in the local vertical ('radial'), the z-direction is in the direction of the orbit normal, and the y-direction is along track direction and it forms a right-handed coordinate system. The origin of the system is at the center of mass of the module. The acceleration and velocity vector is transformed from Moon centered frame to LVLH frame with the following transformation to find the terminal thrust acceleration attitude.

$$R_{MCI_LVLH} = \begin{bmatrix} \frac{\vec{r}}{r} \\ \frac{(\vec{r} \times \vec{v}) \times \vec{r}}{\|(\vec{r} \times \vec{v}) \times \vec{r}\|} \\ \frac{(\vec{r} \times \vec{v})}{\|(\vec{r} \times \vec{v})\|} \end{bmatrix} \quad (3.48)$$

Where \vec{r} and \vec{v} are position and velocity vector in MCI frame. If the acceleration unit vector components represented in LVLH frame ($a_{TLux}, a_{TLuy}, a_{TLuz}$). The thrust acceleration attitude from local horizontal computed as

$$\text{In plane angle} \quad \alpha = \text{atan2}\left(\frac{a_{TLux}}{a_{TLuy}}\right) \quad (3.49a)$$

$$\text{Out of plane angle} \quad \beta = \text{atan}\left(\frac{a_{TLuy}}{a_{TLuz}}\right) \quad (3.49b)$$

To demonstrate the strategy, an altitude of 30 m is chosen at which zero horizontal velocity and appropriate vertical velocity at 30 m to be selected by the optimizer. The altitude may be chosen according to the mission needs. The steps to find the target velocity/position are the following,

The input parameters provided in Table 3.1 are considered for this study. The target conditions to be achieved at 30 m altitude are given in Table 3.24. Because of the assumption of non- rotating Moon and vertical landing, the latitude and longitude are same at 30 m altitude as that of target landing site. Fuel-optimal and energy-optimal DT-DE schemes have been evaluated with this strategy for vertical orientation and

presented in Table 3.25 and 3.26. The flight time from 30 m altitude to touch down is about 4.3 to 4.5 s and the landing mass is 485.6 kg for fuel-optimal and 485.2 kg for energy-optimal DT-DE scheme. The thrust attitude variation is shown in Fig. 3.11 for fuel-optimal and energy-optimal case and the required thrust attitude of 90 deg. is achieved for both cases during the terminal vertical landing phase.

Table 3.24 Target conditions

Parameter	Value
Latitude (deg. North)	16.1508
Longitude (deg.)	0.0
Target Terminal altitude (m)	30
Target Terminal velocity in radial direction (m/s)	Selected by DE
Target terminal velocity in horizontal direction (m/s)	0.0

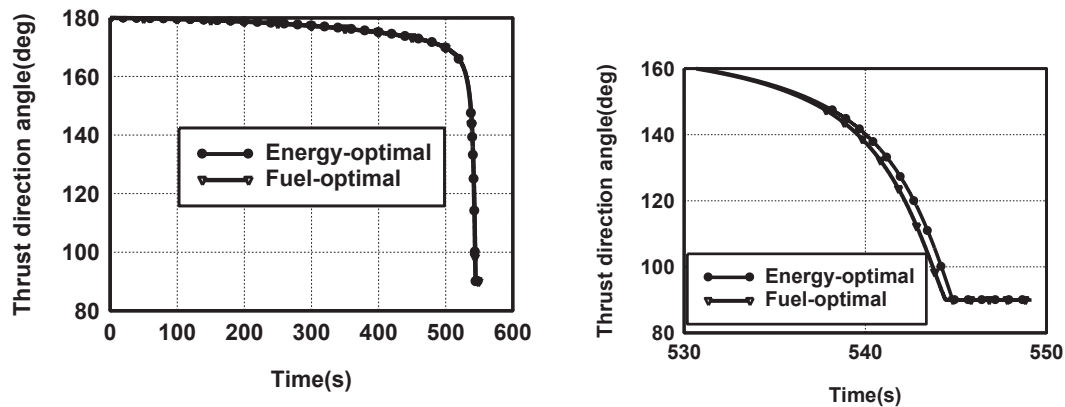


Fig. 3.11. Thrust direction variation for fuel-optimal and energy-optimal DT-DE schemes.

Table 3.25 Performance of the DT-DE scheme (fuel-optimal) for vertical landing

Parameter	DE scheme	DT-DE scheme
Flight Time (s) (touch down time)	548.9	548.91
Time to reach 30m altitude (s)	544.39	544.4
Landing Mass (kg)	485.61	485.6
Zero thrust duration (s)	1.9	2.0
Horizontal velocity @ 30m altitude (m/s)	1.5E-6	4E-6
Vertical velocity @ 30m altitude (m/s)	-13.14	-13.13
Vertical velocity @ touchdown (m/s)	0.01	0.01
Terminal thrust direction from local horizontal (deg.)	90	90

Table 3.26 Performance of the DT-DE scheme (energy-optimal) with terminal vertical thrust direction

Parameter	DE scheme	DT-DE scheme
Flight Time (s) (touch down time)	549.09	549.1
Time to reach 30m altitude (s)	544.8	544.8
Landing Mass (kg)	485.2	485.2
Horizontal velocity @ 30m altitude (m/s)	1.5E-6	2.1E-6
Vertical velocity @ 30m altitude (m/s)	-13.16	-13.16
Vertical velocity @ touchdown (m/s)	0.01	0.01
Terminal thrust direction from local horizontal (deg.)	90	90

3.8 Conclusion

The challenge in determining the initial co-states is dealt through a new computational indirect scheme. The efficiency of the multi-step Differential Transformation (DT) technique in achieving the target site precisely is demonstrated. With a step size of 0.5 s, the deviation in the target site is brought down to 35 cm in position and to 3.6 cm/s in touchdown velocity. The number of unknowns of the two-point boundary value problem is reduced to just one, which removes the complexity in the solution process to a large extent. The Differential Evolution (DE) technique obtains the solution very quickly using the initial co-states determined by the DT technique and the guidelines on the flight time. The optimal landing trajectory is generated quickly without losing the advantages of the indirect scheme. The computational time to generate the optimal solution using the DT- DE scheme is about 35 to 40 s and whereas using the DE scheme, which uses bounds for initial co-states also, it is about 170 s. The computational time for the DT-DE scheme is comparable with a gradient based optimizer that uses the initial co-states determined by the DT technique. Further, the use of the DE technique along with the DT technique avoids non-convergence and local convergence scenarios, which occur when gradient based optimizer is used. The robustness of the scheme is demonstrated through the performance of the proposed DT-DE scheme for different performance measures. The ability of the proposed scheme to introduce coasting during descent is demonstrated.

Chapter 4

Performance and Design analysis using the DT-DE scheme

Chapter Summary

The performance of the DT-DE scheme is assessed for different mission scenarios. The implication on optimal landing mass when the descent is initiated from different periapsis altitudes is assessed. The capability of the DT-DE scheme to introduce coasting or variation of thrust during descent for higher flight durations to land at the pre-fixed target site is demonstrated. A strategy to select a suitable choice of periselinum location and true anomaly of the intermediate orbit to realize this scenario is discussed. An assessment of landing masses for different objectives (i) fuel-optimal and (ii) energy-optimal is presented.

4.1 Optimal Trajectory Design from Different Perilune Altitudes

In Chapter 3, in all the case studied to generate an optimal soft landing trajectory, the powered braking phase is initiated at 15 km altitude (cf. Table 3.1). In this section, the effect of initiating powered phase at different perilune altitudes of intermediate transfer orbit is studied. Both fuel-optimal and energy-optimal trajectories that land at the target site are generated. The results are summarized in Table 4.1 and Table 4.2 for fuel-optimal and energy-optimal (limited thrust) formulations respectively. As expected, with higher perilune altitude, the flight time to touch down increases. The fuel-optimal thrust profiles adjust the zero thrust duration and achieves the target site with a landing mass close to the case of 15 km perilune. In the energy-optimal case, the thrust magnitude is varied to achieve the soft landing at the target site. The thrust profile for the case of perilune altitude of 20 km is shown in Fig.4.1 for fuel-optimal and in Fig. 4.2 for energy-optimal formulations. For about 100 s (from 100 s to 200 s) the thrust

requirement is less than the maximum available thrust level of 2200 N for the energy-optimal formulation. For higher perilune altitudes, the marginal advantage of landing mass for fuel-optimal over energy-optimal increases. In Fig.4.1 (also in Figs. 4.4, 4.8, 5.3 and 5.7) the vertical line during the thrusting phase indicates that thrust becomes zero to achieve maximum landing mass. For many mission scenarios, the fuel-optimal DT guidance provides bang-bang control as the solution in which the engine is to be operated in on-off mode. Practically it may be difficult to operate the main engine in the on-off mode. For practical guidance applications the engine can throttle to a lower limit of 40% or 60% of full thrust. The performance of the algorithm is analyzed in section 5.4.2 for 40 % of lower thrust instead of zero thrust.

Table 4.1 Sensitivity to Perilune altitudes for fuel-optimal trajectory

Perilune altitude (km)	Flight time (s)	Landing mass (kg)	Zero thrust duration (s)
15	543.97	487.03	0.0
20	546.8	487.01	2.97
25	548.5	486.7	4.1
30	552.1	485.6	4.5

Table 4.2 Sensitivity to Perilune altitudes for energy-optimal (limited thrust) trajectory

Perilune altitude (km)	Flight time (s)	Landing mass (kg)
15	543.99	487.01
20	548.21	486.5
25	551.17	485.7
30	554.1	484.5

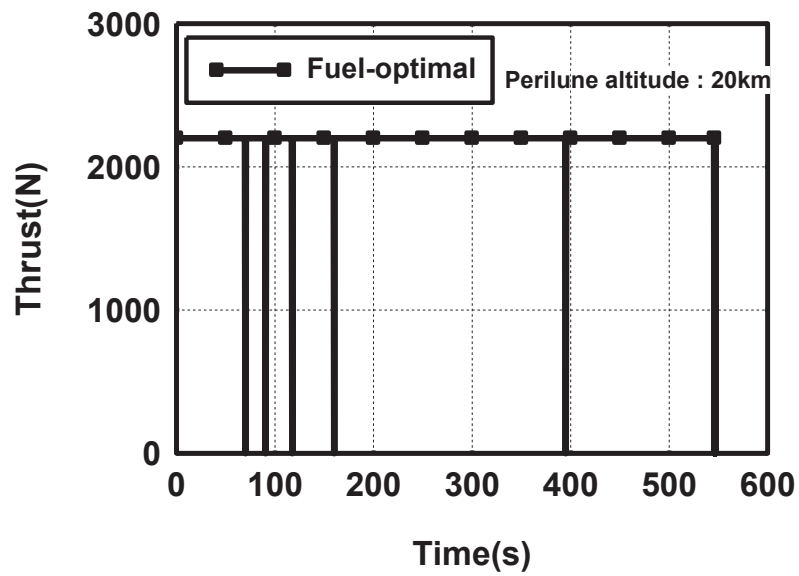


Fig. 4.1. Thrust profile for fuel-optimal formulation for initial perilune altitude of 20 km

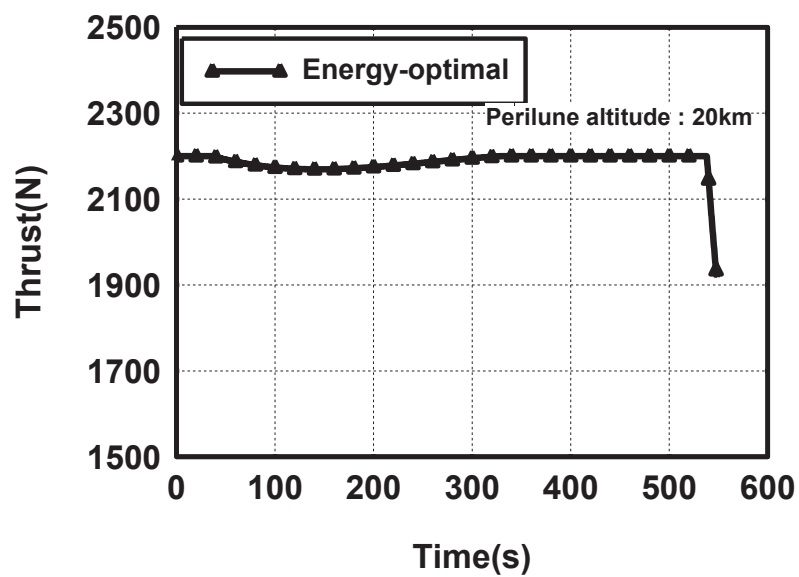


Fig. 4.2. Thrust profile for energy-optimal (limited thrust) formulation for initial perilune altitude of 20 km

4.2 Realization of a Target Site with Different Descent Flight Durations with a Fixed Periapsis Location

With the selection of true anomaly at the start of powered braking, the initial altitude at powered braking changes appropriately to meet the target conditions. For the fuel-optimal case, the thrust throttling time duration varied for the fuel-optimal usage. In the energy-optimal case with limited thrust, the thrust level optimally varied to meet the target conditions.

Usually for soft landing mission studies, the target location will be fixed and the initial state need to select optimally for powered braking initiation. For all cases discussed in Chapter 3, the braking maneuver starts from the perilune of 100x15 km lunar orbit, i.e when true anomaly is zero. In this section, the capability of the DT-DE scheme (for fuel-optimal and energy-optimal formulations) explored for the case with fixed flight time and final target, and the initial true anomaly is optimally selected using DE. With this, the altitude at the initiation of braking maneuver selected by the selection of true anomaly. The different initial and final states are provided in Table 4.3. Here the target is fixed as 0 deg. longitude and 0 deg. latitude below the selected nominal orbital track.

Table 4.3 Input parameters

Parameters	Value
Semi-major axis (m)	1795.5E3
Eccentricity	0.023670287
Inclination (deg.)	90
Argument of perilune (deg.)	0
Longitude of ascending node (deg.)	0
True anomaly (deg.)	Selected using DE
Maximum Thrust (N)	2200
Specific Impulse (s)	315
Mass (kg) @ 100x100km	880.0
Mass (kg) @ 100x15km	874.4
Target Latitude (deg.)	0.0
Target Longitude (deg.)	0.0
Flight time (s)	fixed

4.2.1 Performance of Fuel-optimal DT-DE scheme

For thrust limit cases as in Chapter 3 (Maximum thrust limited to 2200 N), the minimum time required for powered braking is about 544 s (cf. Table 3.3). Therefore, in the present analysis, the flight time fixed higher than 544 s and the different cases with results are provided in Table 4.4. Initial true anomaly is optimally selected to start the landing phase from appropriate altitude in the parking orbit of 100x15 km. Figure 4.3 shows the altitude and latitude profile (longitude is zero throughout the descent phase because inclination is 90 deg.) for the landing trajectory for three cases as in Table 4.4. For these cases the required thrust profile are shown in Fig. 4.4. For higher flight time cases, the trajectory need to be initiated at higher altitude and latitude to land at specified location. With this, the lander module needs to travel at a higher range before touch down. To cover the higher range in an optimal way, the thrust needs to be minimum (cf. Fig. 4.4) during the initial part of the descent. The optimal thrust profile with a higher zero thrust duration, achieves nearly same landing mass for all flight times when the fuel-optimal trajectory is attempted.

Table 4.4 Fuel-optimal DT-DE: touch down parameters with optimum initial true anomaly

Case No.	Flight time (s)	Optimum initial true anomaly	Initial altitude (km)	Initial longitude (deg.)	Initial latitude (deg.)	Final landing mass (kg)	Zero thrust duration (s)
1	600	-19.14	17.24	0.0	-19.14	486.95	55.9
2	800	-30.15	20.5	0.0	-30.15	486.92	255.27
3	1000	-41.1	25.05	0.0	-41.1	486.9	455.3

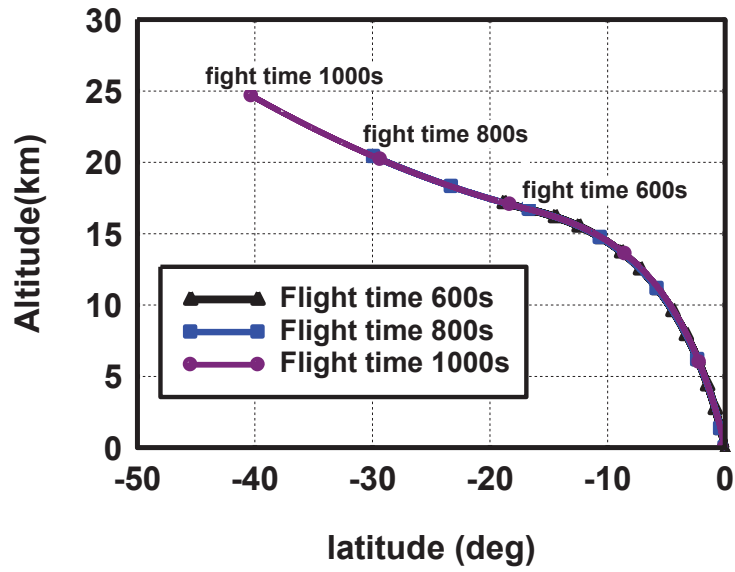


Fig. 4.3. Fuel-optimal trajectory profile for different fixed flight times

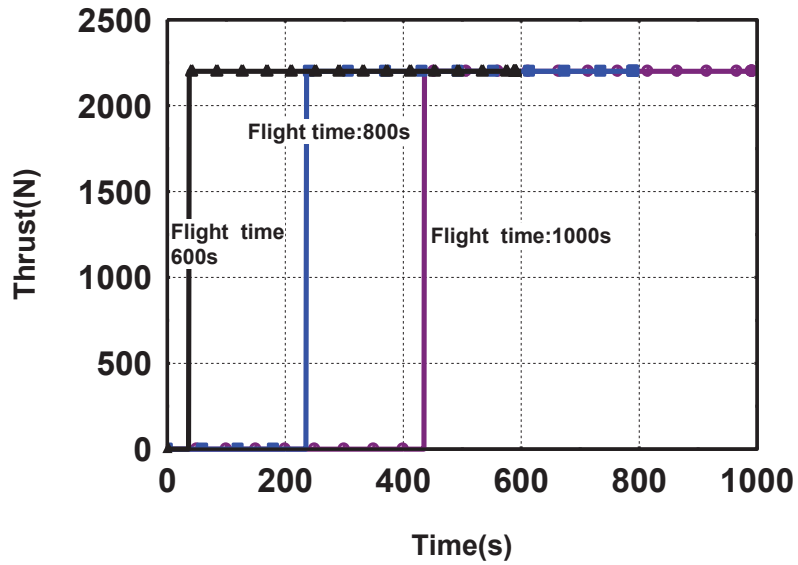


Fig. 4.4. Fuel-optimal thrust profiles for different fixed flight times

4.2.2 Performance of Energy-optimal DT-DE scheme

The initial true anomaly to start the powered landing phase resulting in an appropriate altitude in the parking orbit of 100×15 km is selected using DE. Figure 4.5 shows the altitude and latitude (zero longitude throughout descent) profile for the

landing trajectory for three cases as in Table 4.5. For these cases, the required thrust profiles are shown in Fig. 4.6. For higher flight times, the powered phase needs to be initiated at a higher altitude to realize landing at a specified location and so, the landing module needs to cover a larger range before touch down. To cover larger range in optimal way, the required thrust is lower (cf. Fig. 4.6) during the initial part of the descent. The nonlinear variation of the thrust profile results in an altitude profile that is not similar for all three cases.

Table 4.5 Energy-optimal formulation - touch down parametrs with optimum initial true anomaly

Case No.	Flight time (s)	Optimum initial true anomaly (deg.)	Initial altitude (km)	Initial longitude (deg.)	Initial latitude (deg.)	Final landing mass (kg)
1	600	-18.69	17.14	0	-18.69	486.2
2	800	-29.04	20.11	0	-29.04	484
3	1000	-37.4	23.4	0	-37.4	473.9

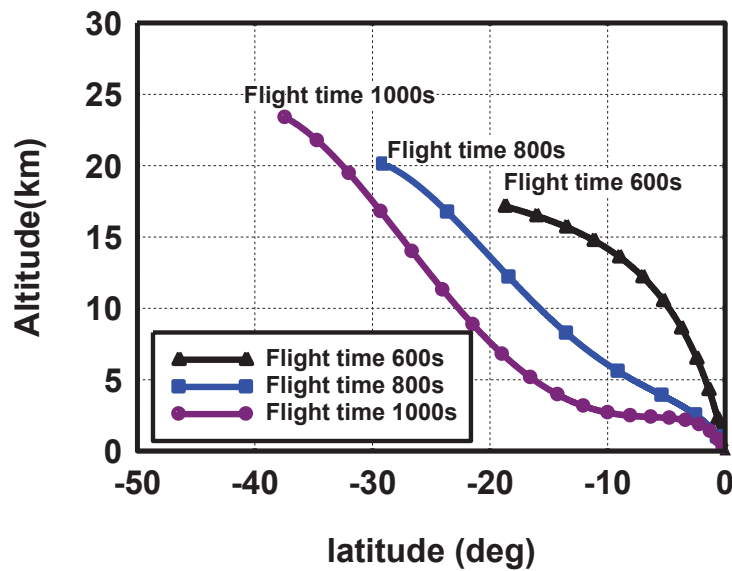


Fig. 4.5. Energy-optimal trajectory profiles for different fixed flight times

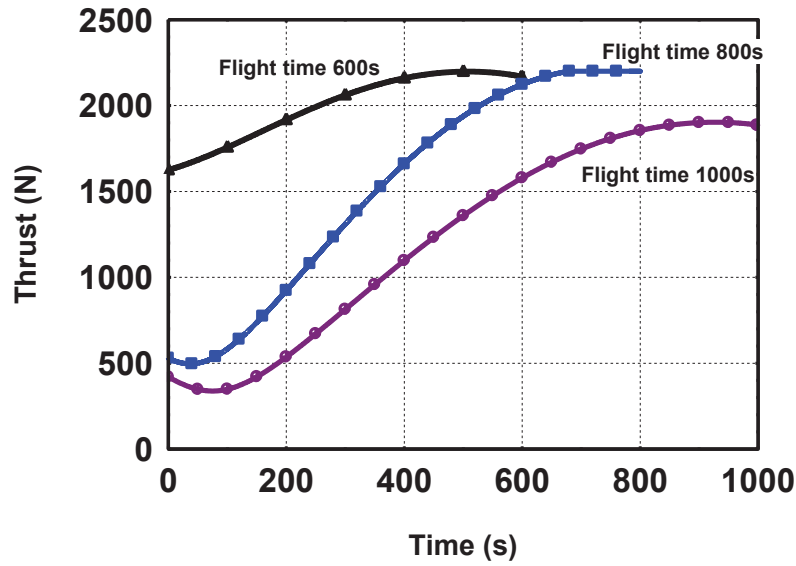


Fig. 4.6. Energy-optimal thrust profiles for different fixed flight times

4.3 Realization of a Target site with Different Descent Flight Durations by the Choice of Periapsis Location

In this section, the capability of the DT-DE schemes (for fuel-optimal and energy-optimal formulation with limited thrust) to reach the selected target site is explored for different flight times. This is achieved by selecting an appropriate argument of perilune using DE. Note that, in the earlier section, the argument of perilune is fixed and the true anomaly was selected using DE to achieve the target. When true anomaly is selected, the altitude at the start of powered phase varies. In this section, because argument of perilune is selected, the powered braking initiation happens always at perilune.

4.3.1 Performance of the Fuel-optimal DT-DE

Figure 4.7 shows the altitude and latitude (zero longitude during descent) profiles for the landing trajectory for three cases as in Table 4.6. For higher flight times, the zero thrust duration (cf. Fig.4.8) is higher (during the initial phase of descent). Therefore, the landing mass for the three cases are nearly same.

Table 4.6 Fuel-optimal DT-DE : Touch down parametrs with optimum initial argument of perilune (AOP)

Case No.	Flight time (s)	Optimum initial AOP (deg.)	Initial longitude (deg.)	Initial latitude(deg.)	Final landing mass (kg)	Zero thrust duration (s)
1	600	-19.11	0	-19.11	486.96	56.05
2	800	-30.1	0	-30.1	486.92	255.27
3	1000	-40.66	0	-40.66	486.91	455.4

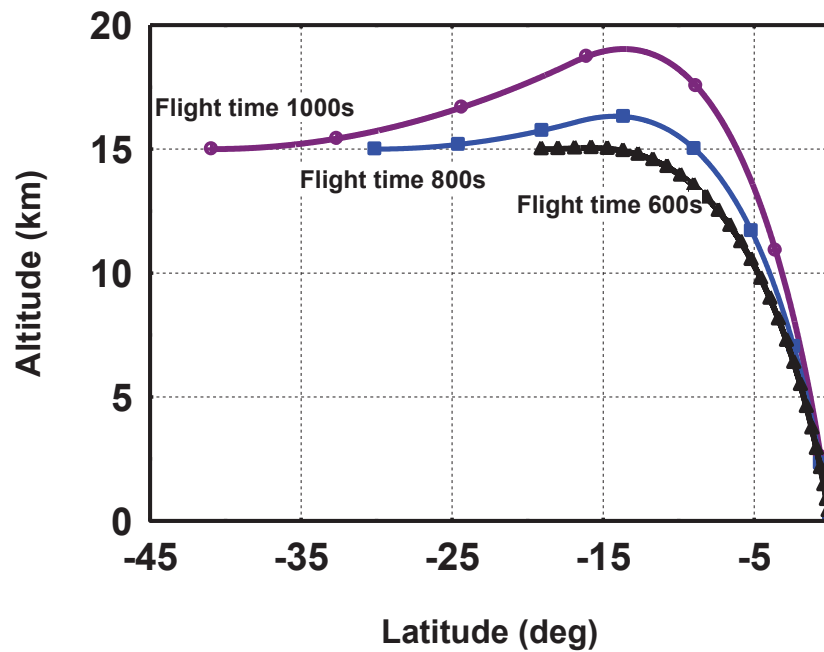


Fig. 4.7. Fuel-optimal trajectory profiles for different fixed flight times

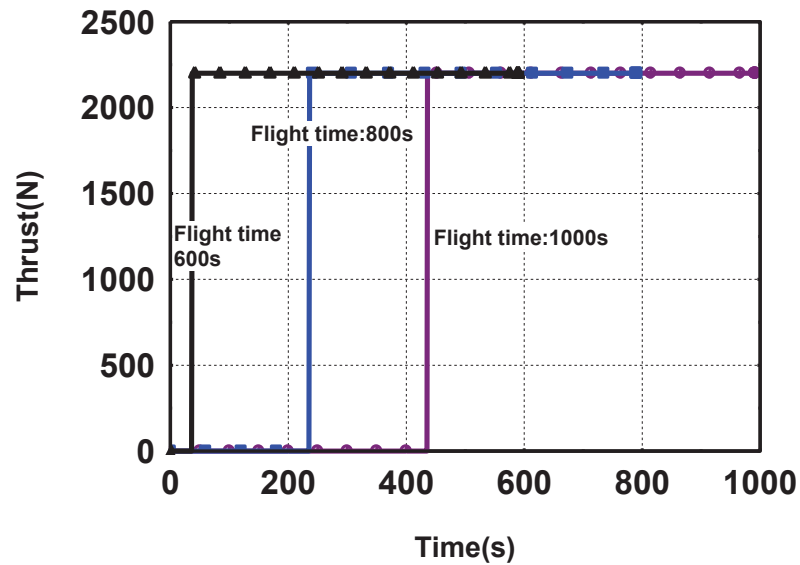


Fig. 4.8. Fuel-optimal thrust profiles for different fixed flight times

4.3.2 Performance of the Energy-optimal Limited Thrust DT-DE

Figure 4.9 depicts the altitude, latitude and longitude profiles for the landing trajectory for three cases as in Table 4.7. For higher flight times the required thrust is lower (cf. Fig.4.10) during the initial phase of descent. The landing mass achieved with energy-optimal formulation results in heavy penalty (cf. Table 4.7) for higher flight times. The penalty for the fuel-optimal formulation is only marginal (cf. Table 4.6).

Table 4.7 Energy-optimal DT-DE : Touch down parameters with optimum initial argument of perilune (AOP)

Case No.	Flight time (s)	Optimum initial Argument of perilune (deg.)	Initial longitude (deg.)	Initial latitude(deg.)	Final landing mass (kg)
1	600	-18.69	0.0	-18.69	486.5
2	800	-29.07	0.0	-29.07	484.1
3	1000	-37.36	0.0	-37.36	474.0

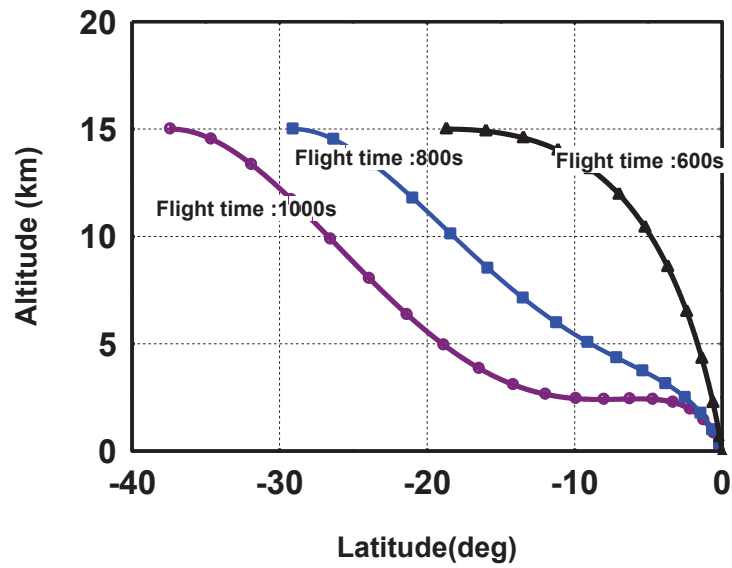


Fig. 4.9. Energy-optimal trajectory profiles for different fixed flight times with optimum initial argument of perilune

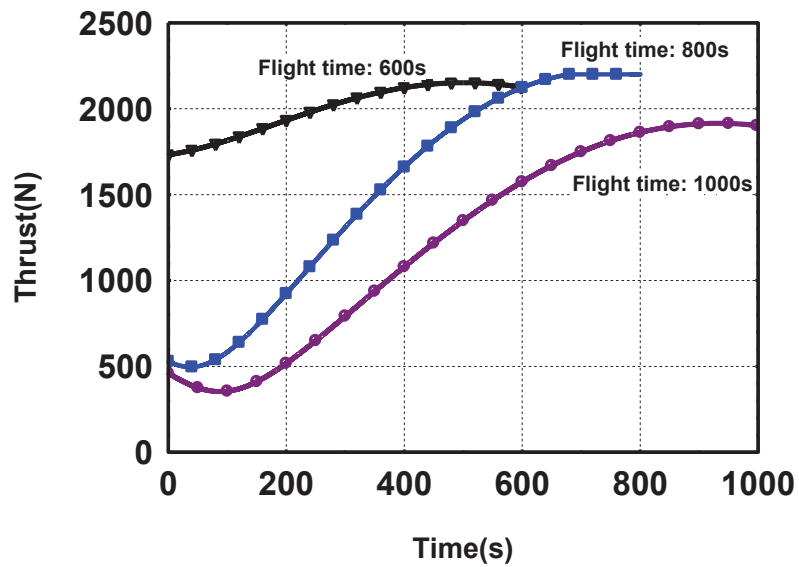


Fig. 4.10. Energy-optimal thrust profiles for different fixed flight times

4.4 Conclusions

The capability of DT-DE schemes (fuel-optimal and energy-optimal) to find the initial conditions of optimal trajectory for different mission scenarios is demonstrated. For higher perilune altitudes, the marginal advantage of landing mass for fuel-optimal over energy-optimal increases. For fuel-optimal formulation, higher flight times result in longer zero thrust duration and hence achieves nearly same landing mass for all flight times. But for energy-optimal formulation achieves soft landing with penalties on the landing mass. When the target site is fixed, the soft landing can be achieved either by changing the initial true anomaly or the argument of perilune. The use of DE is demonstrated to find the appropriate initial true anomaly /argument of perilune. The DT-DE scheme for fuel-optimal adjusts the zero thrust duration to land on the selected target. The DT-DE scheme for energy-optimal computes the required thrust acceleration by varying thrust profile and achieves the target landing conditions. For fuel-optimal trajectories, the penalties on landing mass is only marginal whereas the penalty on landing mass is high for energy-optimal formulation.

Chapter 5

DT Guidance Algorithms for Lunar Pinpoint Soft Landing

Chapter Summary

Guidance schemes with performance measures of (i) fuel-optimal (ii) energy-optimal to realize soft landing at a desired location on the Moon are developed using optimal control laws. The optimal control laws are obtained by solving a two-point boundary value problem formulated based on Pontryagin's principle. The guidance laws, adapted from the optimal control laws, are obtained as a function of unknown co-state variables. The Differential Transformation (DT) technique is employed to determine the unknown co-states at each time instant of landing trajectory using the information on the current vehicle state, target landing site (loaded on-board apriori) and the time-to-go. A simple real time strategy which uses the current and end states is presented to compute the time-to-go, a critical parameter for any guidance scheme. The performance of the simple strategy for time-to-go even when the shape of the trajectory is nonlinear is demonstrated. Extensive analysis evaluating and comparing the proposed guidance schemes is presented. Further, a brief summary of existing guidance algorithms commonly used for planetary landing is provided in this chapter and compared with the DT guidance schemes.

5.1 Introduction

A new algorithm that generates optimal landing trajectories was presented in Chapter 3. Motivated by the use of the Differential Transformation technique, its use to develop an efficient guidance algorithm is attempted. To land at a specified location, the propulsion system must be capable of generating variable thrust through throttling.

Also, if the landing point changes during the powered descent phase, retargeting of landing point with a fixed thrust is not possible. Therefore, any guidance algorithm must be capable of finding the required thrust acceleration vector to meet the terminal boundary conditions. A novel guidance scheme based on Differential Transformation (DT) to land at the specified target is developed and the details are provided in this chapter. As pointed out in Chapter 1, fuel-optimal guidance schemes are scarce in the literature and most of the schemes produce near-optimal guidance by minimizing energy. The proposed DT based guidance scheme provides fuel-optimal guidance in a closed form. Also, the energy-optimal guidance scheme is developed and both of them are evaluated for several mission scenarios. First, a brief summary of existing and commonly used guidance algorithms (i) Explicit guidance algorithm, (ii) Constrained Terminal Velocity Guidance (CTVG) and (iii) Polynomial guidance algorithm for planetary landing are presented in this chapter. Then the DT based algorithm is provided in detail. The DT based proposed schemes help to quantify the landing masses for fuel-optimal and energy-optimal objectives. Other features of the proposed schemes are that they do not assume constant gravity field and are independent of reference trajectory. The numerical integration of co-state dynamics is avoided due to the DT based approach.

5.2 Some Guidance Schemes for Landing at a Specified Location – With Variable Thrust

5.2.1 E-Guidance

E-Guidance algorithm for variable thrust proposed by Cherry (1963, 1964). This guidance algorithm requires information about the current vehicle state vector and the target state vector (position and velocity). The equations of motions are given by

$$\dot{\mathbf{r}} = \mathbf{v} \quad (5.1a)$$

$$\dot{\mathbf{v}} = \frac{-\mu}{r^3} \mathbf{r} + \mathbf{a}_T \quad (5.1b)$$

where $\mathbf{r} = [x, y, z]$, $\mathbf{v} = [v_x, v_y, v_z]$, $\mathbf{a}_T = [a_{Tx}, a_{Ty}, a_{Tz}]$, x, y, z are position and v_x, v_y, v_z are velocity components, r is the radial distance from Moon's centre. The parameters $m, T_{max}, I_{sp}, g, \mu$ are the mass of the lander module, maximum thrust, specific impulse, acceleration due to gravity of Earth (9.80665 ms^{-2}) and gravitational parameter of Moon ($4.902800476\text{E}12 \text{ m}^3\text{s}^{-2}$) respectively. All these quantities are in SI units i.e position in meter and velocity in meter per second. The quantities a_{Tx}, a_{Ty}, a_{Tz} are acceleration components of thrust (T).

Equation (5.1b) is nonlinear and in coupled form. We can linearize and decouple the equations by defining the thrust acceleration components as.

$$a_{Tx} = \frac{\mu}{r^3} x + C_1 + C_2 t \quad (5.1c)$$

$$a_{Ty} = \frac{\mu}{r^3} y + C_3 + C_4 t \quad (5.1d)$$

$$a_{Tz} = \frac{\mu}{r^3} z + C_5 + C_6 t \quad (5.1e)$$

Substituting Eq.(5.1c)-(5.1e) in Eq.(5.1b), then Eq. (5.1b) becomes linearly decoupled and it follows that,

$$\dot{v}_x = C_1 + C_2 t \quad (5.2a)$$

$$\dot{v}_y = C_3 + C_4 t \quad (5.2b)$$

$$\dot{v}_z = C_5 + C_6 t \quad (5.2c)$$

If we get the parameters C_1 to C_6 it is possible to find the required thrust acceleration components using Eq.(5.1c)-(5.1e). Integrating Eqs.(5.2a)-(5.2c) twice from the current time t to the final flight time(t_f) and rearranging the equations to get C_1 to C_6 . The coefficients C_1 to C_6 are derived with terminal boundary conditions of position and velocity and they are the following :

$$\begin{bmatrix} C_1 \\ C_2 \end{bmatrix} = \begin{bmatrix} \frac{4}{t_{go}} & -\frac{6}{t_{go}^2} \\ -\frac{6}{t_{go}^2} & \frac{12}{t_{go}^3} \end{bmatrix} \begin{bmatrix} v_x(t_f) - v_x(t) \\ x(t_f) - (x(t) + v_x(t) t_{go}) \end{bmatrix} \quad (5.3a)$$

$$\begin{bmatrix} C_3 \\ C_4 \end{bmatrix} = \begin{bmatrix} \frac{4}{t_{go}} & -\frac{6}{t_{go}^2} \\ -\frac{6}{t_{go}^2} & \frac{12}{t_{go}^3} \end{bmatrix} \begin{bmatrix} v_y(t_f) - v_y(t) \\ y(t_f) - (y(t) + v_y(t) t_{go}) \end{bmatrix} \quad (5.3b)$$

$$\begin{bmatrix} C_5 \\ C_6 \end{bmatrix} = \begin{bmatrix} \frac{4}{t_{go}} & -\frac{6}{t_{go}^2} \\ -\frac{6}{t_{go}^2} & \frac{12}{t_{go}^3} \end{bmatrix} \begin{bmatrix} v_z(t_f) - v_z(t) \\ z(t_f) - (z(t) + v_z(t) t_{go}) \end{bmatrix} \quad (5.3c)$$

where $t_{go} = t_f - t$.

If required thrust exceeds available maximum thrust, the thrust acceleration is resolved along the unit vector of unlimited thrust acceleration vector.

$$\mathbf{a}_T = \frac{\mathbf{a}_T}{a_T} \frac{T_{max}}{m} \quad (5.3d)$$

The steps of the E-Guidance algorithm are :

1. Specify the total time of powered flight, i.e time-to-go and target position and velocity vectors.
2. From the navigation system obtain current position, velocity and gravity acceleration vectors.
3. Compute the altitude from the position vector or from navigation. Check whether the current altitude is equal to the specified terminal altitude. If equal, landing has occurred otherwise, proceed with the following steps.
4. Set the current ‘time-to-go’ as the difference between the total time of powered flight and the time elapsed.
5. Compute the coefficients C_1 to C_6 (Eqs. (5.3a) – (5.3b)).
6. Compute the components of thrust acceleration vector (cf. Eqs. (5.1c) –(5.1e)) and magnitude. If the thrust magnitude is higher than the available maximum thrust, use the maximum thrust and the unit vector of the required thrust vector (cf. Eq.(5.3d)) to compute the components of acceleration.
7. Repeat steps (2)- (6) until touchdown

5.2.2 CTVG (Constrained Terminal Velocity) Guidance Scheme

This guidance scheme is proposed by Guo et al. (2011) and Hawkins et al. (2011) and it is based on two vectors Viz., ZEM and ZEV (Ebrahimi et.al (2008)). The ZEM (Zero Effort Miss) vector at any time is defined as the deviation of the target location ($\mathbf{r}(t_f)$) (at the end of mission) from the location achieved under zero thrust acceleration from that time until touchdown. At any time, the ZEV vector is defined as the deviation of the target velocity ($\mathbf{v}(t_f)$) from the velocity vector achieved under zero thrust acceleration from that time until touchdown. This algorithm is derived based on the major assumption that the gravitational acceleration is constant. The equations of motion in vector form are given by Eq. (5.1a) and Eq. (5.1b). The soft landing problem is formulated to minimize the integral of the square of acceleration such that ZEM and ZEV are zeroes at touch down and the details are as follows.

Introduce co-state variables ($\mathbf{p} = [p_x, p_y, p_z, p_{v_x}, p_{v_y}, p_{v_z}]$) corresponding to the state variables ($\mathbf{X} = [x, y, z, v_x, v_y, v_z]$). The control variables of the problem are given by $\bar{\mathbf{u}} = (a_{Tx}, a_{Ty}, a_{Tz})$.

$$\min J = \int_{t_0}^{t_f} \Gamma(t) dt = \int_{t_0}^{t_f} \frac{1}{2} (a_{Tx}^2 + a_{Ty}^2 + a_{Tz}^2) dt \quad (5.4)$$

The Hamiltonian for this optimal control problem is,

$$H = \Gamma + \mathbf{p} \dot{\mathbf{X}}^T \quad (5.5)$$

Assuming that the lunar gravitational acceleration \mathbf{g}_l is a constant vector, the co-state equations and the control law are derived. The co-state equations are

$$\dot{\mathbf{p}} = - \left[\frac{\partial H}{\partial x} \frac{\partial H}{\partial y} \frac{\partial H}{\partial z} \frac{\partial H}{\partial v_x} \frac{\partial H}{\partial v_y} \frac{\partial H}{\partial v_z} \right] \quad (5.6a)$$

$$\dot{p}_x = 0.0 \quad (5.6b)$$

$$\dot{p}_y = 0.0 \quad (5.6c)$$

$$\dot{p}_z = 0.0 \quad (5.6d)$$

$$\dot{p}_{v_x} = -p_x \quad (5.6e)$$

$$\dot{p}_{v_y} = -p_y \quad (5.6f)$$

$$\dot{p}_{v_z} = -p_z \quad (5.6g)$$

The control law is given by the optimality condition

$$\frac{\partial H}{\partial \bar{u}} = 0 \quad \forall t \in [t_o, t_f] \quad (5.7a)$$

$$\mathbf{a}_T = -\mathbf{p}_v \quad (5.7b)$$

According to corollary of Pontryagin's principle, when fixed terminal conditions, the co-states at t_f are non-zero. Integrating the co-state equations

$$p_x = p_x(t_f) \quad (5.8a)$$

$$p_y = p_y(t_f) \quad (5.8b)$$

$$p_z = p_z(t_f) \quad (5.8c)$$

$$p_{v_x}(t) = p_{v_x}(t_f) + (t_f - t) p_x(t_f) \quad (5.9a)$$

$$p_{v_y}(t) = p_{v_y}(t_f) + (t_f - t) p_y(t_f) \quad (5.9b)$$

$$p_{v_z}(t) = p_{v_z}(t_f) + (t_f - t) p_z(t_f) \quad (5.9c)$$

The time-to-go is defined as

$$t_{go} = t_f - t \quad (5.10)$$

The thrust acceleration can be found as

$$a_{Tx} = -p_{v_x} = -p_{v_x}(t_f) - t_{go} p_x(t_f) \quad (5.11a)$$

$$a_{Ty} = -p_{v_y} = -p_{v_y}(t_f) - t_{go} p_y(t_f) \quad (5.11b)$$

$$a_{Tz} = -p_{v_z} = -p_{v_z}(t_f) - t_{go} p_z(t_f) \quad (5.11c)$$

To find the required thrust acceleration with Eqs.(5.11a)-(5.11c), the final co-states are required to be known and it can be found by integrating the state equations. With some algebraic manipulations and rearrangements (Guo et al. 2011), the state vector can be obtained as follows:

$$x = x(t_f) - t_{go} v_x(t_f) - \frac{1}{2} t_{go}^2 p_{v_x}(t_f) - \frac{1}{6} t_{go}^3 p_x(t_f) + \frac{1}{2} t_{go}^2 g_{lx} \quad (5.12a)$$

$$y = y(t_f) - t_{go} v_y(t_f) - \frac{1}{2} t_{go}^2 p_{v_y}(t_f) - \frac{1}{6} t_{go}^3 p_y(t_f) + \frac{1}{2} t_{go}^2 g_{ly} \quad (5.12b)$$

$$z = z(t_f) - t_{go} v_z(t_f) - \frac{1}{2} t_{go}^2 p_{v_z}(t_f) - \frac{1}{6} t_{go}^3 p_z(t_f) + \frac{1}{2} t_{go}^2 g_{lz} \quad (5.12c)$$

$$v_x = v_x(t_f) + t_{go} p_{v_x}(t_f) + \frac{1}{2} t_{go}^2 p_x(t_f) - t_{go} g_{lx} \quad (5.13a)$$

$$v_y = v_y(t_f) + t_{go} p_{v_y}(t_f) + \frac{1}{2} t_{go}^2 p_y(t_f) - t_{go} g_{ly} \quad (5.13b)$$

$$v_z = v_z(t_f) + t_{go} p_{v_z}(t_f) + \frac{1}{2} t_{go}^2 p_z(t_f) - t_{go} g_{lz} \quad (5.13c)$$

In the above equations (Eqs. (5.12) and Eq.(5.13)) all quantities are known except the co-states. The co-states are obtained (Guo et al. 2011) by combining Eqs.(5.12) and Eqs. (5.13) and rearranging the terms and they are as follows,

$$p_x(t_f) = \frac{12}{t_{go}^3} (x - x(t_f)) + \frac{6}{t_{go}^2} (v_x + v_x(t_f)) \quad (5.14a)$$

$$p_y(t_f) = \frac{12}{t_{go}^3} (y - y(t_f)) + \frac{6}{t_{go}^2} (v_y + v_y(t_f)) \quad (5.14b)$$

$$p_z(t_f) = \frac{12}{t_{go}^3} (z - z(t_f)) + \frac{6}{t_{go}^2} (v_z + v_z(t_f)) \quad (5.14c)$$

$$p_{v_x}(t_f) = -\frac{6}{t_{go}^2} (x - x(t_f)) - \frac{2}{t_{go}} (v_x + 2 v_x(t_f)) + g_{lx} \quad (5.15a)$$

$$p_{v_y}(t_f) = -\frac{6}{t_{go}^2} (y - y(t_f)) - \frac{2}{t_{go}} (v_y + 2 v_y(t_f)) + g_{ly} \quad (5.15b)$$

$$p_{v_z}(t_f) = -\frac{6}{t_{go}^2} (z - z(t_f)) - \frac{2}{t_{go}} (v_z + 2 v_z(t_f)) + g_{lz} \quad (5.15c)$$

The required thrust acceleration can be computed using Eq. (5.11) and Eqs.(5.15a)-

(5.15c) and it is,

$$a_{Tx} = \frac{6}{t_{go}^2} (x(t_f) - x - t_{go} v_x(t_f)) + \frac{4}{t_{go}} (v_x(t_f) - v_x) - g_{lx} \quad (5.16a)$$

$$a_{Ty} = \frac{6}{t_{go}^2} (y(t_f) - y - t_{go} v_y(t_f)) + \frac{4}{t_{go}} (v_y(t_f) - v_y) - g_{ly} \quad (5.16b)$$

$$a_{Tz} = \frac{6}{t_{go}^2} (z(t_f) - z - t_{go} v_z(t_f)) + \frac{4}{t_{go}} (v_z(t_f) - v_z) - g_{lz} \quad (5.16c)$$

Let $x_t = x(t_f)$; $y_t = y(t_f)$; $z_t = z(t_f)$; $v_{xt} = v_x(t_f)$; $v_{yt} = v_y(t_f)$; $v_{zt} = v_z(t_f)$

Then Eq.(5.16) becomes

$$a_{Tx} = \frac{6}{t_{go}^2}(x_t - x - t_{go} v_{xt}) + \frac{4}{t_{go}}(v_{xt} - v_x) - g_{lx} \quad (5.17a)$$

$$a_{Ty} = \frac{6}{t_{go}^2}(y_t - y - t_{go} v_{yt}) + \frac{4}{t_{go}}(v_{yt} - v_y) - g_{ly} \quad (5.17b)$$

$$a_{Tz} = \frac{6}{t_{go}^2}(z_t - z - t_{go} v_{zt}) + \frac{4}{t_{go}}(v_{zt} - v_z) - g_{lz} \quad (5.17c)$$

The steps of the CTVG algorithm can be summarized as follows,

Steps (1) – (4) are same as in the previous section 5.2.1

5. Compute the components of thrust acceleration vector (cf. Eqs. (5.17a) –(5.17c)) and magnitude. If thrust magnitude higher than the available maximum thrust, use the maximum thrust and the unit vector of required thrust vector (cf. Eq.(5.3d)) to find the components of acceleration.
6. Repeat steps (2)- (5) until touchdown

5.2.3 Polynomial Guidance Scheme

The polynomial approximated acceleration vector $\mathbf{a}(t)$ that passes through initial and target state is used for landing trajectory acceleration profile. This approximated acceleration profile is used to find the thrust acceleration vector. This scheme requires an acceleration profile which satisfies the initial and target states (position, velocity, acceleration). A quadratic acceleration profile is selected and it is of the form

$$\mathbf{a}(t) = \mathbf{C}_0 + \mathbf{C}_1 t + \mathbf{C}_2 t^2 \quad (5.18a)$$

The thrust acceleration vector is given by

$$\mathbf{a}_T(t) = \mathbf{a}(t) - \mathbf{g}_l \quad (5.18b)$$

Where \mathbf{C}_0 , \mathbf{C}_1 , \mathbf{C}_2 are the coefficient (in vector form) to be determined and the details are provided by Wong et al. (2006) and Sostaric and Rea (2005). \mathbf{g}_l is lunar gravitational acceleration vector. With integration the position and velocity equations become

$$\mathbf{v}(t) = \mathbf{C}_0 t + \frac{1}{2} \mathbf{C}_1 t^2 + \frac{1}{3} \mathbf{C}_2 t^3 + \mathbf{v}_0 \quad (5.19)$$

$$\mathbf{r}(t) = \frac{1}{2}\mathbf{C}_0 t^2 + \frac{1}{6}\mathbf{C}_1 t^3 + \frac{1}{12}\mathbf{C}_2 t^4 + \mathbf{v}_0 t + \mathbf{r}_0 \quad (5.20)$$

Solving for the coefficients they are found using the current state vector and the target state vector at final time (t_f).

$$\mathbf{C}_0 = \mathbf{a}_t - 6 \frac{(\mathbf{v}_t + \mathbf{v}_0)}{t_{go}^2} + 12 \frac{(\mathbf{r}_t - \mathbf{r}_0)}{t_{go}^3} \quad (5.20a)$$

$$\mathbf{C}_1 = -6 \frac{\mathbf{a}_t}{t_{go}} + 6 \frac{(5\mathbf{v}_t + 3\mathbf{v}_0)}{t_{go}^2} - 48 \frac{(\mathbf{r}_t - \mathbf{r}_0)}{t_{go}^3} \quad (5.20b)$$

$$\mathbf{C}_2 = 6 \frac{\mathbf{a}_t}{t_{go}^2} - 12 \frac{(2\mathbf{v}_t + \mathbf{v}_0)}{t_{go}^3} + 36 \frac{(\mathbf{r}_t - \mathbf{r}_0)}{t_{go}^4} \quad (5.20c)$$

Where \mathbf{a}_t , \mathbf{v}_t , \mathbf{r}_t are target acceleration, velocity and position vector at final time to be pre-specified.

The different steps of polynomial guidance algorithm can summarize as follows,

1. Steps (1) – (4) are same as in the previous section 5.2.1
5. Calculate the components of the thrust acceleration vector (cf. Eqs. (5.18), Eq.(5.20a)-(5.20c)) and its magnitude. If thrust magnitude higher than the available maximum thrust use the maximum thrust in the direction of the required thrust vector (cf. Eq.(5.3d))
6. Repeat steps (2)- (5) until touch down.

5.3 Differential Transformation Based Guidance Scheme

The proposed new guidance scheme uses Pontryagin's principle of optimal control theory to derive the optimal control laws in which the acceleration vector is represented as a function of co-states. The formulation is the same as the one described in Chapter 3. So, it is not repeated and those equations are referred in this chapter. For dynamics and formulation of the problem, the readers are directed to refer to sections 3.2 and 3.3 respectively. The components of acceleration components and throttling parameter at a particular time instant are obtained for two objectives (i) energy-optimal (ii) fuel-optimal in sections 3.3.1 and 3.3.2 respectively. For completeness, the control laws are reproduced herein for both the objectives. These controls laws are used as the guidance laws to compute the instantaneous acceleration vector. These acceleration

vectors can be obtained if the co-states at that time instant are known. In the proposed scheme, the Differential Transformation technique is used to compute the co-states at each time instant using the time-to-go (t_{go}) and the target state (landing location). A simple strategy to compute the parameter t_{go} is used.

5.3.1 Energy-optimal Guidance Laws

When the thrust level is limited to T_{max} , the thrust acceleration vector (\mathbf{a}_T) is given by (Eq.3.12),

$$k a_{T_x} = -\frac{p_{v_x}}{p_v} \frac{T_{max}}{m} \quad (3.12a)$$

$$k a_{T_y} = -\frac{p_{v_y}}{p_v} \frac{T_{max}}{m} \quad (3.12b)$$

$$k a_{T_z} = -\frac{p_{v_z}}{p_v} \frac{T_{max}}{m} \quad (3.12c)$$

The quantities $a_{T_x}, a_{T_y}, a_{T_z}$ are acceleration components of thrust (T) and k is the throttling parameter. For computation purposes, the parameter ‘ k ’ is set to equal to 1.

The co-state velocity vector is $\mathbf{p}_v = [p_{v_x}, p_{v_y}, p_{v_z}]$ and $p_v = \sqrt{p_{v_x}^2 + p_{v_y}^2 + p_{v_z}^2}$.

5.3.2 Fuel-optimal Guidance Laws

The optimal thrust acceleration components and magnitude are found using the optimality condition and they are as given (Eq. 3.16) below.

$$a_{T_x} = -\frac{k g I_{sp} T_{max} p_{v_x}}{m^2(1-p_m)} \quad (3.16a)$$

$$a_{T_y} = -\frac{k g I_{sp} T_{max} p_{v_y}}{m^2(1-p_m)} \quad (3.16b)$$

$$a_{T_z} = -\frac{k g I_{sp} T_{max} p_{v_z}}{m^2(1-p_m)} \quad (3.16c)$$

$$\sqrt{a_{T_x}^2 + a_{T_y}^2 + a_{T_z}^2} = \frac{T_{max}}{m} \quad (3.16d)$$

where k is throttling parameter (cf. Eq.3.17-Eq.3.18),

$$k = \begin{cases} 0 & \text{for } S > 0 \\ 1 & \text{for } S < 0 \end{cases} \quad \text{and} \quad S = \left(\frac{m(1-p_m)}{g I_{sp}} - \frac{g I_{sp}}{m(1-p_m)} (p_{v_x}^2 + p_{v_y}^2 + p_{v_z}^2) \right)$$

The parameters m, T_{max}, I_{sp}, g are the mass of the lander module, maximum thrust, specific impulse and acceleration due to gravity of Earth (9.80665 ms^{-2}) respectively.

5.3.3 Strategy for Time-to-go

Let the latitudes and longitudes of current and target points are given by ϕ_c, λ_c and ϕ_f, λ_f . Convert the current vehicle velocity vector to local inertial frame on surface as

$$\begin{pmatrix} v_{xg} \\ v_{yg} \\ v_{zg} \end{pmatrix} = \begin{pmatrix} -\sin \phi_c \cos \lambda_c & -\sin \phi_c \sin \lambda_c & \cos \phi_c \\ -\sin \lambda_c & \cos \lambda_c & 0 \\ -\cos \phi_c \cos \lambda_c & -\cos \phi_c \sin \lambda_c & -\sin \phi_c \end{pmatrix} \begin{pmatrix} v_{xc} \\ v_{yc} \\ v_{zc} \end{pmatrix} \quad (5.21)$$

$$\text{and find the velocity Azimuth } A_z = \sin^{-1} \left(\frac{v_{yg}}{\sqrt{v_{xg}^2 + v_{yg}^2}} \right) \quad (5.22)$$

The cross-range and down-range angles ρ_c and ρ_d are given by (Brauer et.al., 1975)

$$\sin \rho_c = -\cos A_z \cos \phi_f \sin(\lambda_c - \lambda_f) + \sin A_z \cos \phi_c \sin \phi_f - [\sin A_z \sin \phi_c \cos \phi_f \cos(\lambda_c - \lambda_f)] \quad (5.23)$$

$$\sin \rho_d = \frac{\sin A_z \cos \phi_f \sin(\lambda_c - \lambda_f) + \cos A_z \cos \phi_c \sin \phi_f - [\cos A_z \sin \phi_c \cos \phi_f \cos(\lambda_c - \lambda_f)]}{\cos \rho_c} \quad (5.24)$$

$$\text{Find the parameter } r_{ave} = \frac{(r_c + r_f)}{2} \quad (5.25)$$

where r_c and r_f are the radius at the current and target points. The down-range (ρ_{dr}) and cross-range are (ρ_{cr}) given by

$$\rho_{dr} = r_{ave} \rho_d \quad (5.26)$$

$$\rho_{cr} = r_{ave} \rho_c \quad (5.27)$$

The parameter t_{go} is computed as the time taken to cover the linear distance between the current and end states if the lander travels with a mean velocity. The mean velocity (v_m) is the average of current and end velocities.

$$v_m = \frac{v_c + v_f}{2} \quad (5.28a)$$

The parameter t_{go} is given by

$$t_{go} = \frac{\sqrt{h^2 + \rho_{dr}^2 + \rho_{cr}^2}}{v_m} \quad (5.28b)$$

where, h is current altitude, ρ_{dr} is down-range to go, ρ_{cr} is cross-range to go, v_c and v_f are current and target velocity magnitudes. The parameter t_{go} becomes indeterminate when both current and target velocities are zeros. The current velocity becoming zero is a very rare occurrence. However, if this occurs it is handled by discontinuing the t_{go} computation within a small threshold value of current velocity. For this scenario, the value for t_{go} is taken as the latest value corresponding to non-zero current velocity. However, in all simulations of this study, this situation did not arise.

5.3.4 Differential Transformation (DT) Based Guidance Algorithms

The instantaneous co-states for a t_{go} value are computed using the Differential Transformation technique. All equations related to finding the initial co-states are the same and hence it not repeated in this chapter. For derivations, refer to section 3.4.2 of Chapter 3. The time-to-go is computed using Eq. (5.28) and the relevant equations required to compute the initial co-states are repeated in the DT based guidance scheme. The steps of the DT based guidance algorithms are designated as Fuel-optimal and Energy-optimal DT guidance schemes, and are as follows:

1. Fix I_{sp} , maximum available thrust level of engine and target state vector (position and velocity vectors) and fix a positive value greater than 1 for the co-state of ' m '.
2. Obtain / compute the current vehicle state (position and velocity vectors) from navigation / numerical integration.
3. Obtain / compute the vehicle altitude information from navigation / numerical integration. If it reaches the required terminal altitude, stop the guidance computation.
4. Compute the parameter time-to-go using the Eq.(5.28)
5. Compute the current co-states using the current vehicle state, target state and time-to-go using the following steps.

- (i) Compute the matrix A (Eq. 5.29) using the Eq. (5.30) for the performance measure of energy-optimal or using the Eq. (5.31) for the performance measure of fuel-optimal.

$$A = \begin{bmatrix} A_1 & B_1 \\ 0 & A_2 \end{bmatrix}_{12 \times 12} \quad (5.29)$$

$$A_1 = \begin{bmatrix} 0 & 0 & 0 & 1 & 0 & 0 \\ 0 & 0 & 0 & 0 & 1 & 0 \\ 0 & 0 & 0 & 0 & 0 & 1 \\ \frac{-\mu}{r^3} & 0 & 0 & 0 & 0 & 0 \\ 0 & \frac{-\mu}{r^3} & 0 & 0 & 0 & 0 \\ 0 & 0 & \frac{-\mu}{r^3} & 0 & 0 & 0 \end{bmatrix} \quad (5.30)$$

$$A_2 = \begin{bmatrix} 0 & 0 & 0 & \frac{\mu(y^2+z^2-2x^2)}{r^5} & \frac{-3\mu xy}{r^5} & \frac{-3\mu xz}{r^5} \\ 0 & 0 & 0 & \frac{-3\mu xy}{r^5} & \frac{\mu(x^2+z^2-2y^2)}{r^5} & \frac{-3\mu zy}{r^5} \\ 0 & 0 & 0 & \frac{-3\mu xz}{r^5} & \frac{-3\mu zy}{r^5} & \frac{\mu(y^2+x^2-2z^2)}{r^5} \\ -1 & 0 & 0 & 0 & 0 & 0 \\ 0 & -1 & 0 & 0 & 0 & 0 \\ 0 & 0 & -1 & 0 & 0 & 0 \end{bmatrix} \quad (5.31)$$

The matrix B_1 is set according to the performance measure. The B_1 matrix for the energy-optimal is,

$$B_1 = \begin{bmatrix} 0 & 0 & 0 & 0 & 0 & 0 \\ 0 & 0 & 0 & 0 & 0 & 0 \\ 0 & 0 & 0 & 0 & 0 & 0 \\ 0 & 0 & 0 & -1 & 0 & 0 \\ 0 & 0 & 0 & 0 & -1 & 0 \\ 0 & 0 & 0 & 0 & 0 & -1 \end{bmatrix} \quad (5.32)$$

and for fuel-optimal case, the matrix B_1 is

$$B_1 = \left(\frac{g I_{sp} T_{max}}{m^2 (1-p_m)} \right) \begin{bmatrix} 0 & 0 & 0 & 0 & 0 & 0 \\ 0 & 0 & 0 & 0 & 0 & 0 \\ 0 & 0 & 0 & 0 & 0 & 0 \\ 0 & 0 & 0 & -1 & 0 & 0 \\ 0 & 0 & 0 & 0 & -1 & 0 \\ 0 & 0 & 0 & 0 & 0 & -1 \end{bmatrix} \quad (5.33)$$

- (ii) Compute the matrix $[A^j]_{12 \times 12}$ [cf. Eq. (5.34)] and the sub matrices A_{j1} and A_{j2} .

where $[A^j]_{12 \times 12} = A \times A \times A \dots \times A$, j times. It is represented as

$$[A^j]_{12 \times 12} = \begin{bmatrix} [A_{j1}]_{6 \times 6} & [A_{j2}]_{6 \times 6} \\ [A_{j3}]_{6 \times 6} & [A_{j4}]_{6 \times 6} \end{bmatrix} \quad (5.34)$$

- (iii) Compute the quantities R [cf. Eq. (5.36)] and Q [cf. Eq. (5.35)] by substituting the value of t_{go} for $(t_f - t_0)$. The number of terms in the series expansion is chosen based on an analysis on the determining the co-states by varying the number of terms.

$$Q = \sum_{j=0}^n \frac{(t_f - t_0)^j}{j!} A_{j1} \mathbf{x}(t_0) \quad (5.35)$$

$$R = \sum_{j=0}^n \frac{(t_f - t_0)^j}{j!} A_{j2} \quad (5.36)$$

- (iv) Compute the co-states at the current time (t_c), using Eq. (5.37) and replacing t_0 with t_c .

$$\mathbf{p}(t_0) = R^{-1} [\mathbf{x}(t_f) - Q] \quad (5.37)$$

6. Compute the required thrust acceleration vector from the current co-states and the thrust magnitude using Eqs. (5.38a)-(5.38c) for the fuel-optimal and Eqs. (5.40a) – (5.40 c) for the energy-optimal formulations.

For the fuel-optimal formulation, the thrust acceleration components and throttling parameter are the following,

$$a_{T_x} = - \frac{k g I_{sp} T_{max} p_{v_x}}{m^2 (1-p_m)} \quad (5.38a)$$

$$a_{T_y} = -\frac{k g I_{sp} T_{max} p_{v_y}}{m^2 (1-p_m)} \quad (5.38b)$$

$$a_{T_z} = -\frac{k g I_{sp} T_{max} p_{v_z}}{m^2 (1-p_m)} \quad (5.38c)$$

$$\sqrt{a_{T_x}^2 + a_{T_y}^2 + a_{T_z}^2} = \frac{T_{max}}{m} \quad (5.39)$$

where k is throttling parameter (cf. Eq.3.17-Eq.3.18),

$$k = \begin{cases} 0 & \text{for } S > 0 \\ 1 & \text{for } S < 0 \end{cases} \quad \text{and} \quad S = \left(\frac{m(1-p_m)}{g I_{sp}} - \frac{g I_{sp}}{m(1-p_m)} (p_{v_x}^2 + p_{v_y}^2 + p_{v_z}^2) \right)$$

For the energy-optimal formulation, the product of the acceleration component and the throttling parameter is considered as a single parameter. For computation purposes, the parameter ' k ' is set to equal to 1. Therefore, the thrust acceleration components and throttling parameter are ,

$$k a_{T_x} = -p_{v_x} \quad (5.40a)$$

$$k a_{T_y} = -p_{v_y} \quad (5.40b)$$

$$k a_{T_z} = -p_{v_z} \forall t \in [t_0, t_f] \quad (5.40c)$$

$$k \sqrt{a_{T_x}^2 + a_{T_y}^2 + a_{T_z}^2} = \frac{\text{Thrust required}}{m} \quad (5.40d)$$

The above energy-optimal control laws (Eq.(5.40)) are valid for unbounded thrust. But, in actual missions the thrust available is limited. If the required thrust computed using the Eq.(5.40d) is higher than the available maximum thrust, the control laws are modified using Pontryagin's principle. According to Pontryagin's principle, the thrust must be chosen satisfying the constraint on the maximum thrust and still minimizing the Hamiltonian. It can easily be verified by selecting the terms that contain control variables that H is minimum when the thrust is set to the maximum permissible value. The unit vector along the co-state of velocity vector, which is optimally computed using Eqs. (5.41a)-(5.41c), is used for thrust direction. Combining these strategies, to suit the limited thrust conditions, the maximum thrust acceleration is resolved along the unit vector of the co-state velocity vector. The energy-optimal control laws that provide the thrust acceleration components are

$$k a_{T_x} = -\frac{p_{v_x}}{p_v} \frac{T_{max}}{m} \quad (5.41a)$$

$$k a_{T_y} = -\frac{p_{v_y}}{p_v} \frac{T_{max}}{m} \quad (5.41b)$$

$$k a_{T_z} = -\frac{p_{v_z}}{p_v} \frac{T_{max}}{m} \quad (5.41c)$$

where

$$p_v = \sqrt{p_{v_x}^2 + p_{v_y}^2 + p_{v_z}^2}$$

To summarize, the Eqs. (5.40a) -(5.40c) are used as control laws if the required thrust is less than the maximum thrust. Otherwise the Eqs. (5.41a) -(5.41c) are used as control laws.

7. Repeat the steps (2) to (6) until target altitude is achieved (corresponding to touchdown or until any interim target state is reached).

In the above algorithm, there exist possibility of matrix R becoming singular (determinant becomes zero). However, the matrix inversion for the matrix R did not cause any problem in all simulations (including the Monte Carlo simulations) of this research work. When such situations occur in the simulations, a strategy to update the co-states is proposed. If the determinant of the matrix R is zero, then the co-states are updated linearly using the previous values using Eqs.(3.9a)-(3.9f). But the matrix becomes indeterminate (mathematically) in the following situations:

- Time-to-go becomes zero

If this occurs, the co-states can linearly be updated (Euler method) from previous values using Eqs.(3.9a)-(3.9f).

- Position and velocity becomes zero

The position components expressed in lunar centred co-ordinate frame and therefore the possibility of zero position is not there. When the velocity becomes zero, the simulation will stop and therefore, there is no computation of matrix R .

5.4 Results and Discussion

The performance of the proposed method is attempted for a lander with a propulsion system as given in Table 5.1. The lander mass is assumed to be 880 kg in a 100 x 100 km lunar orbit and 874.4 kg in 15 x 100 km intermediate lunar orbit after an orbital transfer. Two cases of intermediate orbits as given Table 5.1 have been considered (i) inclination = 90 deg. (ii) inclination = 45 deg. The descent for landing is assumed to occur in the ascending phase of the orbit in the near side. For the guidance scheme, the coordinates of a target landing site are required. The coordinates of landing site obtained in fuel-optimal trajectories with no constraint on the landing sites have been used for the performance assessment. The fuel-optimal trajectories and the resulting landing sites for the two cases are given in Table 5.2. Note that except the coordinates of the landing sites all other parameters are nearly same. As reported in Chapter 3 (section 3.6.5 and 3.6.6), the optimal solutions and the landing site are nearly the same for the energy-optimal open-loop trajectory.

Table 5.1 Input parameters

Parameters	Case1	Case 2
Semi-major axis (km)	1795.5	1795.5
Eccentricity	0.023670287	0.023670287
Inclination (deg)	90	45
Argument of perilune (deg)	0	0
Longitude of ascending node (deg)	0	0
True anomaly (deg)	0	0
Maximum Thrust (N)	2200	2200
Specific Impulse (s)	315	315
Mass at 100km (kg)	880	880
Mass at 15km (kg)	874.4	874.4

Table 5.2 Optimal trajectory parameters and the resulting landing target

Parameter	Case 1	Case 2
Latitude (deg, North)	16.1508	11.46113
Longitude (deg)	0.0	11.46146
Flight time to touch down (s)	543.96	543.98
Landing mass (kg)	487.04	487.01

Problem Definition for Guidance Analysis: A lander in orbits as given in Table 5.1 is to achieve the respective target sites as given Table 5.2. The thrust provided by the propulsion system is limited to 2200 N. As described in section 3.6.2 of chapter 3, the DT parameters (i) DT step size and (ii) number of terms in the series expansion have fixed at 0.5 s and 15 respectively.

5.4.1 Evaluation of Guidance Schemes

Both the fuel-optimal and the energy-optimal DT guidance schemes have been evaluated for the two cases of orbits and are presented in Tables 5.3 and 5.4. The time-to-go is computed and updated for each time step using the procedure given in section 5.3.1. The fuel-optimal DT guidance achieves the target in 552.49 s of which for 7.3 s the thrust is zero. So, thrusting time is only 545.19 s (case 1) which is nearly same as the flight time obtained (cf. Table 5.2) in the open-loop optimal trajectory (544.96 s). The landing mass, for fuel-optimal guidance, is 486.2 kg whereas the energy-optimal guidance lands a mass of 485.8 kg. Although marginal, there is an advantage of 0.4 kg in the case of fuel-optimal DT guidance. The performance of energy-optimal DT guidance is marginally better than (i) CTVG (ii) E guidance schemes. The CTVG scheme is considered for comparison as the performance of the scheme was found to be similar to many other schemes. For CTVG and E guidance schemes, t_{go} is computed using the proposed time-to-go computation (cf. Eq. 5.28) which uses current states and target states. An additional landing mass of 0.2 kg in a reduced flight time (less by 2.6 s) is obtained for energy-optimal DT guidance. Note that the zero thrust duration does not occur for other guidance schemes except for the fuel-optimal DT guidance. The behavior of the schemes are the same for case 2 (inclination = 45 deg.) also.

Table 5.3 Performance of DT Guidance scheme and Comparison with other schemes
(Case 1)

Parameter	Fuel-optimal DT Guidance	Energy-optimal DT Guidance	CTVG	E-guidance
Flight time (s) (touch down time)	552.49	554.96	557.56	557.55
Landing Mass(kg)	486.16	485.79	485.5	485.5
Deviation in target position at touchdown (m)	0.001	5.e-6	4e-5	5e-5
Deviation in velocity at touchdown (m/s)	0.1	0.001	0.005	0.0049
Zero thrust duration (s)	7.3	-	-	-

Table 5.4 Performance of DT Guidance scheme and Comparison with other schemes
(Case 2)

Parameter	Fuel-optimal DT Guidance	Energy-optimal DT Guidance	CTVG	E- guidance
Flight time (s) (touch down time)	552.62	555.09	557.68	557.68
Landing Mass(kg)	486.13	485.75	485.45	485.495
Deviation in target position at touchdown (m)	0.001	5.e-6	4e-5	5e-5
Deviation in velocity at touchdown (m/s)	0.1	0.001	0.005	0.00493
Zero thrust duration (s)	7.3	-	-	-

It is observed that the polynomial guidance fails to converge when t_{go} is updated in real time and works only when a value for t_{go} is fixed at t_0 . This fixed time-to-go is decremented linearly using the propagation/navigation step size. The performance of polynomial guidance is given in Table 5.5 for different t_{go} values varying between 545 s and 585 s. Polynomial guidance works for t_{go} values in the range of 548 s – 581 s for this test case (case 1). This range is applicable only for the case considered in this study. However, it is observed that for any other case also there will be a range of values for t_{go} in which only polynomial guidance works. Note that the landing mass is less by about 1 kg for the 560 s of time-to-go case. Also, it is observed that for all guidance schemes the initial t_{go} value must be more than the optimal flight time of open-loop optimal trajectory.

The altitude profiles for the fuel-optimal and the energy-optimal DT schemes are depicted in Fig. 5.1. Figure 5.2 provides the track of the descent trajectory in terms of down-range and cross-range parameters. The thrust profiles for the fuel-optimal and the energy-optimal guidance schemes are depicted in Fig.5.3 and Fig.5.4 respectively.

Clearly, the fuel-optimal guidance demands either maximum thrust or zero thrust and the thrust demanded by the energy-optimal guidance tapers down in the latter part of the flight. The t_{go} profile with time is given in Fig. 5.5. Initially the value of t_{go} is computed as 581.85 s and later on the value gets reduced to meet the target. Further, the inadequacy of a strategy that fixes t_{go} at an initial time and then linearly decrements instead of updating real time is established in Fig. 5.6(a) and Fig. 5.6(b). In these figures, the propagation step size is 0.5 s which is equivalent to the step size of navigation update. The t_{go} difference which is the difference between the two t_{go} 's determined at two successive propagation steps is plotted for fuel-optimal DT guidance in Fig. 5.6(a) and Fig. 5.6(b) (blown up version of Fig.5.6(a) during 0 s to 450 s). Note that the t_{go} difference is about 0.56 s initially and varies to 0.48 s before resulting in wild variations due to the variations in the demand for thrust between zero and full level. The non-linearity in the trend is clearly seen.

Table 5.5 Performance of polynomial guidance with fixed time-to-go (Case 1)

Parameter	$t_{go} =$ 545 s	$t_{go} =$ 548 s	$t_{go} =$ 555 s	$t_{go} =$ 560 s	$t_{go} =$ 580 s	$t_{go} =$ 585 s
Touch down time (s)	531.6	548	555	560	580	578
Landing Mass (kg)	497.04	486.1	485.7	485.03	481.5	489
Deviation in target position at touchdown (m)	231.8	9E-10	8.E-7	9.E-7	3.E-9	60
Deviation in velocity at touchdown (m/s)	53.9	3.E-7	5.E-9	7E-10	2.E-6	8

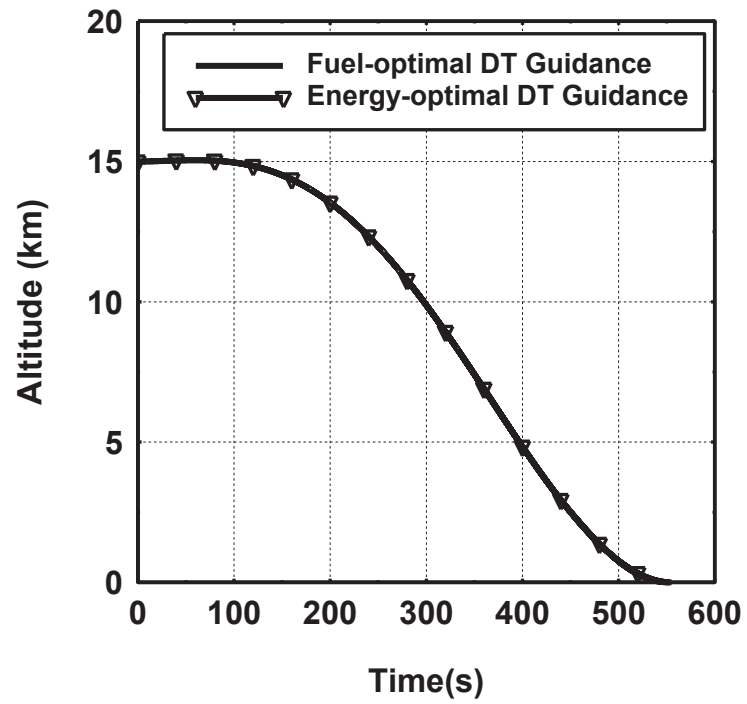


Fig. 5.1. Altitude profile for DT guidance schemes (Case 1).

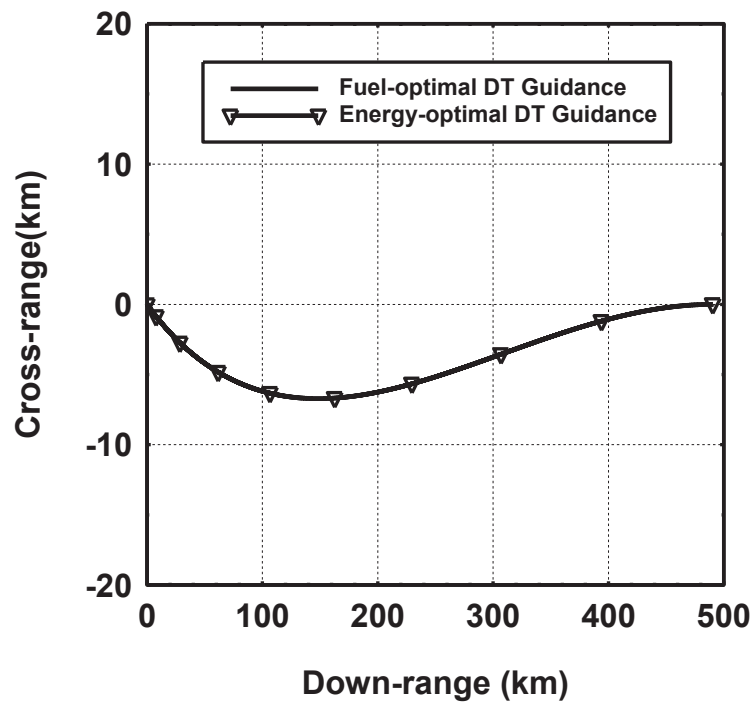


Fig. 5.2. Down-range vs cross-range - Case 1.

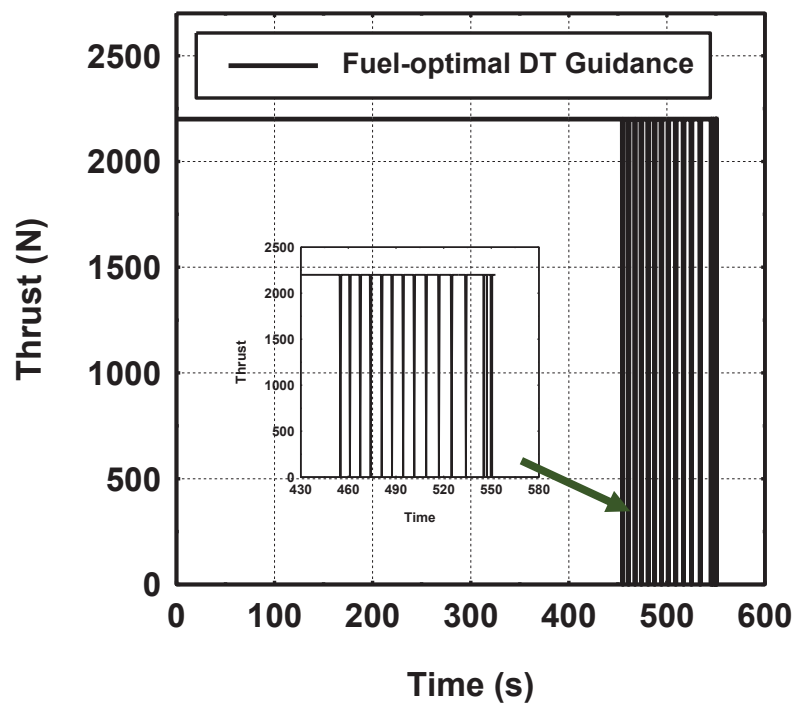


Fig. 5.3. Thrust profile- for fuel-optimal DT guidance (0 %- Case 1).

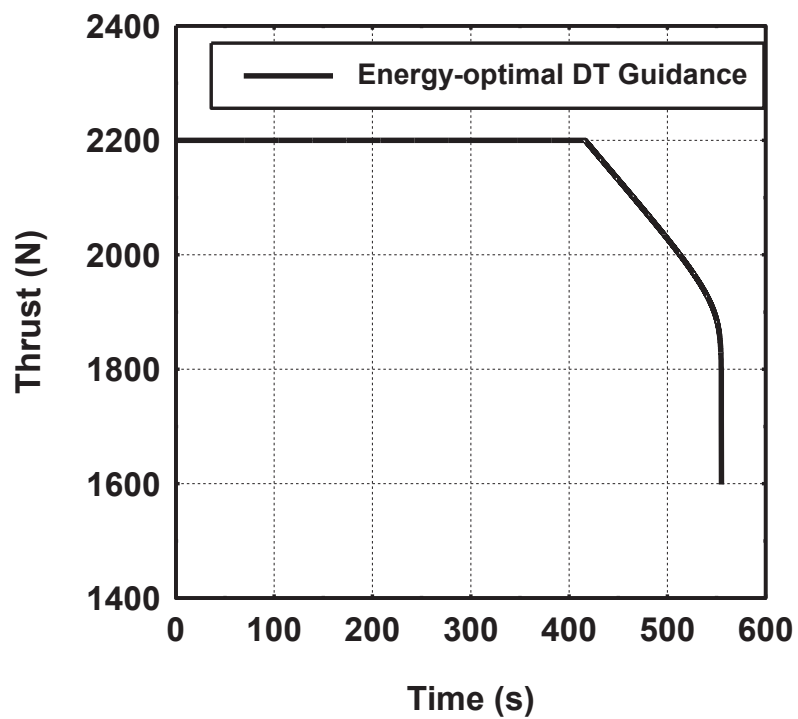


Fig. 5.4. Thrust profile for energy-optimal DT guidance (Case 1).

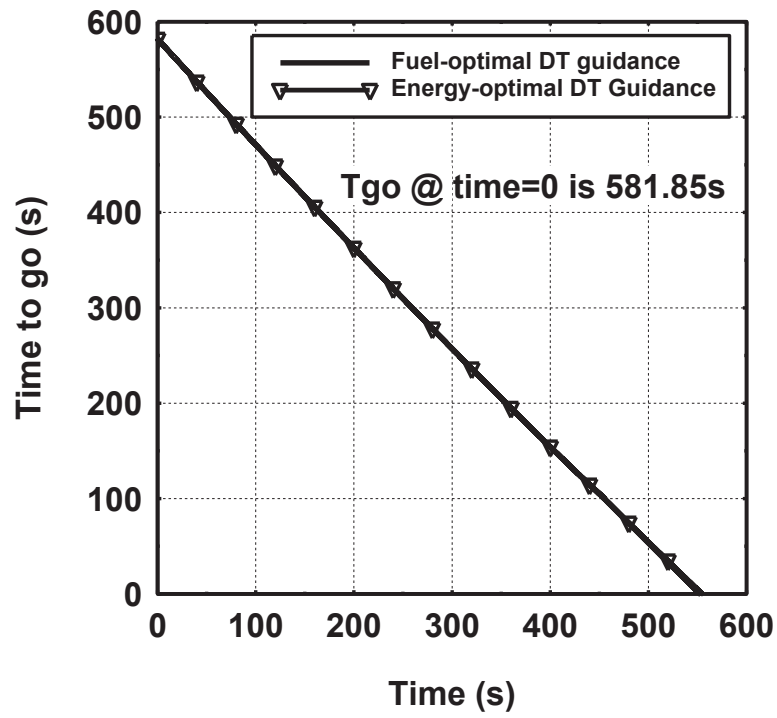


Fig. 5.5. Time vs real time computed time-to-go.

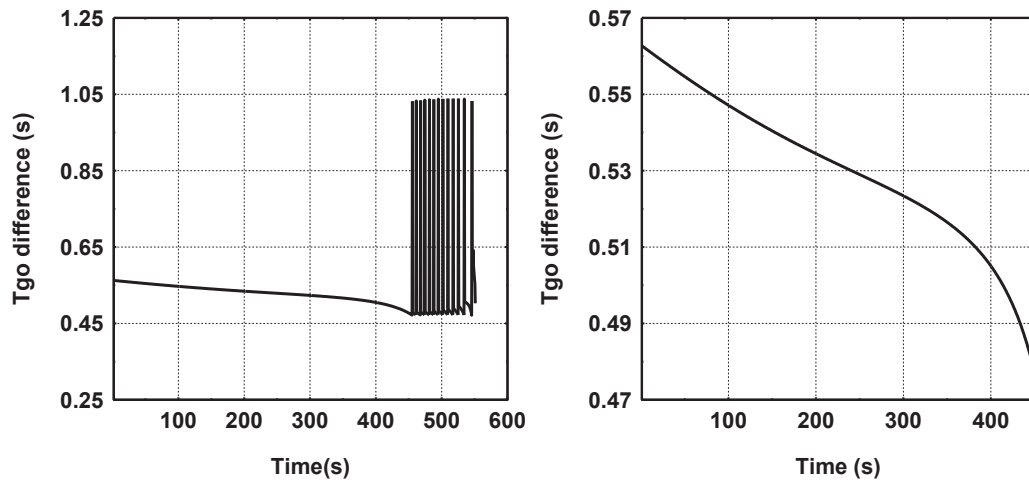


Fig. 5.6a. and Fig.5.6b. The time-to-go difference with propagation steps.

5.4.2 Fuel-optimal DT Guidance for Throttling Engine (40 % - 100 %)

The fuel-optimal DT guidance for case 1 needs the propulsion system to operate with full thrust for a time duration of 545.3 s and with zero thrust for 7.3 s. Practically, it may be difficult to operate the main engine in the on-off mode. In general, the throttling engines operate with a lower limit on throttling. A value of 40% is assumed for evaluating the fuel-optimal DT guidance. That means, during landing the engine is assumed to be operating either with maximum thrust (2200 N for this study) or with minimum thrust (880 N). The target site is kept as same as given Table 5.2. The performance of fuel-optimal guidance for this engine is presented in Table 5.6. The flight time and landing mass for this engine remains nearly same as in the 0% thrust case. But the target is achieved by increasing the time of operation with minimum thrust (40%) by about 4 s. However, the flight time remains the same implying that the total impulse in both the cases is same. The profile of demanded thrust by this engine is provided in Fig. 5.7.

Table 5.6 Performance of fuel-optimal DT guidance with minimum thrust 40 %

Parameter	Minimum thrust = 0%	Minimum thrust = 40%
Target Latitude (deg, North)	16.1508	16.1508
Target Longitude (deg)	0	0
Flight time (s) (touch down time)	552.49	552.52
Landing Mass(kg)	486.16	486.15
Deviation in target position at touch down (m)	0.001	0.001
Deviation in velocity at touch down (m/s)	0.10	0.11
Zero / minimum thrust duration (s)	7.3	11.0

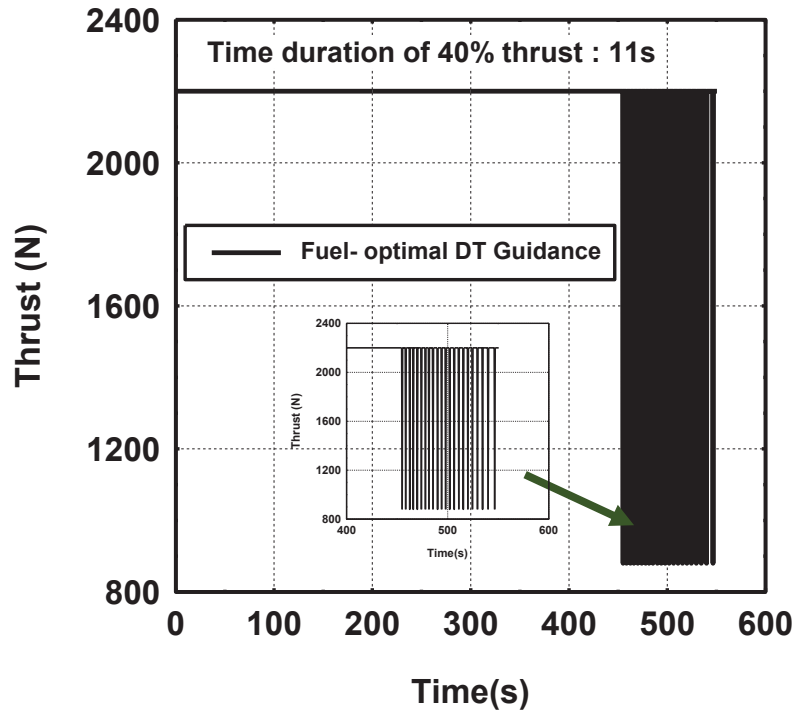


Fig. 5.7. Profile of demanded thrust by fuel-optimal DT guidance (minimum thrust = 40%).

5.4.3 Evaluation of time-to-go Computation Strategy and Guidance Schemes

The t_{go} strategy adapted herein is based on linearity assumption on the trajectory. So, the strategy is tested for various shapes of trajectory. Three thrust levels are considered for this analysis. The optimal landing trajectories are generated first to fix the target sites to be used for guidance schemes. These are tabulated in Table 5.7 for case 1. The first row of Table 5.7 is already reported in Table 5.2.

The fuel-optimal trajectories are plotted in Fig. 5.8. For the thrust levels of 1800 N and 1300 N, the altitude goes up initially and starts coming down compared to the case with thrust level of 2200 N. This type of non-linearity in the trajectory is tested with the t_{go} strategy. The performance of the DT guidance schemes are consolidated in

Table 5.8 and 5.9 for fuel-optimal and energy-optimal respectively. For all thrust levels, the fuel-optimal DT guidance achieves a landing mass very close to the optimal trajectory (cf. Table 5.7). For lower thrust levels the landing masses achieved with fuel-optimal and energy-optimal guidance schemes are different. The reduction in landing mass obtained using energy-optimal DT guidance scheme is about 3 kg. The reduction in landing mass is about 7 kg if CTVG scheme (cf. Table 5.10) is used. The CTVG scheme leads to lower landing masses with lower thrust levels. The performance of E-guidance is same as that of CTVG scheme and so not included herein. The profiles of t_{go} differences are depicted in Fig.5.9 for different thrust levels for the energy-optimal DT guidance. Although the shapes of the trajectories are different, the t_{go} strategy makes the module to land precisely. The trend is same for fuel-optimal also and so not plotted. It can be concluded that for very high thrust to mass ratios, the performance of the fuel-optimal and energy-optimal guidance scheme tends to be the same (in terms of landing masses) whereas for low thrust to mass ratios the reduction in landing masses occur for energy-optimal guidance scheme compared to fuel-optimal guidance scheme.

Table 5.7 Optimal trajectory parameters – Fuel-optimal

Thrust level (N)	Landing mass (kg)	Flight time (s) (Touch down time)	Target Latitude (deg. N)	Target Longitude (deg.)
2200	487.04	543.96	16.1508	0.0
1800	478	695	20.75	0.0
1300	454.2	998.68	29.04764	0.0

Table 5.8 Performance of the fuel-optimal DT guidance scheme

Thrust level (N)	Landing mass (kg)	Target Latitude (deg.N)	Target Longitude (deg.)	Flight time (s) (Touch down time)	Landing position deviation from target (m)	Landing velocity deviation from target (m/s)
2200	486.16	16.15080	0.0	552.49	0.001	0.1
1800	475.24	20.75	0.0	723.3	1.E-5	0.0023
1300	453.9	29.04764	0.0	1009.59	1.E-4	0.01

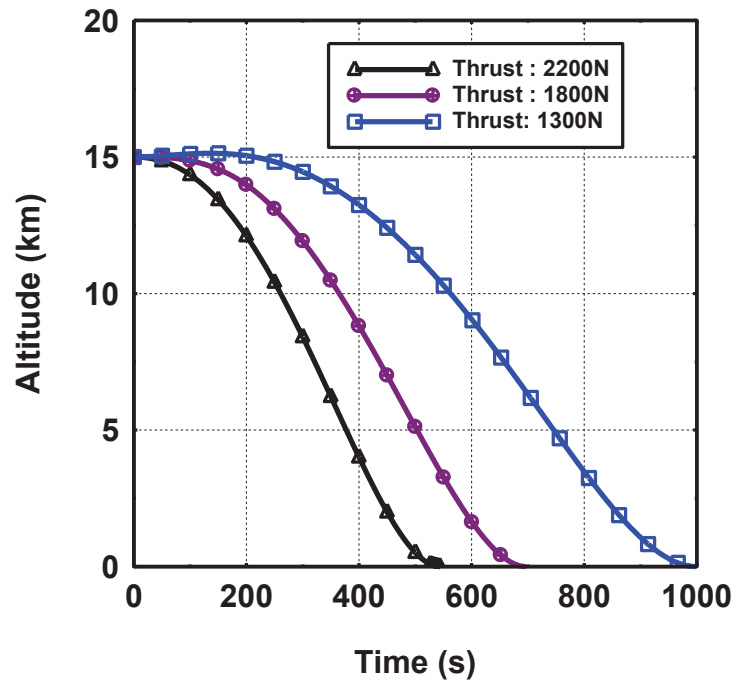


Fig. 5.8. Fuel-optimal trajectories for different thrust levels (case 1).

Table 5.9 Performance of the energy-optimal DT guidance scheme

Thrust level (N)	Landing mass (kg)	Target Latitude (deg.)	Target Longitude (deg.)	Flight time (s) (Touch down time)	Landing position deviation from target (m)	Landing velocity deviation from target (m/s)
2200	485.79	16.15080	0	554.96	5.E-06	0.001
1800	472	20.75	0	746.64	1.E-06	0.002
1300	450.19	29.04764	0	1023.75	2.7E-05	0.005

Table 5.10 Performance of the CTVG scheme

Thrust level (N)	Landing mass (kg)	Target Latitude (deg.)	Target Longitude (deg.)	Flight time (s) (Touch down time)	Landing position deviation from target (m)	Landing velocity deviation from target (m/s)
2200	485.5	16.15080	0	557.56	4.E-5	0.005
1800	470.45	20.75	0	751.5	3.E-5	0.011
1300	446.5	29.04764	0	1051.6	2.E-5	0.012

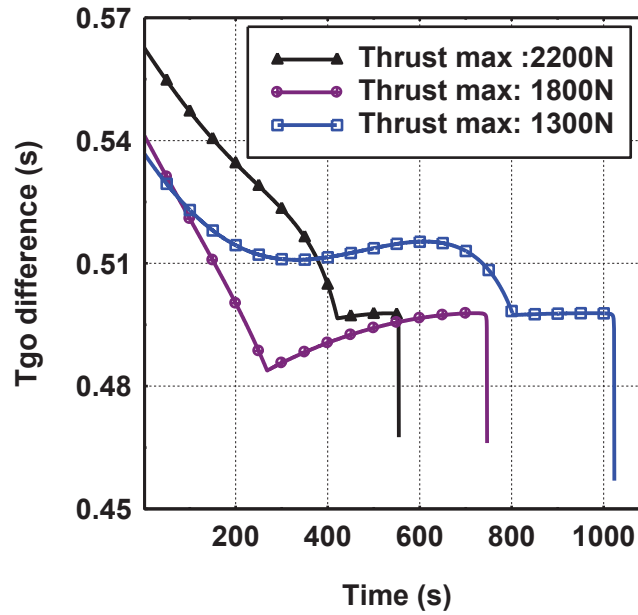


Fig. 5.9. Profiles of time-to-go differences under various thrust levels.

5.4.3.1 Performance comparison of time-to-go computation methods- proposed vs standard method

A standard way of computing time-to-go is as follows:

$$t_{go} = \frac{\rho}{v_{close}} ; \text{ where, } \rho \text{ is current range and } v_{close} = - \text{range rate}$$

The range vector is given by $\boldsymbol{\rho} = \mathbf{r}_C - \mathbf{r}_T$ and $\rho = |\boldsymbol{\rho}|$ where $\boldsymbol{\rho}$ is the current range vector, \mathbf{r}_C is the current position vector and \mathbf{r}_T is the target position vector of landing site.

For the comparative study, the minimum fuel case (Section.5.4.1, minimum fuel guidance case) is used. The use of standard method of time-to-go computation (using range and range rate) makes the module to touch down before the velocity braking ends and it results in large deviation in touch down position (2210 m) and velocity (286 m/s) from the target. The main difference between the two schemes is that in the proposed scheme instantaneous average velocity is used for time-to-go computation whereas in the standard method current range rate (i.e close to current velocity) is used. Therefore, the effect of change in velocity as the module descends is not accounted in the

computation. If the standard scheme is adopted along with the average (mean) range rate, then the position and velocity deviation at touch down will reduce (2.2 m in position and 0.8 m/s in velocity).

5.4.4 Nominal Landing Site with Higher Thrust

Another scenario tested for t_{go} strategy is when the thrust level for guidance is higher than the thrust used to generate the nominal target site (Table 5.7). That means with thrust higher than the nominal thrust (2200 N), achieving the same landing site is attempted. A thrust of 2500 N is used to achieve the landing site that was optimally achievable with a nominal thrust of 2200 N. This strategy is useful to provide margins for the guidance design. The fuel-optimal DT guidance achieves the target (cf. Table 5.11) with an additional landing mass of 2 kg with higher zero thrust duration of 65.5 s (7.3 s for a thrust level of 2200N) whereas the energy-optimal DT guidance achieves the target with a reduction of about 7 kg in the landing mass. For fuel-optimal guidance, the landing mass is higher due to the higher duration of zero thrust to achieve the same target site. For energy-optimal guidance, zero thrust is not possible and the lander needs to cover higher down-range (energy-optimal trajectory with 2500 N will result in a target site with lesser down-range and higher landing mass) to achieve the nominal target site of 2200 N and this results in more flight time with additional landing mass penalty.

Table 5.11 Effect of higher thrust (2500 N) on guidance scheme and time-to-go strategy

Parameter	Fuel-optimal DT Guidance	Energy-optimal DT Guidance	CTVG
Flight time (s) (touch down time)	543.6	593.55	597.5
Landing Mass(kg)	487.4	480.5	479.99
Deviation in target position at touch down (m)	0.001	4.e-6	5e-6
Deviation in velocity at touch down (m/s)	0.11	0.002	0.003
Zero thrust duration (s)	65.5	-	-

5.5 Retargeting Capability

5.5.1 Retargeting Before Start of Powered Braking

If the landing site is changed for some reason, the guidance schemes must be capable of handling the new landing sites. In this section, a mission scenario in which the retargeting is planned before the start of powered braking phase. First, the capability of guidance schemes is evaluated for different sites along the orbit track. For this purpose, instead of the nominal site (16.1508 deg. N , 0 deg.) two retarget sites (i) 18 deg N latitude and 0 deg. longitude (ii) 25 deg. N latitude and 0 deg. longitude are considered. Table 5.12 and Table 5.13 present the performance of guidance schemes. The fuel-optimal DT guidance achieves the retargets without much loss in the landing mass by introducing longer zero thrust duration. The energy-optimal DT guidance achieves the retargeted sites with reduction in landing masses (i.e) 7 kg and 30 kg respectively. The CTVG scheme achieves the retargeted sites with a reduction of 7.5 kg and 32 kg in landing mass respectively. Even with 40% minimum thrust engine, the performance of fuel-optimal DT guidance is similar to zero thrust case.

The cross-track capability for both guidance schemes are assessed and given in Tables 5.14 and 5.15. For this purpose, the longitude of the site is varied keeping latitude same. With the same thrust level, the guidance schemes are able to manage cross-ranges up to 0.8 deg. in longitude that is equivalent to 23 km. Any further change in the latitude becomes not achievable by the guidance schemes. But the cross-range capability increases if the down-range of target site is also increased. For example, for a latitude 16.5 deg., the cross-range capability increases to 2.5 deg. A higher cross-range is achievable in the case of energy-optimal guidance when the more leverage is provided in the down-range. For example, for a target latitude of 17.5 deg. N, the cross-range achievable by fuel-optimal is 3.2 deg. whereas with energy-optimal it is about 5.9 deg. However, there is a heavy penalty (reduction of 35 kg) on landing mass.

Table 5.12 Assessment of retargeting capability (Retarget 1)

Parameter	Fuel-optimal DT guidance		Energy-optimal DT Guidance	CTVG
	Min. thrust = 0%	Min. thrust = 40%		
Flight time (s)	601.4	601.5	660.4	665.2
Landing Mass(kg)	484.8	484.8	476.08	475.48
Zero thrust duration (s)	54.44	90.75	-	-
Deviation in target position at touch down (m)	2.E-4	1.98E-4	8.2E-6	4E-5
Deviation in velocity at touch down (m/s)	0.015	0.015	0.0016	0.012

Table 5.13 Assessment of retargeting capability (Retarget 2)

Parameter	Fuel-optimal DT guidance		Energy-optimal DT Guidance	CTVG
	Min. thrust = 0%	Min. thrust = 40%		
Flight time (s)	730.8	731.5	931.2	948.5
Landing Mass(kg)	484.79	484.9	453.45	451.3
Minimum thrust duration (s)	183.6	315.24	-	-
Deviation in target position at touch down (m)	3.1E-4	2.01E-4	8e-7	3.9e-6
Deviation in velocity at touch down (m/s)	0.017	0.015	0.001	0.003

Table 5.14 Assessment of fuel-optimal DT guidance for cross-range deviation

Target Latitude (deg., North)	Target Longitude (deg.)	Down-range/ Cross- range (km)	Flight time/ Touch down time (s)	Pos.dev from target (m)	Vel.dev from target (m/s)	Zero thrust duration (s)	Landing mass (kg)
16.1508	0.0	492.07 / 0.0	552.49	0.001	0.1	7.3	486.16
16.1508	0.8	492.07/ 23.4	546.1	0.005	0.2	2.41	486.01
16.5	2.5	503.9 / 73.0	558	0.5	1.2	2.1	477.5
17.5	3.2	533.0 / 87.2	605.4	0.63	0.84	43.6	473.6

Table 5.15 Assessment of energy-optimal DT guidance for cross-range deviation

Target Latitude (deg., North)	Target Longitude (deg.)	Down-range /Cross-range (km)	Flight time/Touch down time (s)	Pos.dev. from target (m)	Vel.dev from target (m/s)	Landing mass (kg)
16.1508	0.0	492.07/0.0	554.96	5.e-6	0.001	485.79
16.1508	0.8	492.07/23.4	547.5	0.1	0.8	485.65
16.5	2.5	503.0/73.0	559.5	0.23	0.91	477.1
17.5	5.9	533.0/171.0	641.2	0.33	1.2	437.3

5.5.2 Retargeting During Powered Braking Phase

If the landing site is changed during the powered braking phase for some reason, the capability of the guidance schemes to handle the new landing sites is assessed. For the present study, the following conditions are considered. The nominal target conditions until 7 km altitude is 0.0 deg. longitude and 16.1508 deg. latitude. From 7 km altitude the module is diverted to the new landing target, which is away from the nominal target. Different targets are listed in Table 5.16. For retargeting of 0.2 deg. deviation in both longitude and latitude at 7 km altitude, the landing mass penalty from nominal case of fuel-optimal case (cf. Table 5.16) is about 2 kg. In this case, the zero thrust duration increases to 17.7 s whereas it is 7.3 s for the nominal case. For energy-optimal case (cf. Table 5.17) the landing mass reduction is about 3.6 kg. The profiles of latitude, longitude and altitude profile for nominal and for retarget deviations of 0.2 deg. on both target latitude and longitude for energy-optimal case are shown in Fig. 5.10 (zoomed plot at terminal landing point also provided) and 5.11.

Table 5.16 Assessment of fuel-optimal DT guidance for retargeting at 7km

Target Latitude @ 15km altitude 16.1508 deg.	Target Longitude @ 15km altitude : 0.0 deg.	Flight time/Touch down time (s)	Zero thrust time (s)	Pos.dev. from target (m)	Vel.dev from target (m/s)	Landing mass (kg)
Target Latitude @ 7km altitude (deg., North)	Target Longitude Latitude @ 7km altitude (deg.)					
16.1508	0.0	554.49	7.3	0.001	0.1	486.16
16.1508	0.2	552.3	5.6	0.002	0.05	485.1
16.3508	0.0	564.5	17.8	0.005	0.13	485
16.3508	0.2	565.6	17.7	0.003	0.03	484.2

Table 5.17 Assessment of energy-optimal DT guidance for retargeting at 7km

Target Latitude @ 15km altitude 16.1508 deg.	Target Longitude @ 15km altitude : 0.0 deg.	Flight time/Touch down time (s)	Pos.dev from target (m)	Vel.dev from target (m/s)	Landing mass (kg)
Target Latitude @ 7km altitude (deg. North)	Target Longitude Latitude @ 7km altitude (deg.)				
16.1508	0.0	554.96	5.E-6	0.001	485.79
16.1508	0.2	554.4	2.E-4	0.02	484.7
16.3508	0.0	574.6	4E-4	0.03	483.5
16.3508	0.2	576.6	6E-4	0.1	482.3

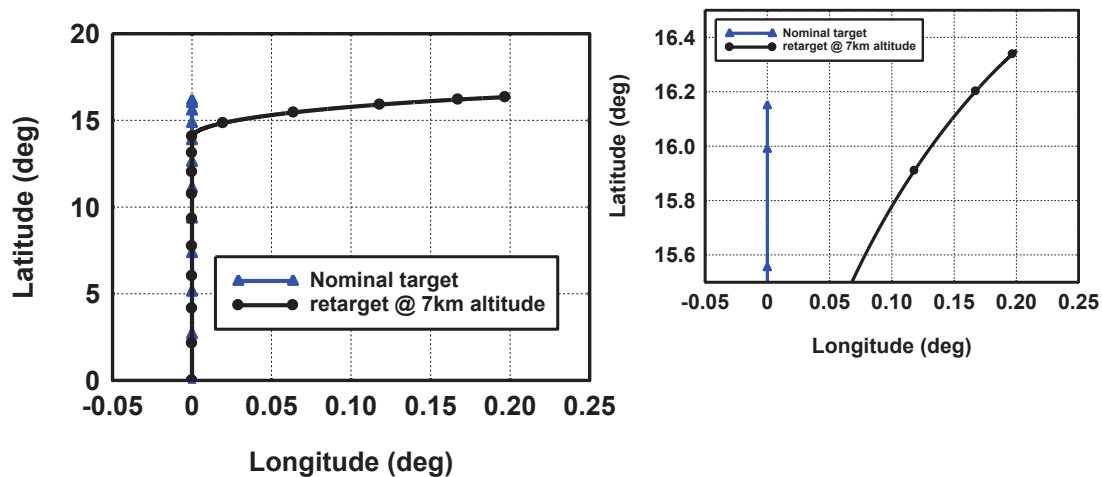


Fig. 5.10. Guided trajectories (latitude vs longitude) for nominal and with retargeting-energy-optimal

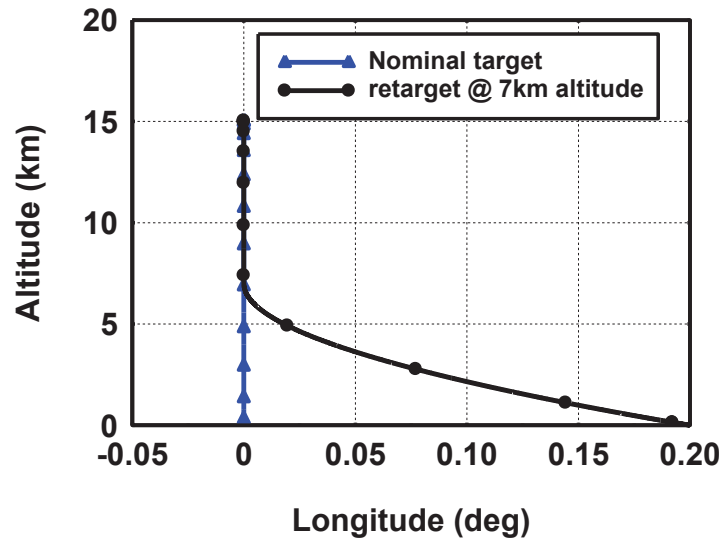


Fig. 5.11. Guided trajectories (altitude vs longitude) for nominal and with retargeting - energy optimal

5.6 Monte Carlo Simulations

To evaluate the robustness of the schemes, Monte Carlo (MC) simulations have been carried out for the case 1 and are reported in Table 5.1. The input parameters and their dispersions are given in Table 5.18. The dispersion on position (1km) is distributed to the components of position and it is 577.35 m in each direction and similarly the dispersion on velocity (10 m/s) on each component of velocity is 5.774 m/s. The results of one thousand MC simulations are presented in Tables 5.19 and 5.20 for the fuel-optimal and the energy-optimal DT guidance schemes respectively. The position and velocity deviation for various cases at touch down for fuel-optimal and energy-optimal simulations are shown in Fig. 5.12 to Fig. 5.15. The touch down time and landing mass for various cases are shown in Fig. 5.16 to Fig. 5.19. The variation in the landing mass is very small (less than 1 kg) for the fuel-optimal DT guidance because zero thrust duration is varied to achieve the landing site. The trend remains the same even with minimum thrust of 40% instead of zero thrust. For energy-optimal guidance, the variation in landing mass compared to the nominal mass is up to 5 kg. Further, the variation in the parameter time-to-go is larger (18.5 s) for energy-optimal guidance

whereas it is 13 s for fuel-optimal guidance. These trends are observed even when uniform distribution is adapted for the dispersions. The efficiency of fuel-optimal DT guidance over energy-optimal DT guidance is clear.

The altitude, downrange and cross range profiles for energy-optimal cases are shown in Fig.5.20. Even when the initial cross range deviation of about 2000 m (cf. Fig. 5.20), the guidance scheme is capable of bringing the vehicle to zero cross range and down range at touch down. For this case, the velocity components are reduced to zero at touch down and it is shown in Fig.5.21.

Table 5.18 Dispersions for Monte Carlo simulation

Parameter	Distribution	Dispersion (3σ)
Position (m)	Gaussian	1000
Velocity (m/s)	Gaussian	10
Specific impulse, Isp (s)	Gaussian	5

Table 5.19 Summary of MC simulations for fuel-optimal DT guidance

Parameter	Landing mass (kg)	Touch down time (s)	Deviation in Target Position (m)	Deviation in Target Velocity (m)
Nominal	486.16	552.49	0.001	0.1
Mean	486.23	552.88	0.0012	0.12
Standard Deviation (1σ)	0.119	2.31	0.00064	0.0363
Minimum	485.9	545.31	1.8e-7	0.0013
Maximum	486.81	558.27	0.0029	0.18

Table 5.20 Summary of MC simulations for energy-optimal DT guidance

Parameter	Landing mass (kg)	Touch down time (s)	Deviation in Target Position (m)	Deviation in Target Velocity (m)
Nominal	485.79	554.96	5e-6	0.001
Mean	485.81	556.45	1.095e-5	0.0064
Standard Deviation (1σ)	1.67	2.92	1.027e-5	0.0041
Minimum	480.16	546.33	1.97e-9	4.36e-7
Maximum	492.27	564.8	3.56e-5	0.0148

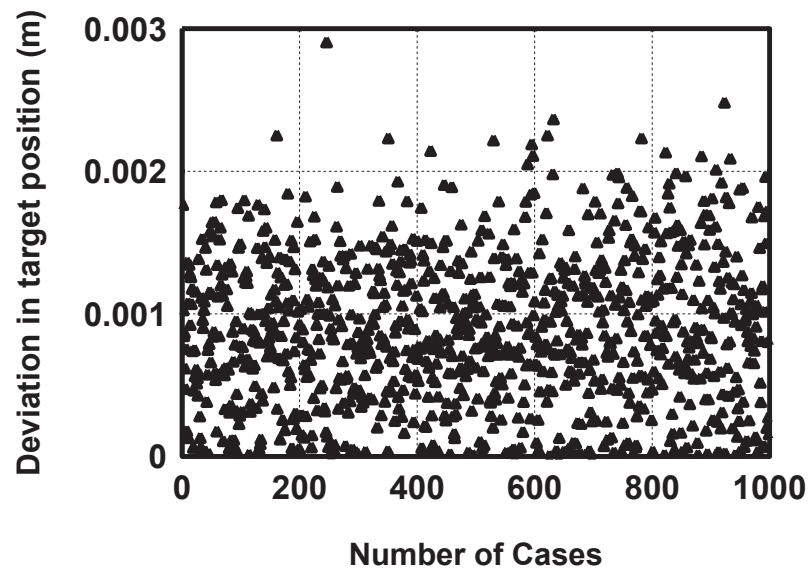


Fig. 5.12. Position deviation from target at touch down (fuel-optimal)

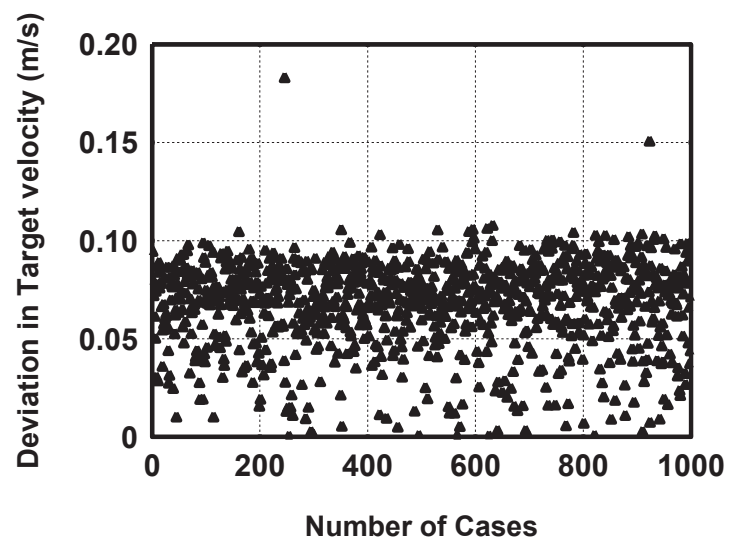


Fig. 5.13. Velocity deviation from target at touch down (fuel-optimal)

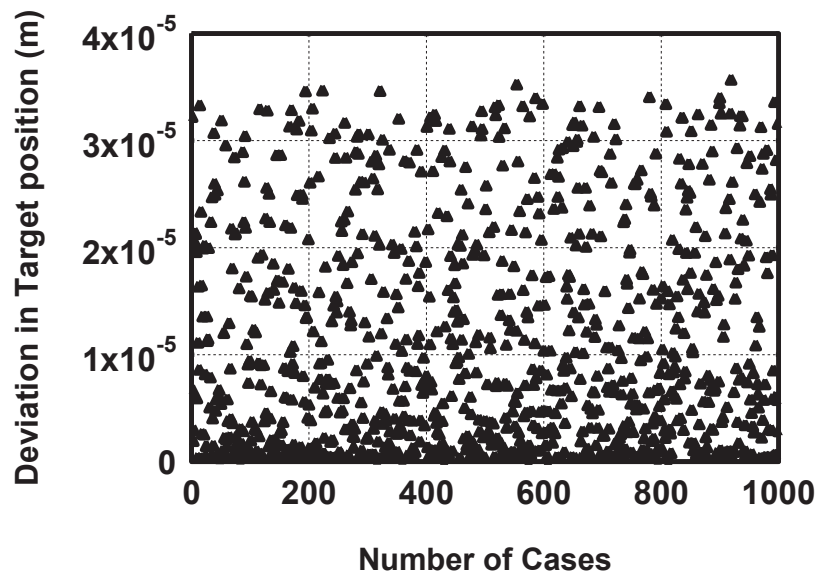


Fig. 5.14. Position deviation from target at touch down (energy-optimal)

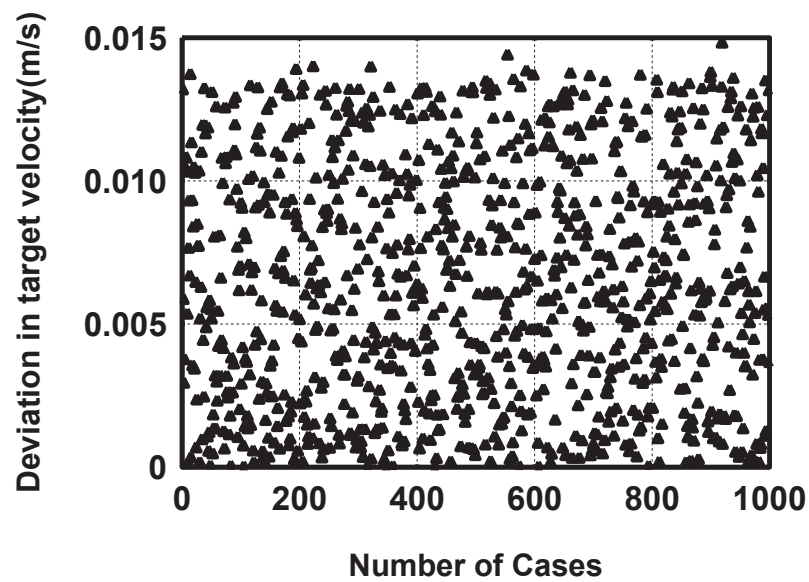


Fig. 5.15. Velocity deviation from target at touch down (energy-optimal)

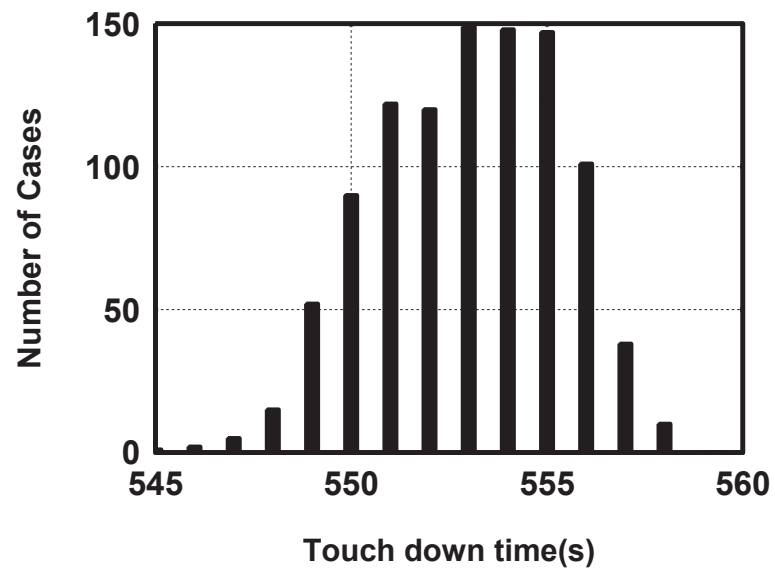


Fig. 5.16. Touch down (flight) time vs number of fuel-optimal simulations

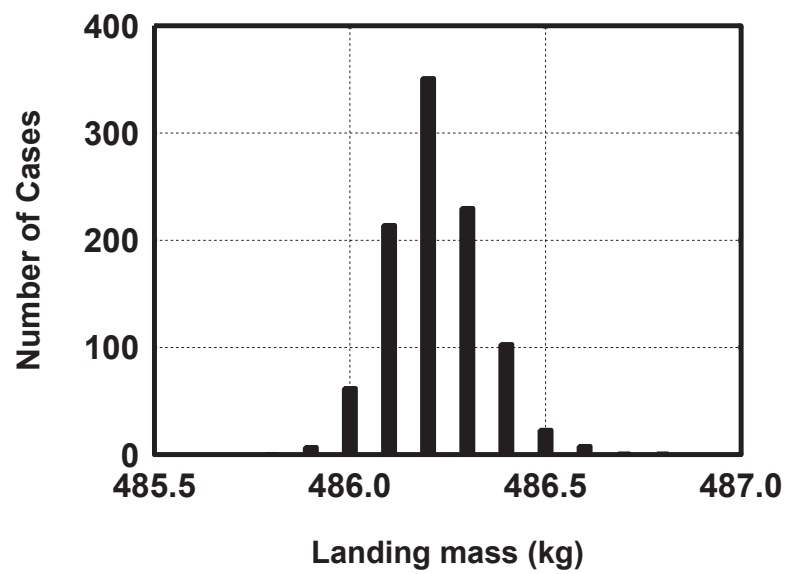


Fig. 5.17. Landing mass vs number of fuel-optimal simulations

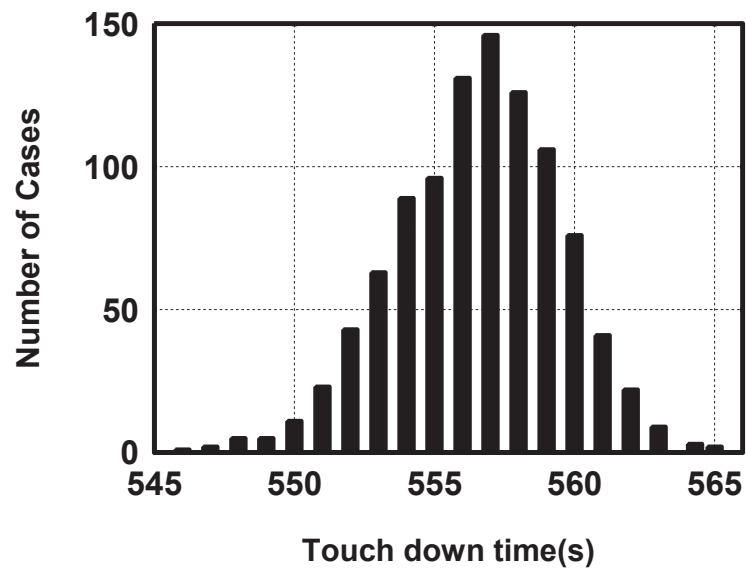


Fig. 5.18. Touch down time vs number of energy-optimal simulations

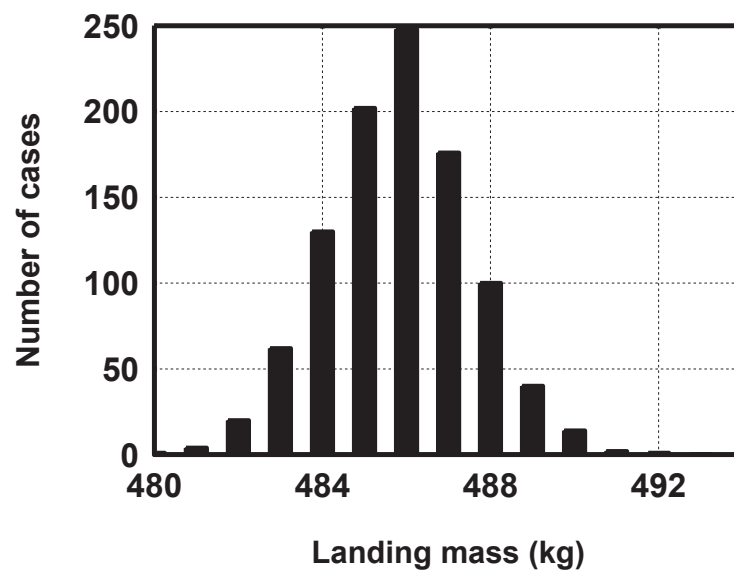


Fig. 5.19. Landing mass vs number of energy-optimal simulations

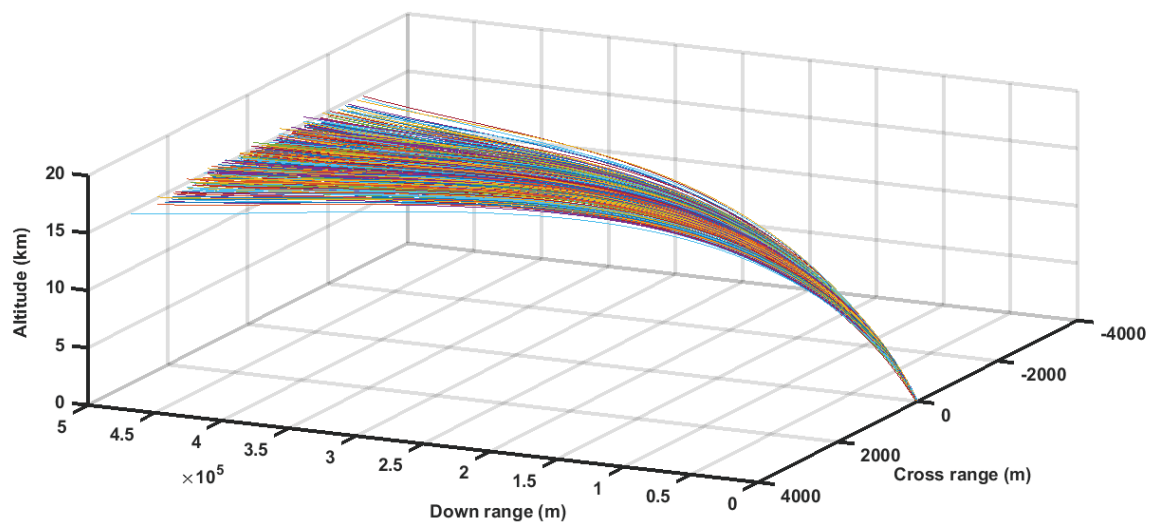


Fig. 5.20. Altitude, downrange and cross range profiles of energy-optimal simulations

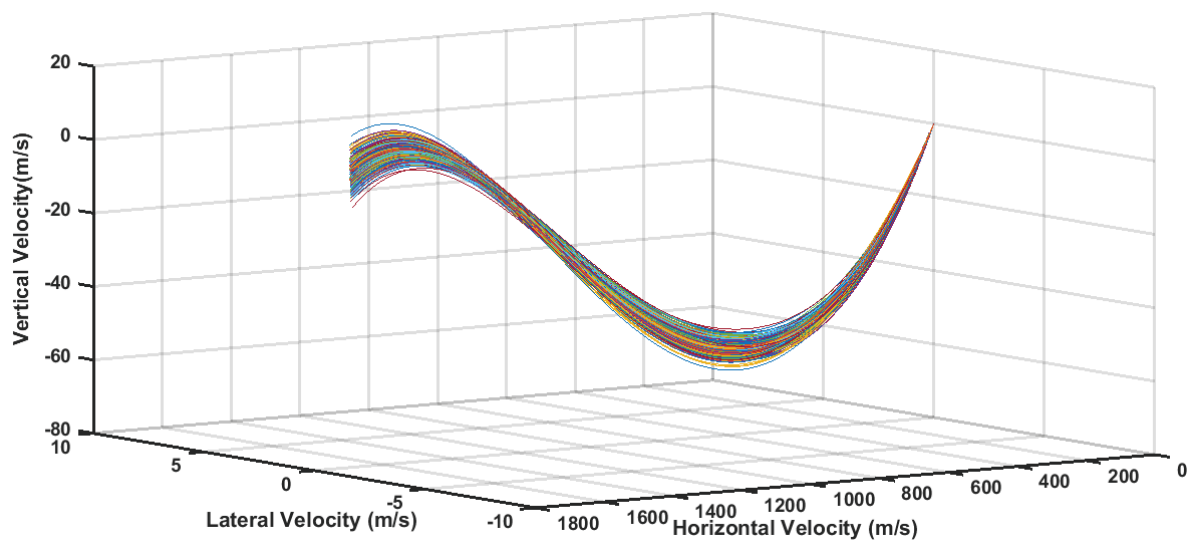


Fig. 5.21. Velocity components – energy-optimal simulations

5.7 Constraint on Lander Terminal Thrust Attitude

In all the above analysis, the guidance schemes achieve the specified landing target point with null altitude and null velocity. The attitude at touchdown is not targeted. In these cases, thrust attitude at the time of touchdown is found to be around 140 deg. from local horizontal. To achieve vertical landing during touch down a strategy is introduced in this section. In this strategy, the horizontal velocity is nullified and an appropriate vertical velocity is achieved at a chosen altitude. This strategy results in zero acceleration components (except vertical) at the chosen altitude ensuring vertical orientation for landing. The appropriate vertical velocity is computed from the one-dimensional kinematics equation $v^2 = u^2 + 2aS$. To demonstrate, an altitude of 30 m is chosen at which zero horizontal velocity and vertical velocity of -13 m/s are to be achieved. The vertical velocity is computed by assuming 2200 N thrust and 493 kg mass of the module. The altitude can be chosen according to the mission needs.

The input parameters provided in Table 5.1 are considered for this study. The target conditions to be achieved at 30 m altitude are given in Table 5.21. Because of the assumption of non- rotating Moon and vertical landing, the latitude and longitude are same at 30m altitude as that of target landing site. Both the fuel-optimal and energy-optimal DT guidance schemes have been evaluated with this strategy for vertical orientation and presented in Table 5.22. The flight time from 30 m altitude to touch down is about 4.6s and the landing mass is 485.6 kg for fuel-optimal and 485.2 kg for energy-optimal scheme. In both cases, the landing mass is about 0.6 kg less compared to the cases (cf. Table 5.3) without terminal thrust attitude constraint. The thrust attitude variation is shown in Fig. 5.22 for fuel-optimal and energy-optimal schemes and the required thrust attitude of 90 deg. is achieved for both cases during the terminal vertical landing phase.

Table 5.21 Target conditions

Parameter	Value
Latitude (deg., North)	16.1508
Longitude (deg.)	0.0
Target Terminal altitude (m)	30
Target Terminal velocity (m/s)	-13m/s in radial direction

Table 5.22 Performance of DT guidance schemes with terminal vertical thrust direction

Parameter	Fuel-optimal DT guidance	Energy-optimal DT guidance
Time to reach 30m altitude (s)	548.3	549.1
Flight Time (s) (touch down time)	552.85	553.65
Landing Mass(kg)	485.6	485.2
Zero thrust duration (s)	6.9	-
Horizontal velocity @ 30m altitude (m/s)	1.5E-6	2.5E-6
Vertical velocity @ 30m altitude (m/s)	-13.03	-13.1
Vertical velocity @ touchdown (m/s)	0.013	0.14
Terminal thrust direction from local horizontal (deg.)	90	90

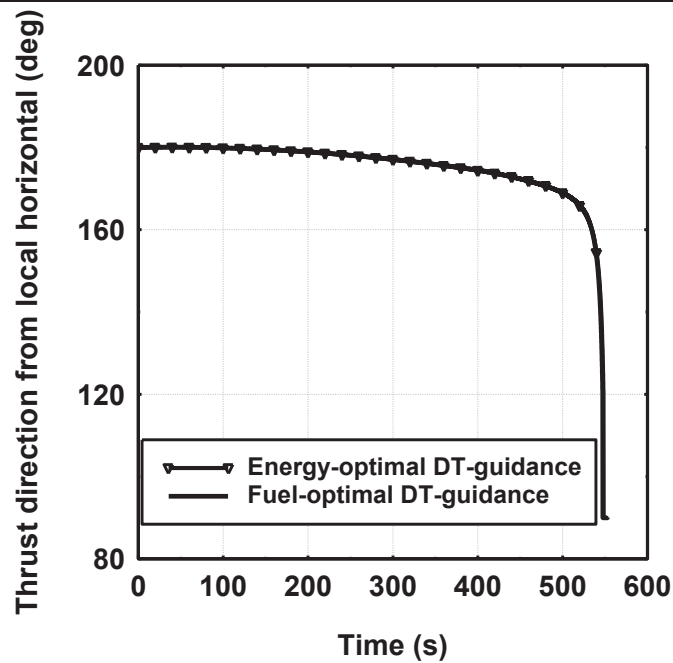


Fig. 5.22. Thrust direction variation for fuel-optimal and energy-optimal guidance scheme.

5.8 Conclusions

The fuel-optimal DT guidance scheme performs very well in different mission scenarios. The scheme is capable of introducing minimum thrust or no thrust duration during powered descent to achieve the target site. The landing mass difference between the DT energy-optimal guidance and open-loop optimal trajectory are within 1 to 1.5 kg only. The difference between the landing masses achieved using open loop fuel-optimal trajectory formulation and fuel-optimal DT guidance scheme is only marginal (less than 1 kg) for all nominal thrust levels. Reduction in landing masses is observed for lower nominal thrust levels when energy-optimal guidance is used. For a nominal thrust of 1800 N the achieved landing mass is less than the optimal mass by about 3 kg. The reduction in landing mass (about 7 kg) is more with other guidance schemes such as CTVG. The performance of DT fuel-optimal guidance is independent of the thrust to mass ratios. The performance of the simple strategy for the computation of real time time-to-go is demonstrated for nonlinear shapes of trajectory. The insufficiency of linear decrement of the parameter time-to-go for guidance command generation is established. The decrement in time-to-go in the proposed simple strategy varies between 0.47 s and 0.56 s instead of 0.5 s with linear decrement. The strategy works well for the cases with different thrust levels, retargeted sites etc. The advantage of this strategy is that the information of flight time prior to the mission is not necessary. When a nominal target site (obtained with some nominal thrust level) is targeted with higher thrust, the fuel-optimal DT guidance scheme achieves the target with higher landing mass by introducing higher zero-thrust duration. In the same scenario, the energy-optimal DT guidance achieves the target with reduced landing mass. The proposed guidance schemes are capable of realizing the retargeted target sites. When the retargeted sites are along the orbital track, the fuel-optimal DT guidance achieves the target with only marginal loss in landing mass whereas energy-optimal guidance schemes achieve the retargeted sites with heavy penalty on landing mass. The capability of both the guidance schemes in achieving the off-track retargeted sites is found to be limited. The variation in the landing mass with fuel-optimal guidance is less than 1 kg under Monte Carlo

dispersion studies. The use of energy-optimal guidance results in larger variation (5kg) in the landing mass.

Chapter 6

Conclusions and Future Scope of Work

The soft landing on the Moon is formulated as an optimal control problem and is transformed into a Two Point Boundary Value Problem (TPBVP). As a first step, planar motion for landing trajectory design is considered and this problem is evaluated using different solution scheme. Six direct and indirect schemes have been evaluated using two evolutionary optimization methods i.e Particle Swarm Optimization (PSO) and Differential Evolution (DE) along with MATLAB based gradient optimization method for soft landing trajectory optimization. Both the evolutionary optimization methods are found to be capable of locating the optimum solution even with very wide bounds. However, PSO requires more function evaluations compared to DE to arrive at the global optimum. Gradient-based optimization methods requires reasonable accurate initial guess of the solution. Apart from good initial guesses, the solution accuracy of the direct approach depends on the number of discrete thrust direction angular rates at different time intervals and their interpolation schemes. For a new problem, a prior information about nature of the solution is unknown. Therefore, the indirect approach using DE technique is followed for further research on design of optimal soft landing trajectory on the Moon.

A novel computational scheme is developed for open loop lunar soft landing trajectory computation by combining Differential Transformation (DT) technique and Differential Evolution (DE). This computational scheme is called DT-DE scheme. The required thrust acceleration vector at every computational time interval is computed using DT scheme by determining the co-states. The single unknown variable in this formulation is flight time and it is selected using DE, which removes the complexity in the solution process to a large extent.

Three performance measures i) time-optimal ii) fuel-optimal iii) energy-optimal with and without thrust limit are considered for the formulation and their performances are compared with detailed analysis. The summary of findings and conclusions from the analysis studies is as follows:

- The efficiency of the DT technique in achieving the target site precisely is demonstrated.
- Differential Evolution technique obtains the solution very quickly using the initial co-states determined by DT technique and the guidelines on the flight time. The optimal landing trajectory is generated quickly without losing the advantages of the indirect scheme. The computational time (CPU time) to generate the optimal solution using the DT- DE scheme is about 35 to 40s and whereas using the DE technique alone, which uses bounds for initial co-states also, it is about 170s.
- The computational time for DT-DE scheme is comparable with a gradient based optimizer (to select flight time) that uses the initial co-states determined by DT technique.
- The use of the DE technique along with the DT technique avoids non-convergence and local convergence scenarios, which occur when gradient-based optimizer is used.
- The robustness of the DT-DE scheme is demonstrated for different performance measures.
- The ability of the proposed scheme to introduce coasting during descent is demonstrated.
- The capability of the DT-DE schemes (fuel-optimal and energy-optimal) to find the initial conditions of the optimal trajectory for different mission scenarios is demonstrated.

- Usually for soft landing mission, the target location will be fixed and the initial state need to select optimally for powered braking initiation. When the target site is fixed, the soft landing can be achieved either by changing the initial true anomaly or the argument of perilune. The use of DE is demonstrated to find the appropriate initial true anomaly or argument of perilune to land at the selected target. The fuel-optimal formulation adjusts the zero thrust duration to achieve the fixed target state. The energy-optimal formulation computes the required thrust acceleration by varying thrust profile and achieves the target landing conditions.
- When descent phase is initiated at higher perilune altitudes, there is marginal advantage of landing mass for fuel-optimal over energy-optimal strategies and it increases when altitude increases.
- For fuel-optimal trajectories, higher flight times result in longer zero thrust duration and achieve nearly same landing mass for all flight times. But for energy-optimal formulation achieves soft landing with penalties on the landing mass.

The DT based proposed guidance schemes help quantify the landing masses for fuel-optimal and energy-optimal objectives. The important findings from the studies are summarized as follows,

- The fuel-optimal DT guidance scheme performs very well in different mission scenarios. The scheme is capable of introducing minimum thrust or no thrust duration during powered descent to achieve the target site. The difference between the landing masses achieved using open-loop optimal trajectory formulation and the fuel-optimal DT guidance scheme is marginal (less than 1 kg) for all nominal thrust levels.

- There is reduction in landing masses for lower nominal thrust levels when energy-optimal guidance is used. For a nominal thrust of 1800 N the achieved landing mass is less than the optimal mass of open-loop trajectory by about 3 kg. The reduction in landing mass (about 7 kg) is more with other guidance schemes such as CTVG.
- The performance of the simple strategy for the real-time computation of time-to-go is demonstrated even for nonlinear shapes of trajectory. The insufficiency of linear decrement of the parameter time-to-go for guidance command generation is established. The decrement in time-to-go in the proposed simple strategy varies between 0.47 s and 0.56 s instead of 0.5 s with linear decrement. The strategy works well for the cases with different thrust levels, retargeted sites etc.
- When a nominal target site (obtained with some nominal thrust level) is targeted with higher thrust, the fuel-optimal DT guidance achieves the target with higher landing mass by introducing higher zero-thrust duration. In the same scenario, the energy-optimal DT guidance scheme achieves the target with reduced landing mass.
- When higher thrust ($2500 \text{ N} > \text{nominal thrust } 2200 \text{ N}$) is used the fuel-optimal DT guidance achieves the nominal target with an additional landing mass of 2 kg with higher zero thrust duration of 65.5 s (7.3 s for a thrust level of 2200 N) whereas the energy-optimal DT guidance achieves the target with a reduction of about 7 kg in the landing mass.
- For very high thrust to mass ratios, the performance of the fuel-optimal and energy-optimal guidance schemes tends to be the same (in terms of landing masses) whereas for low thrust to mass ratios the reduction in landing masses occur for energy-optimal guidance scheme compared to the landing mass obtained using fuel-optimal guidance scheme.
- The proposed guidance schemes are capable of realizing the retargeted target sites. When the retargeted sites are along the orbital track, the fuel-optimal DT guidance achieves the target with only marginal loss in

landing mass whereas energy-optimal guidance schemes achieve the retargeted sites with heavy penalty on landing mass. The capability of both the guidance schemes in achieving the off-track retargeted sites is found to be limited.

- The variation in the landing mass with fuel-optimal guidance is less than 1 kg under Monte Carlo dispersion studies. The use of energy-optimal guidance results in variation of 5kg in the landing mass.

Future Scope

The compatibility of the thrust on/off switching frequency with the actual thrusters is not considered in this thesis. The limitations of the actual thrusters can be modeled as constraints and a feasible solution can be obtained. This work is proposed for the future.

The DT based scheme can be explored for Mars soft-landing scenario with appropriate aerodynamic force model for atmospheric phase of trajectory.

References

1. Acikmese, B., Blackmore, L., 2011. Lossless Convexification for a class of optimal control problems with nonconvex control constraints. *Automatica*, 47(2), 341-347.
2. Acikmese, B., Blackmore, L., Scharf, D. P., Wolf A., August 2008. Enhancements on the convex programming based powered descent guidance algorithm for Mars landing. AIAA/AAS Astrodynamics Specialist Conference and Exhibit, Honolulu, AIAA-2008-6426.
3. Acikmese, B., Ploen, S. R., 2007. Convex programming approach to powered descent guidance for Mars landing. *Journal of Guidance, Control, and Dynamics*, 30(5), 1353–1366.
4. Ashok Kumar, Y., MIP Project team, 2009. The Moon Impact Probe (MIP) on Chandrayaan-1. *Current Science*, 96(4), 540-543.
5. Banerjee, A., Padhi, R., 2017. An optimal explicit guidance algorithm for terminal descent phase of lunar soft landing. AIAA Guidance, Navigation and Control Conference, Grapevine, Texas, 9 - 13 January 2017, AIAA 2017-1266.
6. Banerjee, A., Padhi, R., March 2020. Multiphase MPSP guidance design for lunar soft landing. *Transactions of Indian National Academy of Engineering*, DOI: 10.1007/s41403-020-00090-1
7. Banerjee, A., Padhi, R., Vatsal, V., 2015. Optimal guidance for accurate lunar soft landing with minimum fuel consumption using model predictive static programming. 2015 American Control Conference, Palmer House Hilton July 1-3, 2015, Chicago, IL, USA.
8. Ben Asher, J., 2010. Optimal control theory with aerospace applications, AIAA education series.
9. Bennett, F. V., 1970. Apollo lunar descent and ascent trajectories. NASA TMX-58040.
10. Bennett, F.V., 1972. Apollo experience report-mission planning for lunar module descent and ascent. NASA Technical Note, NASA TN D-6846.

11. Bennett, F.V., Price, T.G., 1964. Study of powered-descent trajectories for manned lunar landings. NASA TN D-2426.
12. Benson, D. A., Huntington, G.T., Thorvaldsen, T., Rao, A.V., 2006. Direct trajectory optimization and co-state estimation via an orthogonal collocation. *Journal of Guidance, Control and Dynamics*, 29(6), 1435-1440.
13. Betts, J. T., 1998. Survey of numerical methods for trajectory optimization. *Journal of Guidance, Control and Dynamics*, 21(2), 193-207.
14. Bishop, R.H., Azimov, D. M., 2008. Improved Apollo targeting for on-board lunar landing site re-designation. *New trends in astrodynamics and applications*, Milan, Italy, June 30-July 2, 2008.
15. Blackmore, L., Acikmese, B., Scharf, D., 2010. Minimum landing-error powered descent guidance for Mars landing using convex optimization. *Journal of Guidance, Control and Dynamics*, 33(4), 1161-1171.
16. Brauer, G. L., Cornick, D. E., Habegar, A. R., Peterson, F.M., Stevenson, R., 1975. Program to Optimize Simulated Trajectories, POST- formulation manual. NASA CR-132689.
17. Bryson, A., Ho, Y. C., 1975. *Applied Optimal Control - Optimization, Estimation and Control*. Hemisphere Publishing Company
18. Cavoti, C. R., September 1966. Minimum-fuel, two-impulse, soft lunar landing orbits. Technical report, Space Sciences Laboratory, General Electric Company, NASA-CR-65554.
19. Cheng, R. K., Meredith, C., Conrad, D., 1966. Design considerations for surveyor guidance. *Journal of Spacecraft and Rockets*, 3(11), 1569-1576.
20. Cheng, R. K., Pfeffer, I., 1962. Terminal guidance system for soft lunar landing. *Progress in Astronautics and Rocketry*, 8, 217-239.
21. Cheng, R.K., Conrad, D.A., 1964. Design considerations for the Surveyor terminal descent system. *AIAA/ION Astrodynamics, Guidance and Control Conference*, Los Angeles, California, AIAA-64-644.
22. Cherry, G.W., 1963. A unified explicit technique for performing orbital insertion, soft landing and rendezvous with a throttle able rocket propelled space vehicle.

- AIAA guidance and control conference, Aug 12-14, 1963, MIT Cambridge, Massachusetts, AIAA-63-335.
23. Cherry, G.W., 1964. A general explicit optimizing guidance law for rocket propelled spaceflight. AIAA/Astroynamics Guidance and Control Conference, Aug 24-26, 1964, Los Angeles, California, AIAA-64-638.
 24. Citron, S. J., Dunin, S. E., and Meissinger, H. F., 1964. A terminal guidance technique for lunar landing. AIAA Journal, 2(3), 503–509.
 25. Conway, B.A., 2012. A survey of methods available for the numerical optimization of continuous dynamic systems. Journal of Optimization Theory and Application, 152, 271–306.
 26. D'Souza, S. N., Klijn, N., S., 2014. Survey of planetary entry guidance algorithms. Progress in Aerospace Sciences, 68, 64-74.
 27. Donna Lu., 2020. To the moon and back. New Scientist, 248(3310), 8-9.
 28. D'Souza, C. N., 1997. An optimal guidance law for planetary landing. Proceedings of the AIAA conference on Guidance, Navigation, and control, LA, U.S.A, AIAA-97-3709.
 29. Ebrahimi, B., Bahrami, M., Roshanian, J., 2008. Optimal sliding-mode guidance with terminal velocity constraint for fixed-interval propulsive maneuvers. Acta Astronautica, 62(10-11), 556-562.
 30. Taheri, E., Nan, I. Li, Kolmanovsky I., 2016. Co-states initialization of minimum-time low thrust trajectories using shape-based methods. American Control Conference, Boston, MA, USA, July 6-8, 2016.
 31. Ennico, K., Shirley, M., Colaprete, A., Osetinsky, L., 2012. The lunar crater observation and sensing satellite (LCROSS) payload development and performance in flight. Space Science Reviews, 167, 23-69.
 32. Fahroo, F., Ross, I. M., 2001. Co-state estimation by Legendre pseudo spectral method. Journal of Guidance, Control and Dynamics, 24(2), 270-277.

33. Fahroo, F., Ross, I. M., 2004. Pseudospectral method knotting methods for solving optimal control problems. *Journal of Guidance, Control, and Dynamics*, 27, 397-405.
34. Foing, B.H., et al., 2005. SMART-1 after lunar capture-first results and perspectives. *Journal of Earth System Sciences*, 114(6), 689-697.
35. Furfaro, R., Cersosimo, D., Wibben, D. R., 2013. Asteroid precision landing via multiple sliding surfaces guidance techniques. *Journal of Guidance, Control, and Dynamics*, 36(4), 1075-1092.
36. Furfaro, R., Selnick, S., Cupples, M. L., and Cribb, M. W., February 13-17, 2011. Non-linear sliding guidance algorithms for precision lunar landing. *Advances in the Astronautical Sciences*, Vol.140, 21st AAS/AIAA Space Flight Mechanics Meeting, New Orleans, Louisiana.
37. Gerth, I., Mooij, E., 2014. Guidance for autonomous precision landing on atmosphere less bodies. *AIAA Guidance, Navigation and Control Conference*, 13-17 January 2014, Maryland, USA, AIAA-2014-0088.
38. Gong, Q., Fahroo, F. and Michael Ross, I., 2008. Spectral algorithm for Pseudospectral methods in optimal control. *Journal of Guidance, Control and Dynamics*, 31(3), 460-471.
39. Guo, J. A., Han, C. Y., 2009. Design of guidance laws for lunar pinpoint soft landing. *AAS/AIAA Astrodynamics Specialist Conference*, 9-13 August 2009, Washington, AAS 09-431.
40. Guo, Y., Hawkins, M. and Wie, B., 2013. Waypoint-Optimized Zero-Effort-Miss/Zero-Effort-Velocity feedback guidance for Mars landing. *Journal of Guidance, Control and dynamics*, 36(3), 799-809.
41. Guo, Y., Hawkins, M. and Wie, B., 2012. Waypoint-Optimized Zero-Effort-Miss/Zero-Effort-Velocity feedback guidance for Mars landing. *AAS/AIAA Astrodynamics specialist conference*, 13-16 August 2012, Minneapolis, Minnesota, USA, AAS 12-196.

42. Guo, Y., Hawkins, M., and Wie, B., 2011. Optimal feedback guidance algorithms for planetary landing and asteroid intercept. AAS/AIAA Astrodynamics specialist conference, July 31-August 4, 2011, Girdwood, Alaska, USA, AAS 11-588.
43. Hall, B. A., Dietrich, R. G., and Tiernan, K. E., 1963. A minimum fuel vertical touchdown lunar landing guidance technique. AIAA Guidance and Control Conference, Cambridge, MA, 12-14 August 1963, <https://doi.org/10.2514/6.1963-345>.
44. Hargraves, C. R., Paris, S. W., 1987. Direct trajectory optimization using nonlinear programming and collocation. *Journal of Guidance Control, and Dynamics*, 10(4), 338-342. doi: 10.2514/3.20223.
45. Hassan, R., Cohanin, B.W., Oliver De, 2005. A comparison of Particle Swarm Optimization and Genetic algorithm. 46th AIAA/ASME/ASCEAHS/ASC Structures, Structural Dynamics and Materials conference, Austin, Texas, 18-21 April 2005, AIAA 2005-1897.
46. Hawkins, M., 2005. Constrained Trajectory Optimization of a Soft Lunar Landing from a Parking Orbit. Master of Science thesis, Massachusetts Institute of Technology.
47. Hawkins, M., Guo, Y., and Wie, B., 2011. Guidance algorithms for asteroid intercept missions with precision targeting requirements. AAS/AIAA Astrodynamics specialist conference, July 31-August 4, 2011, Girdwood, Alaska, USA, AAS 11-531.
48. Hawkins, M., Guo, Y., and Bong Wie, 2012. ZEM/ZEV feedback guidance application to fuel-efficient orbital maneuvers around an irregular shaped Asteroid, AIAA Guidance, Navigation and Control conference, Minnesota, August 13-16, 2012, AIAA-2012-5045.
49. Henzeh L., Dong-Hyun C., Donghoon K., 2016. An optimal trajectory design for the lunar vertical landing. *ProcIMechE Part G: Journal of Aerospace Engineering*, 230(11), 2077–208.
50. Huang, R., Hwang, I., and Corless, M., 2009. A new nonlinear model predictive control algorithm using Differential Transformation with application to

- interplanetary low-thrust trajectory tracking. American Control Conference, St. Louis, MO, USA, June 10-12, 2009, 4868-4873.
51. Hubbard, G. S., Binder, A. B., Feldman, W., 1998. The lunar prospector discovery mission: mission and measurement description. *IEEE transactions on Nuclear Science*, 45(3), 880-887.
 52. Huiping C., Lin M., Kexin W., Zhijiang S., Zhengyu S., 2017. Trajectory optimization for lunar soft landing with complex constraints. *Advances in Space Research* 60(2017), 2060–2076.
 53. Hwang, I., Li. J., Du, D., February 2008. A numerical algorithm for optimal control of a class of hybrid systems: Differential Transformation based approach. *International Journal of Control*, 81(2), 277-293.
 54. Ingoldby, R. N., 1978. Guidance and control system design of the Viking planetary lander. *Journal of Guidance, Control and Dynamics*, 1(3), 189–196.
 55. Je Liuyu, Zhou., Yuanqing, Xia., 2014. Improved ZEM/ZEV feedback guidance for Mars powered descent phase. *Advances in Space Research*, 54, 2446–2455.
 56. Jenkins, R. M., Hartfield Jr., R. J., 2012. Hybrid Particle Swarm: Pattern Search Optimizer for Rocket Propulsion Applications. *Journal of Spacecraft and Rockets*, 49(3), 512-521.
 57. Jennings, L.S., Fisher, M.E., Teo, K.L., Goh, C. J., 1991. MISER3: Solving optimal control problems - an update. *Advance Engineering Software*, 190–196.
 58. Kawakatsu, Y., Kaneko, Y., Takizawa, Y., 1998. Trajectory design of SELENE lunar orbiting and landing. *Proceedings of the AAS/GSFC international symposium on Space Flight Dynamics*, Greenbelt, Maryland, USA, 100(1), AAS98-320.
 59. Kirk, D. E., 1970. *Optimal Control Theory: An Introduction*. Prentice Hall
 60. Klumpp, A. R., 1968. A manually retargeted automatic landing system for the lunar module (LM). *Journal of Spacecraft and Rockets*, 5(2), 129-138.
 61. Klumpp, A. R., 1971. Apollo guidance, navigation, and control: Apollo lunar-descent guidance. Technical report, R-695, MIT Charles Stark Draper Laboratory.
 62. Klumpp, A. R., 1974. Apollo lunar descent guidance. *Automatica*, 10, 133—146.

63. Kozynchenko, A. I., 2010. Enhancing the maneuvering capabilities of a lunar landing module using predictive guidance algorithms. *Acta Astronautica*, 67,406–416.
64. Lee, A. Y., 2011. Fuel-efficient descent and landing guidance logic for a safe lunar touchdown. *AIAA Guidance, Navigation, and Control Conference*, 8-11 August 2011, Portland, Oregon, AIAA 2011-6499.
65. Lee, A. Y., Ely, T., Strahan, A., Riedel, J., Ingham, M., Wincentsen, J., and Sarani, S., 2010. Preliminary design of the guidance, navigation and control system of the Altair lunar lander. *AIAA Guidance, Navigation, and Control Conference*. 2-5 August 2010, Toronto, Canada, AIAA 2010-7717.
66. Li, M.D., Macdonald, M., McInnes, C.R., and Jing, W. X., 2010. Analytical landing trajectories for embedded autonomy. *Proceedings of the institution of Mechanical Engineers, Part G, Journal of Aerospace Engineering*, 224(11), 1177-1191.
67. Lunghi, P., Armellini, R., Di Lizia, Pierluigi, Lavagna, M., 2016. Semi-analytical adaptive guidance computation based on differential algebra for autonomous planetary landing. *Proceedings of 26th AAS/AIAA Space Flight Mechanics Meeting*, in: *Advances in the Astronautical Sciences*, 158, 2003-2022.
68. Lunghi, P., Lavagna, M., 2015. A semi-analytical guidance algorithm for autonomous landing. *Advances in Space Research*, 55, 2719-2738.
69. Mason, M., Brainin S. M., 1962. Descent trajectory optimization for soft lunar landings. *Aerospace Engineering*, 21(4), 54-55, 82-91.
70. Mathavaraj, S., Pandiyan, R., Padhi, R., 2017. Constrained optimal multi-phase lunar landing trajectory with minimum fuel consumption. *Advances in Space Research*, 60(2017), 2477-2490.
71. McInnes, C. R., 1995. Path shaping guidance for terminal lunar descent. *Acta Astronautica* 36(7), 367-377.
72. McInnes, C. R., 1996. Nonlinear transformation methods for gravity-turn descent. *Journal of Guidance Control and Dynamics*, 19(1), 247–248.
73. McInnes, C. R., 1999. Direct adaptive control for gravity turn descent, *Journal of Guidance Control and Dynamics*, 22(2), 373-375.

74. McInnes, C. R., 2003. Gravity-turn descent from low circular orbit conditions. *Journal of Guidance Control and Dynamics*, 26(1), 183-185.
75. Meditch, J. S., 1964. On the problem of optimal thrust programming for a lunar soft landing. *IEEE Transactions on Automatic Control*, 9(4), 477-484.
76. Mehedi, I., Kubota, T., 2011. Advanced guidance scheme for lunar descent and landing from orbital speed conditions. *Transaction of Japan Society for Aeronautical and Space Sciences*, 54(184), 98-105.
77. Najson, F., Mease, K., 2006. Computationally inexpensive guidance algorithm for fuel-efficient terminal descent. *Journal of Guidance, Control and Dynamics*, 29(4), 955-964.
78. Nozette, S., 1995. The Clementine mission: past, present and future. *Acta Astronautica*, 35(1), 161-169.
79. Olds, A. D., and Kluever, C.A., Cupples, M., 2007. Interplanetary mission design using Differential Evolution. *Journal of Spacecraft and Rockets*, 44(5), 1060-1070.
80. Park, B. G., Ahn, J. S., and Tahk, M. J., 2011. Two-dimensional trajectory optimization for soft lunar landing considering a landing site. *International Journal of Aeronautical Space Sciences*, 12(3), 288-295, The Korean Society for Aeronautical and Space Sciences.
81. Park, B. G., and Tahk, M. J., 2011. Three-dimensional trajectory optimization of soft lunar landings from the parking orbit with considerations of the landing Site. *International Journal of Control, Automation and Systems* (2011) 9(6):1164-1172.
82. Lu, P., 2018. Propellant-optimal powered descent guidance. *Journal of Guidance, Control, and Dynamics*, 41(4), 813-826.
83. Lu, P., 2019. Augmented Apollo powered descent guidance. *Journal of Guidance, Control, and Dynamics*. 42(3), 447-457.
84. Lu, P., Brunner, C.W., Stachowiak, S. J., Mendeck, G. F., Tigges, M.A., Cerimele, C.J., 2017. Verification of a fully numerical entry guidance algorithm, *Journal of Guidance, Control and Dynamics*, 40(2), 230-247.
85. Ploen, S.R., Acikmese, A.B., and Wolf, A., August 21-24, 2006. A comparison of powered descent guidance laws for Mars pinpoint landing. *Proceedings of*

AIAA/AAS Astrodynamics Specialist Conference and Exhibit, Keystone, CO, USA, AIAA2 006-6676.

86. Pontani, M., Cechheti, G., Teofilatto, P., 2015. Variable time neighboring optimal guidance: part 2: Application to lunar descent and soft landing. *Journal of Optimization Theory and Applications*, 166(1), 93-114.
87. Pontani, M., Conway, B., A., 2010. Particle Swarm Optimization applied to space trajectories. *Journal of Guidance, Control and Dynamics*, 33(5), 1429-1441.
88. Pontani, M., Ghosh, P., Conway, B. A., 2012. Particle Swarm Optimization of multiple-burn rendezvous trajectories. *Journal of Guidance, Control and Dynamics*, 35(4), 1192-1207
89. Pukhov, G. E., 1981. Expansion formulas for differential transforms. *Cybernetics and System analysis*, 17(4), 460–464.
90. Ramanan, R.V. and Madanlal, 2005. Analysis of optimal strategies for soft landing on the Moon from lunar parking orbits. *Journal of Earth System Sciences*, 114(6), 807-813.
91. Rao, A. V., 2009. A survey of numerical methods for optimal control. *Astrodynamics Specialist Conference*, August 9-13, 2009, Pittsburgh, Pennsylvania, AAS 09-334, 135 (1), 497-528.
92. Rao, A. V., Benson, D. A., Darby, C. L., Patterson, M. A., Francolin, C., Sanders, I., and Huntington, G. T., 2010. GPOPS: A MATLAB software for solving multiple-phase optimal control problems using the Gauss pseudospectral method. *ACM Transactions on Mathematical Software*, 37(2) , Article no. 22, March-April 2010.
93. Rea. J., Bishop, R. H., 2010. Analytical dimensional reduction of a fuel optimal powered descent sub problem. *AIAA Guidance, Navigation, and Control Conference*. Toronto, Ontario Canada, AIAA-2010-8026,
94. Shuang, L., Xiuqiang J., Ting T., 2016. Guidance summary and assessment of the Chang'e-3 powered descent and landing, *Journal of Spacecraft and Rockets*, 53(2), 258-277.

95. Sostaric, R. R., Rea, J. R., 2005. Powered descent guidance methods for the Moon and Mars. AIAA Guidance, Navigation, and Control Conference and Exhibit, San Francisco, California, AIAA 2005-6287.
96. Steinfeld B., Grant M., Matz D., Braun R., Barton G, 2010. Guidance, navigation, and control system performance trades for Mars pinpoint landing. *Journal of Spacecraft and Rockets*, 47(1), 188-198.
97. Storn, R., Price, K., 1997. Differential Evolution – A simple and efficient heuristic for global optimization over continuous spaces. *Journal of Global Optimization* 11(4), 341–359.
98. Stryk, O., 1993. Numerical solution of optimal control problem by direct collocation. *Optimal control theory and numerical methods*, International series of Numerical Mathematics, 111, 129-143
99. Subchan, S. and Zikowski, R., 2009. Computational optimal control, tools and practice. John Wiley and Sons Ltd.
100. Topcu, U., Casoliva, J., and Mease, K. D., 2007. Minimum-fuel powered descent for Mars pinpoint landing. *Journal of Spacecraft and Rockets*. 44(2), 324-331.
101. Tu, L., Yuan, J., Luo, J., Ning, X. and Zhou, R., 2007. Lunar soft-landing rapid trajectory optimization using direct collocation method and nonlinear programming. *Proceeding of second international conference on spatial information technology*, Wuhan, China, 6795(4).
102. Uchiyama, K., Shimada, Y., 2002. Tracking control to near-optimal trajectory for a lunar lander. *Proceedings of the Twenty-Third International Symposium on Space Technology and Science*, 977– 982.
103. Uchiyama, K., Shimada, Y., Ogawa, K., 2005. Minimum Jerk guidance for lunar lander. *Transactions of Japan Society for Aeronautical and Space Science*, 48(159), 34-39.
104. Ueno, S., Yamaguchi, Y., 1999. 3-Dimensional near-minimum fuel guidance law of a lunar landing module. AIAA Guidance, Navigation, and Control Conference and Exhibit, Portland, AIAA- 99-3983.

105. Uesugi, K., 1996. Results of the MUSES-A “HITEN” mission. *Advances in Space Research*, 18(11), 69-72.
106. Vasik, M. M., Floberghagen, R., 1998. Optimal trajectories for lunar landing mission. *Proceedings of the AAS/GSFC international symposium on Space Flight Dynamics*, Greenbelt, Maryland, USA, 100(1), AAS 98-321.
107. Vasile, M., and Minisci, E., Locatelliz, M., 2008. On testing global optimization algorithms for space trajectory design. *AIAA/AAS Astrodynamics specialist conference and Exhibit*, Honolulu, Hawaii, 18-21 August 2008, AIAA 2008-6277.
108. Vasile, M., and Minisci, E., March-April 2010. Analysis of some global optimization algorithms for space trajectory design. *Journal of Spacecraft and Rockets*, 47(2), 334-344.
109. Venkataraman, P., 2009. *Applied Optimization with MATLAB Programming*. John Wiley & Sons Inc.
110. Venter, G., Sobieski, J. S., 2003. Particle Swarm optimization. *AIAA journal*, 41(8), 1583-1589.
111. Wang, D., Huang, X., and Guan, Y., 2008. GNC system scheme for lunar soft-landing spacecraft. *Advances in Space Research*. 42(2), 379-385.
112. Wilhite, A. W., Wagner J., 2008. Lunar module descent mission design. *AIAA/AAS Astrodynamics Specialist Conference and Exhibit*, August 18-21, 2008, Honolulu, Hawaii, USA, AIAA 2008-6939.
113. Won, M., Hedrick, J., 1996. Multiple surface sliding control of a class of uncertain nonlinear systems. *International Journal of Control*, 64, 693-706.
114. Wong, E. C., Singh, G., Masciarelli, J. P., 2006. Guidance and control design for hazard avoidance and safe landing on Mars. *Journal of Spacecraft and Rockets*, 43(2). 379-384.
115. Zhou, J., Teo, K., Zhou, D., Zhao, G., 2010. Optimal guidance for lunar module soft landing. *Non-linear dynamics and Systems theory*, 10 (2010), 189-201